AN ULTIMATE STRENGTH APPROACH TO FLEXIBLE PAVEMENT DESIGN

NORMAN W. McLEOD

INTRODUCTION

Until very recently, airport and highway engineers have been rather fortunate in that almost any reasonably well designed mixture of gravel or crushed stone and asphalt has had sufficient stability for pavements for the weights and intensities of traffic to which they have been subjected on airports and rural highways. Similarly, crushed gravel or crushed stone, and even pit-run gravel, have provided adequate stability for the underlying base courses. The truth of this statement is verified by the fact that hundreds of millions of square yards of flexible pavements have been laid on highways and airports all over the world without any test for stability having been made on either the base course or surfacing materials. The ultimate arbitrament of traffic has demonstrated that stable pavement structures have generally been obtained in spite of this lack of formal stability tests.

In the past, most bituminous pavements have been designed and constructed on the basis of previous experience with the same or similar materials, and with no laboratory control apart from occasional extraction, gradation, and density tests. Base course materials have been selected on the basis of their visual appearance, guided occasionally by a sieve analysis sometimes augmented by a plasticity index determination. Formal stability tests for either the design or construction control of base course and surfacing materials have been the exception rather than the rule. Many organizations laying large areas of flexible pavement each year do not specify a stability requirement of any kind for either the base or surface courses.

This fortuitous circumstance, namely that most granular base and sub-base materials, and most reasonably well designed bituminous surfaces, have had adequate stability for the traffic loads to which they have been exposed in the past is largely responsible for the fact that we still know very little about the fundamental factors on which the stability of a flexible pavement depends. If the materials themselves had had less inherent

[1] Engineering Consultant, Department of Transport, Ottawa, Canada.

stability, or if the unit pressures of traffic had frequently exceeded the stability of either the flexible pavement structure as a whole, or of one or more of its layers, highway and airport engineers would have been forced long ago to investigate the basic factors upon which the stability of every part of a flexible pavement depends. It appears that we are just entering the stage where these fundamentals must be studied.

Since World War II, the advent of jet aircraft with tire pressures of 200 to 300 p.s.i., and the possibility that these inflation pressures may be further increased, has made it necessary to re-examine our current more or less lackadaisical approach to all phases of flexible pavement design. Tire inflation pressures of this magnitude create high shearing stresses in the portion of the surface and base course close to the loaded area. To resist these high shearing stresses, surfacing and base course materials with high shearing strengths are required. Consequently, airport engineers have been forced to give more attention to methods for measuring the strength or stability of base course and surfacing materials. To a somewhat similar degree, the increasing number of heavy axle loadings on highways is forcing highway engineers also to devote more attention to these problems of flexible pavement stability.

An accurate formulation or statement of any problem is the first important step toward its solution. If the stability of flexible pavements is to be investigated, what stability criteria are to be employed? For this paper, it is assumed that every flexible pavement must satisfy each of the following three stability requirements, which formulate the stability problem in this case:

1. The overall thickness of sub-base, base course, and bituminous surface must be adequate to protect the subgrade from failure under the stresses transmitted from the loaded area.
2. The shearing strengths of the materials in layers close to the loaded area must be greater than the shearing stresses caused by high inflation pressures, which tend to cause failure along shear surfaces entirely within the base course and bituminous surface.
3. The stability of each individual layer, sub-base, base course, and bituminous surface, must be greater than the tendency of the layer to fail by being squeezed out laterally under the applied load. For example, the bituminous surface must be stable enough to resist being squeezed out between the tire and base course.

The first of the above three requirements of flexible pavement design has already received considerable study (1, 2, 3, 4, 5, 6, 7, 8, 9) by means of methods that are either wholly empirical, entirely theoretical, or a combination of both. The author has outlined a rational solution to the third problem in previous papers (10, 11, 12, 13, 14, 15), insofar as the stability of the bituminous pavement itself is concerned. While it deals to some extent with each of the above three flexible pavement stability requirements, it is the principal purpose of the present paper to investigate the second problem, and to re-examine the first, on the basis of an ultimate strength approach to flexible pavement design.

CONSIDERATIONS THAT LEAD TO AN ULTIMATE STRENGTH APPROACH TO FLEXIBLE PAVEMENT DESIGN

The composite cross-section of a flexible pavement, consisting of the three principal layers, subgrade, base course, and bituminous surface, is illustrated in Figure 1. Both empirical and rational methods are available for determining the stability of each of these three layers, and of the flexible pavement as a whole.

Among the empirical methods, the C.B.R. and Marshall methods of the Corps of Engineers, the Hveem stabilometer, and North Dakota cone are well known. While empirical methods are widely used in the flexible pavement field, they have the serious disadvantage that they have been developed for a specific set of conditions, and cannot be safely employed under new and different circumstances until investigated for these. It is because they have no theoretical background that the use of empirical tests is so limited, and cannot be extrapolated from one situation to another without careful pretesting for every set of conditions. Furthermore, the factor of safety represented by the use of empirical methods cannot be determined, and they may at times lead to either serious overdesign or underdesign due to their neglect of important variables.

In 1943, Professor Burmister (16) proposed a rational method of design for the layered system represented by a flexible pavement. In Burmister's method, each layer, subgrade, base course, and bituminous surface, is assumed to consist of perfectly elastic material. Consequently, insofar as its strength is concerned, the most important characteristic of the material in each layer is its modulus of elasticity. For any measured or given moduli

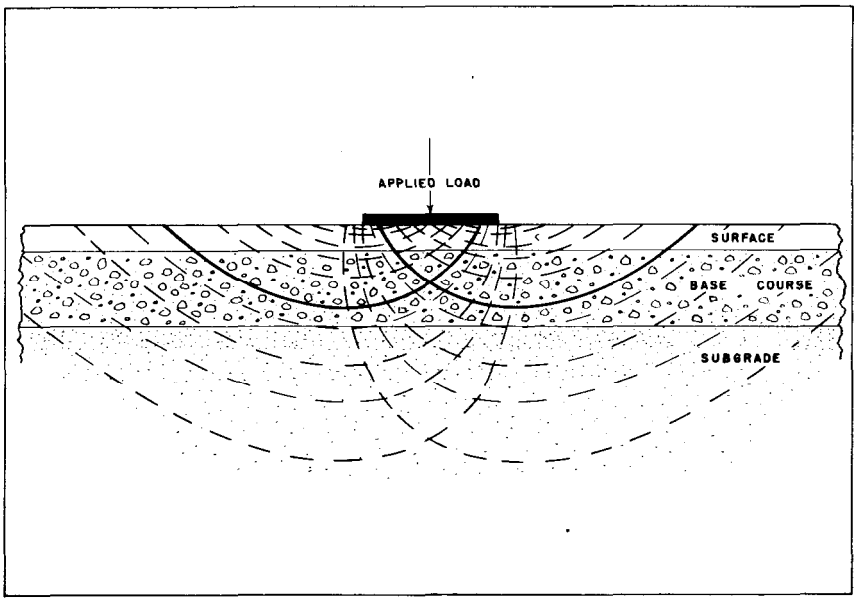

Fig. 1. Diagram of Shear Planes Under a Loaded Area.

of elasticity for the subgrade, base course, and bituminous surface, and for any specified deflection of the surface of the pavement under the applied load within the elastic range, the required thickness of flexible pavement can be determined. Partly because of its own individual merit, and partly because of its stimulation toward organized rational thought in this field, Professor Burmister's theory represents an outstanding contribution to flexible pavement design.

The principal criticism of the Burmister theory concerns its assumption that the soils, aggregates, and bituminous mixtures that make up the various layers of a flexible pavement, function as perfectly elastic materials; that is, they obey Hooke's law, and strain is proportional to stress. The actual behaviour of many of these is far from elastic. Another criticism is that a critical surface deflection must be arbitrarily assumed, since information does not exist to indicate what this deflection should be and how it should vary with size of contact area, intensity of inflation pressure, thickness of flexible pavement, etc. Furthermore, the moduli of elasticity of many cohesionless base course aggregates and bituminous paving mixtures seem to lie within a similar range. Wherever this occurs, Burmister's method in-

dicates them to be of equivalent strength in flexible pavement design. Results developed later in the present paper indicate that this may not be true. Finally, an elastic theory is subject to the general criticism that the factor of safety against ultimate failure is not known.

It has been frequently observed that when an earth road consisting of a relatively soft homogeneous clay or loam is overloaded by traffic a rut forms in each wheel path and upheaval of the displaced material occurs on both sides of the lane. It is also a matter of relatively common observation that when a flexible pavement consisting of subgrade, base course, and bituminous surface is overloaded by traffic, similar rutting and upheaval develops. Therefore, in a qualitative way at least, failure of the layered system of a flexible pavement when overloaded by wheeled traffic seems to follow the general pattern of failure of a homogeneous soil that has been overstressed by traffic. In both of these cases, failure occurs because the applied wheel load exceeds the ultimate strength of the roadway structure. Expressed in another way, failure takes place because the applied shearing stress exceeds the shearing resistance of the loaded material.

These various considerations have led the author to a different rational approach to flexible pavement design. Professor Burmister's theory is based upon the assumptions of a critical surface deflection, and of elastic performance of the materials in the different layers. In the present paper, an attempt will be made to analyse the flexible pavement problem on the basis of shearing stress versus shearing resistance. Since the ultimate strength of the flexible pavement is employed, which is far beyond any elastic range of loading the structure may have, the method described in this paper is based upon the plastic rather than the elastic behaviour of the materials in the various layers of the flexible pavement.

LOGARITHMIC SPIRAL METHOD FOR DETERMINING THE ULTIMATE STRENGTH OF SOILS

Various investigators have studied the problem of the ultimate bearing capacity of homogeneous soils. Equations for ultimate strength have been proposed by Prandtl (17), Terzaghi (18), Krey (19), Fellenius (20), Meyerhof (21), and others. It is beyond the scope of this paper to review each of these critically. However, reference will be made to the principles on which several are based, in order to point out the reasons for the selection of the logarithmic spiral method adopted in this paper.

One of the earliest simple methods proposed for calculating the ultimate strengths of homogeneous soils was the Terzaghi-Hogentogler equation (22-23). This was based upon the assumption of failure along the straight line shear planes ab and bc in Figure 2(a). Failure occurs when the shearing strength stress exerted on these shear planes by the applied load exceeds the shearing strength. The shearing resistance of the soil along these failure planes is given by the well-known Coulomb equation $s = c + n \tan \phi$. From the nature of this equation, it is apparent that any factor that will increase the normal pressure n on the plane of failure will add to the magnitude of the $n \tan \phi$ term of the Coulomb equation and thereby increase the shearing strength s of the soil.

The Terzaghi-Hogentogler equation overlooks the possibility that the applied load itself may increase the normal pressure n

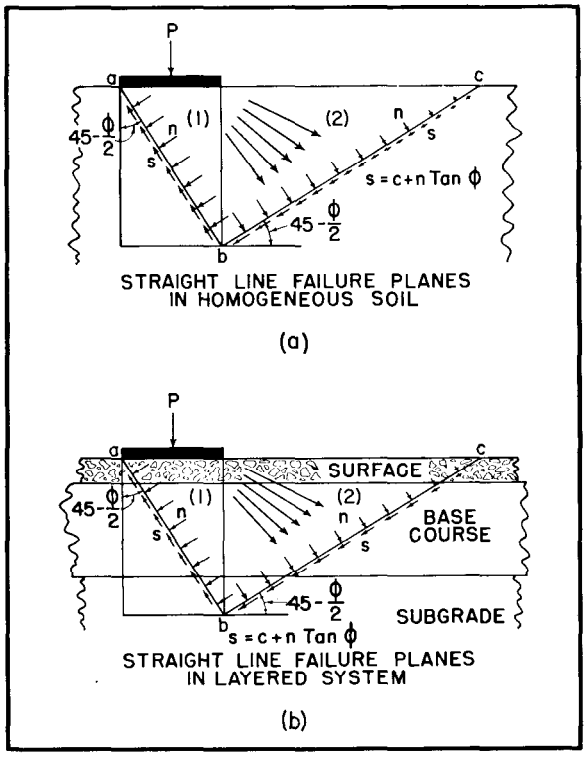

Fig. 2. Straight Line Failure Planes.

on the failure plane bc in Figure 2(a). Investigations by Housel (24), and by Davis and Woodward (25, 26), have shown that spreading of the applied load outward with depth below the loaded area may add considerably to the magnitude of the normal pressure n exerted on the failure plane bc. Neglect of this factor makes the Terzaghi-Hogentogler equation for ultimate bearing capacity ultra-conservative.

On the other hand, the manner in which an applied load spreads outward with depth in a homogeneous soil is not known precisely. In the region close to the loaded area at least, this depends upon such factors as the nature of the soil, how the load is applied, e.g. rigid or flexible bearing, etc. As a consequence, the way in which the normal stress n, due to this spreading of the applied load with depth, varies in magnitude along the failure plane bc is not accurately known and must also be assumed. The calculated ultimate strength in turn will be no more accurate than this assumption. In addition, even after this distribution of normal stress n has been assumed, the summation of the total shearing resistance s, acting along the surface of failure, is not a simple matter, since the n $\tan\phi$ term of the shearing strength varies from point to point along the failure surface.

The principal problem, therefore, in obtaining a reasonably accurate ultimate strength value for a homogeneous soil, even on the basis of the simple failure planes in Figure 2(a), is due to uncertainty concerning the magnitude and distribution of the normal stress n acting on the failure plane bc. It should be particularly noted that this introduces equal uncertainty into the value of the n $\tan\phi$ term of the Coulomb equation for the shear strength s of each individual element of length along the failure surface bc.

Recent theoretical studies of the shape of the pressure bulb in a layered system by Fox (27) at the National Physical Laboratory in England have shown that the pattern of pressure distribution on horizontal planes below a loaded surface is still less certain for a layered than for a homogeneous system. Consequently, if it is not easy to determine the ultimate bearing capacity of a homogeneous soil on the basis of the simple straight line failure planes of Figure 2(a), it is still more difficult to do so for the layered system of Figure 2(b). In both cases, accurate values for the shearing resistance s can not be calculated because the magnitude and distribution pattern of the normal pressure n on the plane of failure is not definitely known.

The circular arc failure curve proposed by Fellenius (20) can be used for the determination of the ultimate strength of a

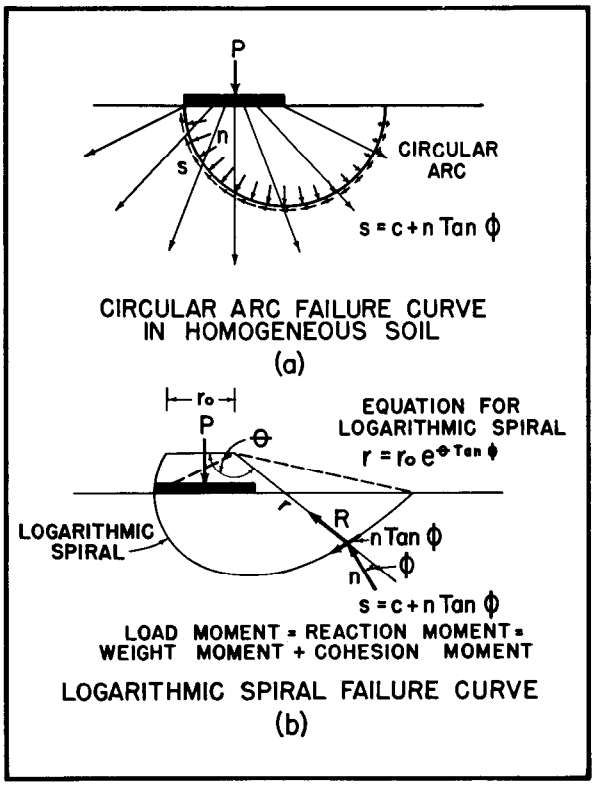

Fig. 3. Curved Line Failure.

homogeneous soil, Figure 3(a). The critical circular arc is found by trial and error and is the arc along which the shearing resistance of the soil will support the lowest ultimate load. The ultimate strength is obtained by equating the moment of applied load about the centre of the critical circular arc to the reaction moment about the same point. The reaction moment consists of the summation of the tangential shearing resistance on all elements of the circular arc multiplied by the radius of the arc. Here again, however, the same difficulty that has already been described in connection with Figures 2(a) and 2(b) still arises. The magnitude of the normal pressure n acting on each element of the circular arc is not definitely known. Consequently, the value of the n tanϕ term of the Coulomb equation for shearing resistance acting tangentially along each element of the circular arc cannot be determined without making assumptions concerning

the pattern of lateral distribution of the applied load below the loaded area. The calculated ultimate strength can be no more accurate than these assumptions. In addition, the calculation of the part of the reaction moment due to the n $\tan\phi$ portion of the tangential shearing resistance along the circular arc of Figure 3(a) is a time-consuming task, particularly since the centre of the critical circular arc must be found by trial and error. These difficulties with the n $\tan\phi$ term do not arise, of course, when applying Fellenius' method to homogeneous cohesive soils for which the angle of internal friction $\phi = 0$.

When discussing the determination of the ultimate bearing capacity of a homogeneous soil by the methods illustrated in Figures 2(a), 2(b), and 3(a), it has been shown that a major difficulty arises because the value of the normal stress n to be used in the Coulomb equation for shearing strength, $s = c + n \tan\phi$, is not accurately known. This problem leads to considering whether there is any alternative approach to the calculation of ultimate bearing capacity, which would eliminate the n $\tan\phi$ term of the Coulomb equation, and substitute for it some other quantity that can be accurately measured or calculated.

As illustrated in Figure 3(b), the assumption of a logarithmic spiral failure curve, for which the angle between the radius vector and the normal to the curve is equal to the angle of internal friction ϕ, meets these requirements, provided the ultimate strength is obtained by equating the load moment to the reaction moment. Two symmetrical spiral failure curves normally occur about a strip load, but to save space in Figure 3(a) the spiral on only one side is shown. Figure 3(b) demonstrates that the resultant of the intergranular normal (n) and frictional (n $\tan\phi$) forces acting at any point along a logarithmic spiral is directed to the origin of the spiral. Consequently, since the moment arm is zero, the moment of the resultant of the intergranular stresses (n and n $\tan\phi$), at any point along the spiral, about the origin of the spiral, is always zero. On the other hand, due to the shape of the logarithmic spiral, there is a greater weight of material within the spiral to the right than to the left of the vertical through the origin. This creates a weight moment about the origin of the spiral.

For the friction moment due to the n $\tan\phi$ term of the Coulomb equation in the case of the circular arc of Figure 3(a) and other failure surfaces, therefore, the logarithmic spiral failure curve of Figure 3(b) substitutes a weight moment. As previously pointed out, the term n $\tan\phi$ is difficult to evaluate precisely. On the other hand, the weight moment of a logarithmic spiral

failure curve can be readily calculated to any desired degree of accuracy.

The significance of each term of the general equation for the logarithmic spiral,

$$r = r_0 e^{\theta \tan \phi} \quad (1)$$

is illustrated in Figure 3(b):

- r_0 is the initial radius vector;
- r is any other radius vector;
- θ is the angle between the two radius vectors r_0 and r, and is measured in radians;
- e is the base of natural logarithms and is equal to 2.71828; and
- ϕ is the angle of internal friction of the material subjected to load.

When calculating the ultimate strength of a homogeneous soil on the assumption of a logarithmic spiral failure curve, the well-known principle of mechanics that for equilibrium the sum of the moments of the forces about any point must be equal to zero is employed. In this case, it is most convenient to select the origin of the spiral as the point about which the moments are to be taken.

At equilibrium,

load moment = reaction moment = weight moment plus cohesion moment.

The load moment is obtained by multiplying the total load by the moment arm. The reaction moment consists of two quantities, the weight moment and the cohesion moment.

Since more material is contained within the spiral to the right than to the left of the vertical through its origin, this unbalanced weight results in a weight moment. If the material under load possesses any cohesion, its cohesion c acts as a shearing resistance along the entire length of the spiral. The summation of the moments for cohesion c for each element of length of the spiral about the spiral's origin gives the cohesion moment.

Mr. E. S. Barber (28) has published several tables of basic data that simplify calculations involving the logarithmic spiral. These tables enable the weight moment and the cohesion moment for the critical spiral, and the ultimate strength to be more readily determined for loads applied to homogeneous soils with different c and ϕ values.

The principles involved in the determination of the ultimate strength of a homogeneous soil by means of a logarithmic spiral failure curve are illustrated by a sample calculation in Appendix A, and can be very easily described. By trial and error, the location of the origin of the spiral along which the shearing resistance of the soil will support the smallest ultimate applied load is found. In this trial and error method, the load moment is equated to the sum of the weight moment and the cohesion moment for each trial spiral selected. This approach is, therefore, somewhat similar to that employed in the circular arc method for determining the stability of slopes.

The origin of the critical spiral determined by the trial and error method lies on a radius vector through an extremity of the loaded area and making a positive angle θ_1 with the horizontal, Figure 19. For cohesionless soils, the origin of this spiral is at the intersection of this radius vector with the vertical marking 75 per cent of the distance toward the opposite extremity of the loaded area (Appendix D). For cohesive soils with zero angle of internal friction, the origin of the spiral is at the intersection of the radius vector with the vertical through the opposite extremity of the loaded area (Appendix D). For soils with both c and ϕ values, the origin of the critical spiral lies on the radius vector at its intersection with a vertical somewhere between 75 and 100 per cent of the distance toward the opposite extremity of the loaded area (Appendix D). The angle $\theta_1 = 23.2^0$ for the critical spiral for homogeneous cohesive soils for which the angle of internal friction $\phi = 0$, and increases as ϕ is increased. θ_1 approaches ϕ for values of ϕ greater than 45^0.

To simplify the calculations, unless specifically stated to be otherwise, all data in this paper pertain to the condition of strip loading; that is, for a loaded area which is very long in proportion to its width. The contact area of a loaded tire is elliptical in outline, but the calculations for ultimate strength for this shape of contact area become quite complicated. Other investigators (29, 30) have found that the ultimate unit load supported by a homogeneous cohesive soil on a square or round bearing area is from 20 to 30 per cent higher than the ultimate unit pressure supported by the same soil on a strip load of the same width.

To save space in Figures 3(a), 19, and in other diagrams of this paper, only one logarithmic spiral failure curve, passing through the left extremity of the loaded area and extending toward the right, is shown. In all cases, however, a similar logarithmic spiral failure curve passing through the right extremity of the

loaded area and extending toward the left also exists. The two spirals are symmetrical about the mid ordinate of the loaded area.

THE ULTIMATE STRENGTH OF HOMOGENEOUS SOILS

Since it represents the simplest case, the application of the logarithmic spiral method to the determination of the ultimate strength of a homogeneous soil will be considered first. In terms of flexible pavement design, this corresponds to a surface treatment of negligible influence and thickness, placed on a great depth of homogeneous soil.

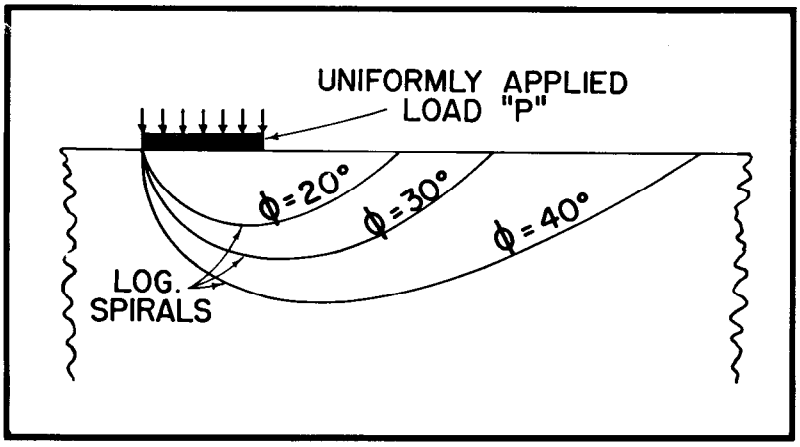

Fig. 4. Influence of Size of Angle of Internal Friction on the Position of the Log. Spiral Failure Curve.

Figure 4 demonstrates how the reaction moment increases with increasing angle of internal friction ϕ of the homogeneous soil being loaded to failure. The logarithmic spiral becomes longer as ϕ becomes greater. This increases both the weight moment and the cohesion moment, which together make up the total reaction moment. Figure 4 also illustrates very clearly how a weight moment is substituted for a friction moment ($n \tan\phi$) in the case of cohesionless soils.

In Figure 5, the increase in the ultimate strength q for a strip load 10 inches wide is illustrated as the angle of internal friction ϕ of a homogeneous cohesionless soil is increased. For highway and airport construction, reasonably well-compacted cohesionless

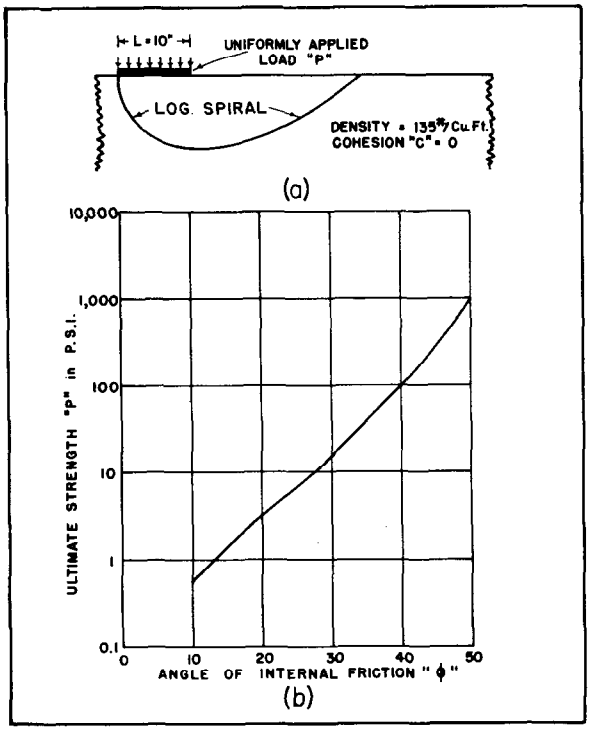

Fig. 5. Influence of Angle of Internal Friction On the Ultimate Strength of a Cohesionless Soil.

soils would have angles of internal friction normally ranging from about 30 to 50° or slightly higher. On the basis of a logarithmic spiral failure curve, and the other conditions illustrated in Figure 5(a), it is shown in the graph of Figure 5(b) that as the angle of internal friction ϕ changes from 30 to 50°, the ultimate strength q of a cohesionless soil increases from about 16 p.s.i. to about 1,000 p.s.i.

Figure 6 demonstrates the large increase in ultimate strength q that would be possible if the angle of internal friction ϕ of a soil were maintained constant at 35°, while its cohesion c was increased from 0 to 14 p.s.i. For the conditions illustrated in Figure 6(a), it is observed from the graph of Figure 6(b) that the ultimate strength q is increased from 37 p.s.i. when c = 0, to 342 p.s.i. when c = 5 p.s.i., to 883 p.s.i. when c = 14 p.s.i. Nijboer (31) has reported the results of some triaxial tests on a sand in both the dry and moist states. No difference in the angle of internal friction ϕ occurred between the moist and dry condition

in these tests. However, he found that the cementing or binding effect of the moisture films on the moist sand provided a value for cohesion c = 1.4 p.s.i. Of particular interest, therefore, is the increase in ultimate strength q from 37 p.s.i., when c = 0 and $\phi = 35^0$, to 125 p.s.i., when c = 1.4 p.s.i. and $\phi = 35^0$, shown in Figure 6(b). This is at least qualitatively in keeping with the large variation in the ultimate strength of beach sand between the moist and dry states that is a matter of common experience.

Roads through large areas of sand in Nebraska, Florida, and elsewhere, were unstable under traffic until stabilized by the addition of bituminous binders. Figure 6 explains very clearly why the incorporation of bituminous binders increased the bearing capacity of the sand in these cases. The cohesionless sand with its inherently low ultimate strength was converted to a material with much greater ultimate strength by the addition of bituminous cements that provided cohesion c.

Natural deposits of the good gravel aggregates required for stable base courses are becoming depleted. While large deposits of sands and inferior gravels are still readily available, their

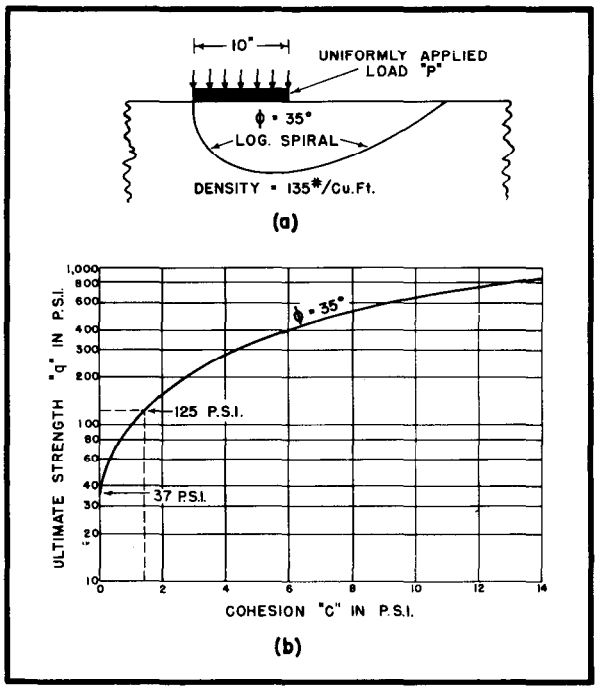

Fig. 6. Influence of Cohesion On Ultimate Strength.

stability is too low for service as base course materials, particularly for traffic on tires inflated to high pressures, which may cause failure within the base. Figure 6 demonstrates that by the use of a suitable binder the stability of these inferior aggregates could be increased to the extent required for good base course performance. For example, from a comparison of Figure 5(b) and 6(b), it is seen that if to an inferior aggregate with an angle of internal friction $\phi = 35^0$ a binder can be added to give a cohesion c = 1.0 p.s.i. without decreasing ϕ, its ultimate strength q becomes 100 p.s.i., Figure 6(b), which is the same as the ultimate strength of a cohesionless gravel for which $\phi = 40^0$, Figure 5(b). If to the material for which $\phi = 35^0$, the added binder gives cohesion c = 6 p.s.i. with no reduction in ϕ, its ultimate strength becomes 403 p.s.i., Figure 6(b), which is identical with the ultimate strength of a cohesionless gravel for which $\phi = 46^0$ 30', Figure 5(b). Similarly, for $\phi = 35^0$ and c = 14 p.s.i., Figure 6(b), the ultimate strength q = 883 p.s.i. is the same as that for a cohesionless gravel for which $\phi = 49^0 30'$, Figure 5(b). Therefore, it is possible by the addition of a suitable binder to a cohesionless sand or gravel of low stability to increase its shearing strength or stability to equal that of a cohesionless aggregate of high stability.

Similarly, by adding a suitable binder to increase the cohesion c of loam soils that already have a low cohesion c and an intermediate angle of internal friction ϕ, their ultimate strength q, or stability, can be increased to equal that of good cohesionless base course aggregates. Although it is probably not always clearly recognized, this is one of the objectives of the stabilization of both cohesive and cohesionless soils for base course construction.

It is highly significant that attempts at the stabilization of heavy clay soils with bituminous binders have not been successful so far. It is believed that failure in this respect is explained by Figure 8. The angle of internal friction ϕ of moist heavy clays encountered in the field is very low, and may frequently approach zero. Figure 8 shows that for a given ultimate strength requirement, if the angle of internal friction ϕ approaches zero, the cohesion c must be correspondingly high. With heavy clay soils at normal field moisture content, the required increase in cohesion c is difficult to obtain by the addition of bituminous binders, since the total liquid content tends to hold cohesion c to a relatively low value. Cohesion c would be expected to increase as the penetration of the bituminous binder was decreased. However, bituminous binders of low penetration would be difficult to

mix with fine textured heavy clay soils, particularly if moist, unless used in the form of cutbacks or emulsions. If the latter are employed, there is the further problem of aeration of the soil-bitumen mixture to a sufficient degree. The successful stabilization of heavy clay soils with bituminous binders would seem to require either drying the clay to a low moisture content, or employing some other mechanical or chemical treatment to increase its angle of internal friction to a value approaching 20 to 30° before the bituminous cement is added.

When adding binders to cohesionless soils (and even to cohesive soils), it must be kept in mind that many binders can function as lubricants as well as cements. When functioning as lubricants, they tend to reduce the angle of internal friction. The cementing action of many binders increases up to a certain binder content, after which the lubricating effect becomes predominant as more binder is added. When the lubricating effect becomes sufficiently pronounced, the decrease in the angle of internal friction ϕ may be large enough that the ultimate strength q may be lowered materially, even though the cohesion c may still be increasing. Figure 7 shows assumed values for ϕ and c for a cohesionless aggregate with an angle of internal friction $\phi = 40^0$, as a binder is added to it. The curve for ultimate strength q in

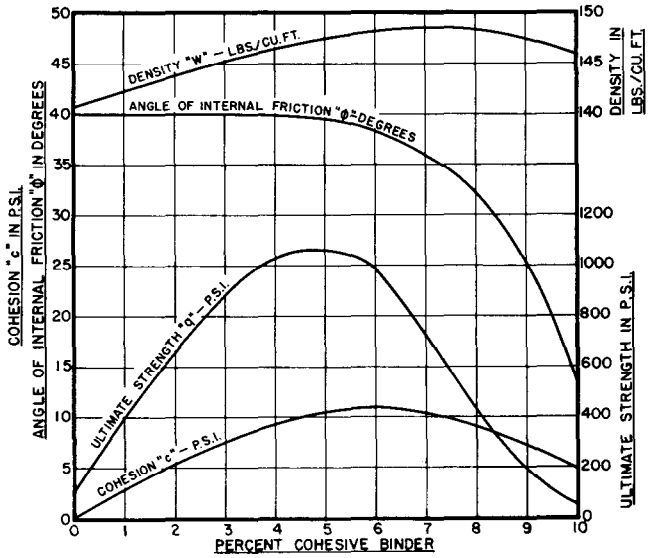

Fig. 7. Influence of the Addition of a Cohesive Binder On the Ultimate Strength of a Cohesionless Soil.

Figure 7 indicates that q increases to a maximum of 1,060 p.s.i. at a binder content of 4.8 per cent, after which it decreases as further binder is added. At a binder content of 10 per cent, the ultimate strength q is *less than that of cohesionless aggregate by itself.* Figure 7 emphasizes the need for careful investigation of the influence of any proposed binder on the ultimate strength or stability of a soil to determine that even small percentages of the binder do not decrease rather than increase the stability or ultimate bearing capacity of the soil.

Figures 6(b) and 7 demonstrate the increase in stability of relatively unstable cohesionless materials that may occur as a cohesive binder is added. They also imply that the stability of even a highly stable cohesionless base course aggregate can be further increased when necessary by the addition of a binder that will give cohesion c without materially decreasing its angle of internal friction ϕ.

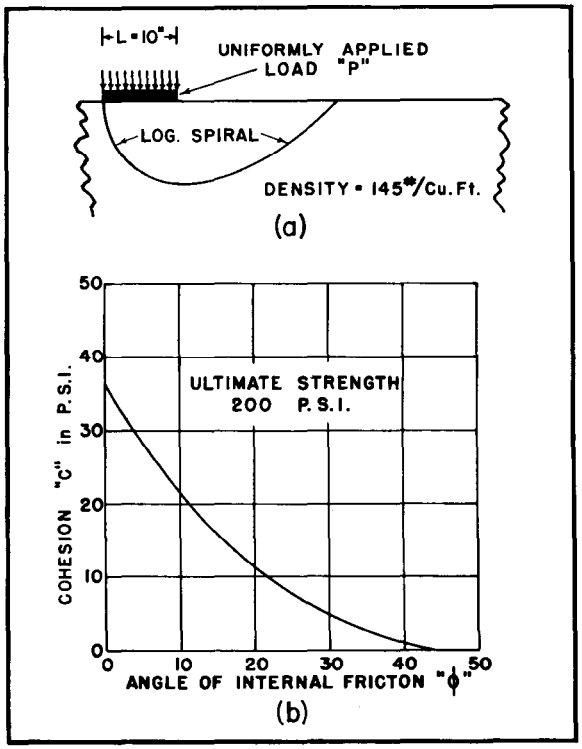

Fig. 8. Corresponding Values of "c" and "ϕ" Required to Provide An Ultimate Strength of 200 p.s.i.

Figure 8 illustrates the various combinations of values of c and ϕ for soil materials that are required for a constant ultimate strength q of 200 p.s.i. Figure 8 shows that soils for which c = 36.4 p.s.i. and $\phi = 0$, c = 21.5 p.s.i. and $\phi = 10^0$, c = 11 p.s.i. and $\phi = 20^0$, c = 5 p.s.i. and $\phi = 30^0$, c = 1 p.s.i. and $\phi = 40^0$, or c = 0 p.s.i. and $\phi = 44^0$, etc., would all have an ultimate strength of 200 p.s.i. Figure 8, therefore, demonstrates further the principle already implied in Figures 6 and 7, that a certain required ultimate strength or stability can be obtained by combining a low angle of internal friction ϕ with a high cohesion c, intermediate values of c and ϕ, or a high angle of internal friction ϕ with a low cohesion c.

Figures 4, 5, 6, 7, and 8 all refer to the ultimate strength of homogeneous soils as determined by means of the logarithmic spiral approach. It is realized that ultimate strength values for homogeneous soils can be determined by means of equations for bearing capacity that have been developed by other investigators. For comparative purposes, the ultimate strength values for homogeneous soils given by several of the better known equations for bearing capacity are listed in Table I.

Table I. Ultimate Bearing Capacity of Homogeneous Soils

Strip Loading
Width of Loaded Strip = 10 inches
Soil Density = 135 lbs. per cu. ft.

Bearing Capacity Formula	Ultimate Strength Values in p.s.i. when			
	c = 5 p.s.i. $\phi = 0$	c = 5 p.s.i. $\phi = 20^0$	c = 5 p.s.i. $\phi = 35^0$	c = 0 $\phi = 40^0$
Terzaghi-Hogentogler	20	45	94	8.5
Terzaghi	28.5	92	307	51
Prandtl	25.7	74	117	-
Fellenius	27.6	-	-	-
Logarithmic Spiral	27.6	90	338	101

From the data of Table I, it is apparent that the logarithmic spiral provides values for the ultimate strengths of cohesive soils (columns 2, 3, and 4 in Table I), that are similar to those given by some other bearing capacity equations. For cohesionless soils, on the other hand, the right hand column in Table I shows that the logarithmic spiral gives ultimate strength values which are considerably higher than those derived by other methods.

Davis and Woodward (25) report making over 100 bearing capacity tests on sands. Table II contains data taken from their paper, in which they compared the measured ultimate strength

of a sand with those calculated by means of several bearing capacity equations. In addition, an ultimate strength value calculated on the basis of the logarithmic spiral method employed for the present paper has been included.

Table II. Ultimate Bearing Capacity of Cohesionless Soil

Strip Loading
Loaded Strip 1 inch wide; 10 and 24 inches long
$c = 0$, $\phi = 36^0$
Density = 102 lbs. per cu. ft.

Bearing Capacity Formula	Ultimate Strength in p.s.i.
Actual Load Test (Davis and Woodward)	14 to 20
Terzaghi-Hogentogler	0.4
Terzaghi	1.5
Logarithmic Spiral	3.4

While Table II shows that all of the bearing capacity values calculated by means of the theoretical methods are several times less than that measured by the actual load test on this sand, the ultimate strength calculated by the logarithmic spiral approach comes closest to the measured value. On this basis, it might be concluded that the logarithmic spiral gives an ultimate strength value for the cohesionless soil ($\phi = 40^0$) in Table I, that is only less conservative than those of the other methods. However, in spite of the fact that the logarithmic spiral method gives best agreement with the measured bearing capacity value in Table II, it should be mentioned that other investigators have reported good checks between measured values of the ultimate strength of cohesionless soils and those calculated by other bearing capacity formulae, such as Terzaghi's. It is generally agreed that we still have a great deal to learn about the bearing capacity of soils, and this is emphasized by the variations in the data of Tables I and II.

Table III indicates that the large difference between the ultimate strength value measured by Davis and Woodward for a sand understood to be cohesionless, and the values calculated by several theoretical bearing capacity equations, Table II, might possibly be due at least in part to the existence of a very small quantity of cohesion c in the sand. For the strip loading width of 1 inch, which they used for the data of Table II, the information in the second and third columns on the left of Table III indicates that on the basis of the logarithmic spiral method the calculated ultimate strength would be 3.43 p.s.i. if $c = 0$, and 14.3 p.s.i. if $c = 0.15$ p.s.i. Consequently, an actual existence of

Table III. Influence of Width of Loaded Area and of Small Values of Cohesion c on the Ultimate Strength of a Cohesionless Soil When Calculated by the Logarithmic Spiral Method

Strip Loading
Width of Loaded Area = L = 1 inch and 10 inches
Density of Sand = 102 lbs. per cubic foot
Angle of Internal Friction $\phi = 36^{\circ}$

	When L = 1.0 inch			When L = 10 inches	
	Cohesion c in p.s.i.				
	c = 0	c = 0.15	c = 1	c = 0	c = 1
Ultimate Strength in psi.	3.43	14.3	74	34.3	107.8

cohesion c = 0.15 p.s.i. in the sand with which Davis and Woodward were working would account for the entire difference between their measured value of ultimate strength, 14 p.s.i., and the value of 3.43 p.s.i. calculated by the logarithmic spiral method on the assumption that the sand was entirely cohesionless. A cohesion c = 0.15 p.s.i. is so small that it is within the range of experimental error for most triaxial or direct shear tests and would ordinarily be overlooked or disregarded. It should be recognized that this small value of cohesion c = 0.15 p.s.i. would not necessarily be due to the presence of a binder. Any characteristic of the sand that would lead to the existence of this small intercept on the ordinate axis of the Mohr or Coulomb diagram (the shear strength value at zero normal stress on the plane of failure commonly called cohesion c) would give the large increase in the ultimate strength of the sand that has been listed in Table III. While this small cohesion c, if it actually existed in the sand used by Davis and Woodward, may have been due to some characteristic other than moisture, it might be mentioned that small quantities of adsorbed moisture can influence the physical properties of sand. This has been pointed out by investigators (32) who have endeavoured to standarize a given sand for use in the sand method for controlling the compaction of soils in the field. Moisture contents as low as 0.25 per cent have been reported to affect the density of a calibrated sand (passing No. 40, retained No. 60 sieve) by as much as 5 pounds per cubic foot (32).

Table III also demonstrates that the existence of small values of cohesion c in a sand thought to be cohesionless has a much greater influence on ultimate strength values calculated by the logarithmic spiral method for very narrow than for wide strip

loads. When the width of the loaded strip is only 1 inch, a value for cohesion c = 1.0 p.s.i. increases the ultimate strength from 3.43 p.s.i. (for c = 0), to 74 p.s.i., which is 21.6 times as large. On the other hand, for a strip load 10 inches wide, a cohesion c = 1.0 p.s.i. increases the ultimate strength from 34.3 p.s.i. (for c = 0), to 107.8 p.s.i., which is only 3.1 times as large. The possibility for unusual results due to unsuspected characteristics of a cohesionless material is, therefore, much greater for very small than for large loaded areas.

It has been shown in Table III that an unsuspected very small value for cohesion c might account for the large difference observed by Davis and Woodward (25) between calculated and their actually measured values of the ultimate strength of the cohesionless sand with which they were working. This difference might also be explained by an increase in density throughout the volume of sand influenced by the applied load, since an increase in the density of the sand would be expected to increase its angle of internal friction. Consequently, both the density and angle of internal friction of the sand might have been greater throughout the volume of sand under stress than tests made on the sand in bulk had indicated. It can be calculated by the logarithmic spiral method that, if due to an increase in density, the angle of internal friction throughout the stressed volume of sand were increased to about 44° from the 36° actually reported, this would account for the entire difference between the ultimate strength of 3.4 p.s.i. calculated by the logarithmic spiral method described in this paper, and the ultimate strength of 14.3 p.s.i. (14 to 20 p.s.i.) actually measured by Davis and Woodward (25), since the ultimate strength calculated by the logarithmic spiral method for a cohesionless sand with an angle of internal friction of about 44° is 14.3 p.s.i., but is only 3.4 p.s.i. for similar sand with an angle of internal friction of 36°. Consequently, for the cohesionless sand with which Davis and Woodward were working, the difference between calculated and their measured values of ultimate strength noted in Tables II and III might be explained by the presence of an unsuspected small value of cohesion c, by an increase in the angle of internal friction ϕ during the test itself, or it could be due to the existence of unknown factors that are overlooked in the theoretical methods of calculation, or to the fundamental inability of the theoretical methods to calculate ultimate strength values equal to those actually measured.

It is instructive that Davis and Woodward (25) report that the shape of the failure surface observed in their bearing capacity tests is a logarithmic spiral.

THE ULTIMATE STRENGTH OF A TWO-LAYER SYSTEM

So far the logarithmic spiral method has been applied to the determination of the ultimate strength of homogeneous soils. In this section an attempt will be made to apply this method to the determination of the ultimate bearing capacity of a two-layer system consisting of a bituminous surface resting on a great thickness of base course. This pertains to the condition where the critical logarithmic spiral failure surface along which shear failure is assumed to occur is located entirely within the base and surface course. This situation is not uncommon, since great thicknesses of granular base are sometimes used for both airport and highway construction. For this case, the base course, including sub-base, is considered to be so thick that the tendency for failure within the base and surface is much greater than within the subgrade.

Figure 9 considers the case of a bituminous pavement 2 inches thick for which c = 10 p.s.i. and $\phi = 40^0$, resting on a great depth of base of cohesionless material. The ultimate strength of the combined base and surface are to be investigated as the angle of internal friction of the base course is varied from 30^0 to 40^0, 50^0, and 60^0.

The principal problem in connection with Figure 9, insofar as this paper is concerned, is how the critical logarithmic spiral failure curve is to be located through the two layers (surface and base), each with quite different c and ϕ values. The approach to this problem employed in this paper is illustrated in Appendix B, but in essence it involves the determination of c and ϕ values for an equivalent homogeneous material having the same ultimate strength as the layered system of the flexible pavement. The ultimate strength of this equivalent homogeneous material can then be calculated on the basis of a logarithmic spiral failure surface, as described earlier in the paper, and illustrated in Appendix A. The entire procedure requires a trial and error approach involving the use of successive approximations, and consists of the following steps, which, by way of example, are based on the conditions of Figure 9(a) with $\phi = 45^0$ for the base:

1. As the first step, c and ϕ values must be assumed for the equivalent homogeneous material that is to have the same ultimate strength as the layered system of Figure 9. With more experience, it may be possible to assume a set of c and ϕ values in this first step that are not greatly different from the ultimate values determined at the end of the successive approximation procedure. This may shorten the number of

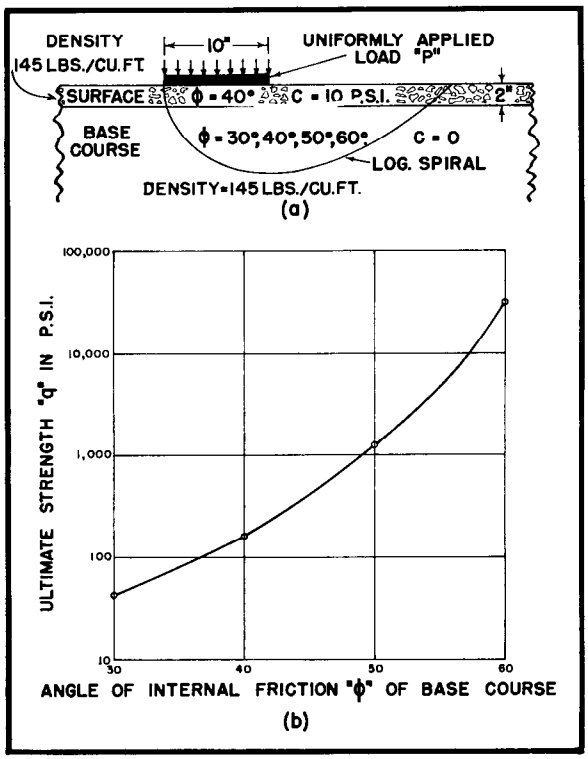

Fig. 9. Influence of Size of Angle of Internal Friction On the Ultimate Strength of a Flexible Pavement.

trials required. As indicated by the set of sample calculations for this particular example in Appendix B, however, the c and ϕ values selected for the first trial were those of the cohesionless base course itself (c = 0 p.s.i., $\phi = 45^0$). For the first trial, therefore, the c and ϕ values assumed for the hypothetical homogeneous material that is to be equivalent in strength to the two-layer system of Figure 9(a) were c = 0 p.s.i. and $\phi = 45^0$.

2. Determine the critical logarithmic spiral for a homogeneous material for which c = 0 p.s.i. and $\phi = 45^0$, by the method outlined in an earlier part of this paper and illustrated in Appendix A. Calculate the ultimate strength q for this material, which is found to be 318.5 p.s.i. (Appendix B).
3. Calculate the complete length of this spiral within the base and surface, and also the exact length of each of the two portions of the spiral that lie entirely within the surface course.

4. Using the length of the spiral within the surface course where $\phi = 40^0$, and the length of the spiral within the base course where $\phi = 45^0$, calculate an overall arithmetic average value for ϕ for the entire length of the spiral within the base and surface. This gives a value for $\phi = 44^0 48'$ (Appendix B).
5. Find an overall average value for cohesion c for the entire length of spiral within the base and surface, on the basis that c = 10 p.s.i. for the surface course, but is zero for the base course. This can be done in either of two ways. First, by spreading the cohesion c = 10 p.s.i. for the part of the spiral within the bituminous surface over the entire length of the spiral as an arithmetic average; that is, the part of the length of the spiral entirely within the bituminous surface multiplied by cohesion c = 10 p.s.i., must be equal to the total length of the spiral within the base and surface multiplied by this overall average value for c. Second, by equating the sum of the cohesion moments for the two parts of the spiral entirely within the surface course, to the cohesion moment for the entire spiral within the base and surface resulting from the use of an overall average value for cohesion c. The limited number of calculations made to date indicate that a lower value for cohesion c may always result from the use of the first method. It might be generally favoured, therefore, since a lower value for c results in a more conservative value for ultimate strength. For the present paper, the data for the various diagrams have been calculated partly by one method, and in part by the other. On the basis of the first method, the overall average value of cohesion c for the first trial spiral is c = 0.404 p.s.i. (Appendix B).
6. For the second trial (approximation), determine the critical logarithmic spiral for a homogeneous material for which c = 0.404 p.s.i. and $\phi = 44^0 48'$. Calculate the ultimate strength q for this material, which is found to be 383.2 p.s.i.
7. Repeat steps 3, 4, and 5, on the basis of this second logarithmic spiral and obtain average values for c and ϕ to be used for the third approximation. The new average values found for c and ϕ are c = 0.401 p.s.i. and $\phi = 44^0 48'$ (Appendix B).
8. For the third trial (approximation), determine the critical logarithmic spiral for a homogeneous material for which c = 0.401 p.s.i. and $\phi = 44^0 48'$ (Appendix B). For this spiral the calculated ultimate strength q = 382.8 p.s.i.
9. Repeat for as many trials as are necessary to reduce the difference between the ultimate strength values for two successive approximations to an acceptable percentage.

Table IV summarizes the c, ϕ, and ultimate strength q values for each of three trial critical logarithmic spirals resulting from these successive approximations. It will be observed that the ultimate strength values for succeeding approximations are alternately on one side of the final value that would result from many successive approximations and then on the other, Figure 21, with the differences between successive approximations gradually becoming smaller. The difference in ultimate strength q between the second and third successive approximations is only 0.1 per cent. Consequently, in this case the second successive approximation provides a value for ultimate strength q that would usually be sufficiently accurate for practical design.

On the basis of this logarithmic spiral approach, therefore, the ultimate strength of the layered system of Figure 9(a) in which a 2-inch bituminous surface, for which c = 10 p.s.i. and $\phi = 40^0$, is placed on a great depth of cohesionless base course for which $\phi = 45^0$, is considered to be equal to the ultimate strength, q = 382.8 p.s.i., of a homogeneous material for which c = 0.401 p.s.i. and $\phi = 44^0 48'$ (third successive approximation in Table IV).

Table IV. Ultimate Strength of Two-Layer System

For Surface Course c = 10 p.s.i., $\phi = 40^0$
For Base Course c = 0 p.s.i., $\phi = 45^0$
Thickness of Surface Course = 2 inches
Density of Base and Surface Course = 145 lbs./cu. ft. = 0.839 lbs./cu. in.
Values of c, ϕ, and q for Successive Trials
Strip Loading
Width of Loaded Strip = L = 10 inches

Successive Approximation No.	Cohesion c p.s.i.	Angle of Internal Friction ϕ	Ultimate Strength q p.s.i.
1	0	45^0	318.5
2	0.404	$44^0 48'$	383.2
3	0.401	$44^0 48'$	382.8

The ultimate strength value, q = 382.8 p.s.i., for successive approximation No. 3 in Table IV for a layered system consisting of a two-inch bituminous surface for which c = 10 p.s.i. and $\phi = 40^0$ on a great depth of cohesionless base for which $\phi = 45^0$ can be read with reasonable accuracy from the graph in Figure 9(b). This graph indicates that the ultimate strength of the layered system illustrated in Figure 9(a) increases rapidly as the angle of internal friction ϕ of the base course is increased from 30^0 to 40^0 to 50^0. The layered system of Figure 9(a), for

which the angle of internal friction ϕ of the base course is 60°, is probably of little more than academic interest insofar as normal aggregates are concerned, since its ultimate strength, q = 30,000 p.s.i., is far above the crushing strength of the grains and could not be attained in practice.

Figure 9 emphasizes the increase in resistance to failure along shear surfaces entirely within the base and bituminous surfacing that results from increasing the angle of internal friction ϕ of a great depth of cohesionless base course material beneath a given bituminous surface.

It is instructive to compare Figure 9 with Figure 5 since both pertain to systems in which the angle of internal friction ϕ of a great depth of cohesionless base course material is varied. Figure 9 differs from Figure 5 only in that a two-inch bituminous surface, for which c = 10 p.s.i. and ϕ = 40° has been substituted in Figure 9 for the top two inches of the base course in Figure 5. For ϕ = 50° in the base course, the bituminous surface in Figure 9 has the effect of decreasing ϕ from 50° to 40° in the top two inches of Figure 5, but at the same time introduces cohesion c = 10 p.s.i. into this layer. Nevertheless, Figures 5(b) and 9(b) show that when the base course has an angle of internal friction ϕ = 50°, the single-layer system of Figure 5 and the two-layer system of Figure 9 both have an ultimate strength of about 1,000 p.s.i. Consequently, introducing a cohesion c = 10 p.s.i. into the top 2 inches of Figure 9(a) just balances the effect of decreasing ϕ from 50° to 40° in this layer, insofar as ultimate strength is concerned. When the base course has an angle of internal friction ϕ = 40° in both cases, the ultimate strength of the single layer system of Figure 5 is 105 p.s.i., while that of the two-layer system of Figure 9 is 160 p.s.i., an increase of about 52 per cent. In this case, since the angle of internal friction ϕ is the same for both systems, the increase in ultimate strength is due entirely to the cohesion c of the two-inch bituminous surface of Figure 9. For the case where the base course has an angle of internal friction ϕ = 30°, the ultimate strength increases from 16 p.s.i. in Figure 5 to 42 p.s.i. in Figure 9, an increase of about one hundred and sixty per cent. This increase is due partly to increasing ϕ from 30° to 40° in the top 2 inches, and partly to the introduction of cohesion c = 10 p.s.i. into this two-inch layer. The small difference in density, 135 pounds per cubic foot for Figure 5, and 145 pounds per cubic foot for Figure 9, does not appreciably affect the comparison that has been made. This comparison between Figure 5 and Figure 9 illustrates the important effect

that the introduction of cohesion c into even a part of a layered system has on its ultimate strength.

Figure 10 illustrates the increase in ultimate strength of a layered system consisting of a bituminous surface on a great thickness of a given cohesionless base course for which $\phi = 40^0$, as the thickness of a bituminous surface is increased from 0 to 6 inches. Two graphs are shown in Figure 10(b). The upper graph, labelled "Full Cohesion," assumes full development of the cohesion of the bituminous surface at both ends of the

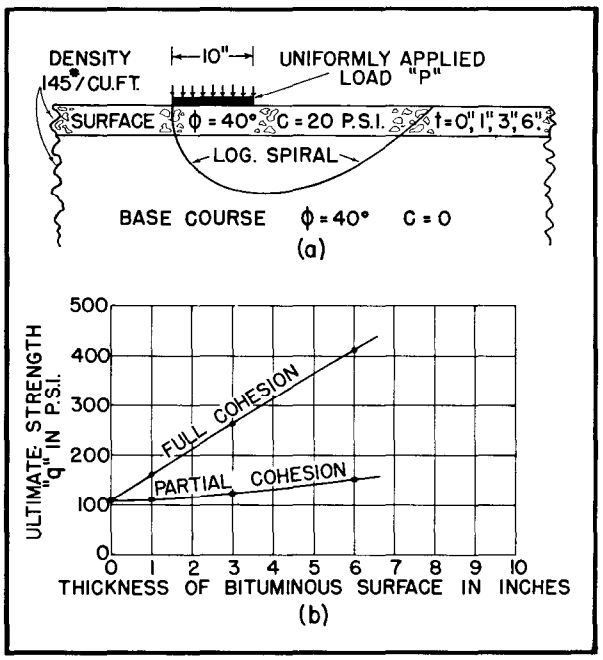

Fig. 10. Influence of Bituminous Pavement Thickness On the Ultimate Strength of a Flexible Pavement.

logarithmic spiral. The graph labelled "Partial Cohesion" is based on the possibility that the structure might have failed before any of the cohesion of the bituminous surface along the right hand side of the spiral has been mobilized. In this latter case, it is assumed that only the cohesion of the bituminous surface traversed by the left hand side of the spiral of Figure 10(a) is fully developed; that is, the portion of the spiral just under the left hand extremity of the loaded area.

Figure 10(b) indicates that if the cohesion of the bituminous surface is fully mobilized where it is traversed by both ends of the spiral, the ultimate strength of the layered system of Figure 10(a) increases from 105 p.s.i. for zero thickness of bituminous surface, to 260 p.s.i. for 3 inches, to 410 p.s.i. for 6 inches of bituminous surface.

On the other hand, if the cohesion of the bituminous pavement is developed only where it is cut by the left hand side of the logarithmic spiral, the graph of Figure 10(b) labelled "Partial Cohesion" shows that the ultimate strength of this layered system increased from 105 p.s.i. for zero thickness of bituminous surface, to 120 p.s.i. for a thickness of 3 inches, to 160 p.s.i. for a 6-inch thickness of bituminous surface.

Experimental data are required to determine which of the curves of Figure 10(b), or whether some other relationship, applies in actual practice. Nevertheless, when the base course itself is not highly stable, Figure 10 indicates that a greater thickness of well designed and constructed bituminous surface of good stability may increase the overall resistance of the base and surface to shearing failure under high tire pressures.

It should be particularly noted in Figure 10 that the angle of internal friction for both the base and surface course is exactly the same, $\phi = 40^0$. This selection was made deliberately to demonstrate that the increase in ultimate strength with increase in surface thickness is due entirely to the introduction of cohesion c into the two-layer system by means of the bituminous binder of the surface course. Consequently, Figure 10 provides further evidence of the important influence that the presence of cohesion c in the surface course, in the base course, or in both, can have on the ultimate strength of a two-layer system.

It should be emphasized that the ultimate strength values that have been given in this section pertain only to resistance to failure along shear surfaces that lie entirely within the base and surface.

SQUEEZING FAILURE OF BITUMINOUS SURFACE BETWEEN TIRE AND BASE

Figure 11 demonstrates the possibility of another type of flexible pavement failure that must always be investigated, particularly where high tire inflation pressures are involved.

Figure 11(a) shows that a great thickness of cohesionless aggregate, for which $\phi = 47^0$ and $c = 0$, has an ultimate strength of 467 p.s.i. Figure 11(b) indicates an ultimate strength of

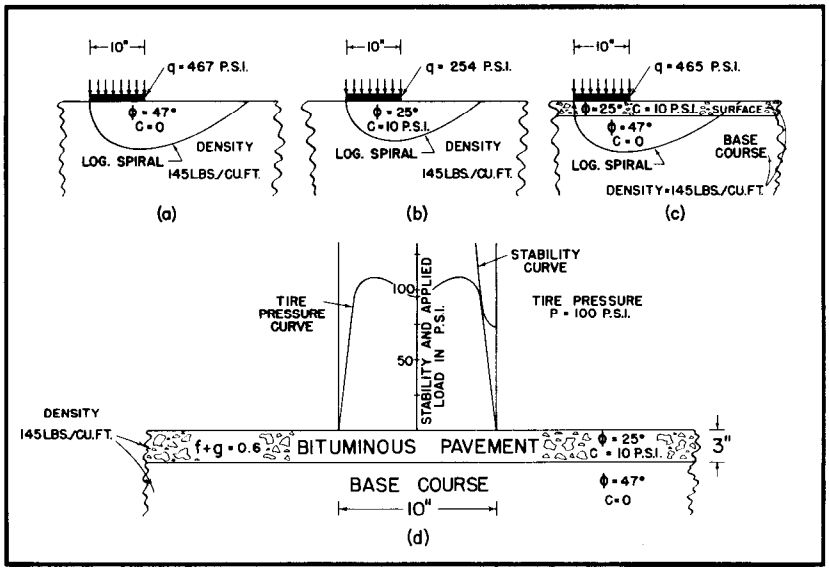

Fig. 11. Illustrating Failure Criteria For Flexible Pavements.

254 p.s.i. for a great thickness of bituminous surfacing material for which c = 10 p.s.i. and $\phi = 25^0$. Combining these materials in the two-layered flexible pavement structure illustrated in Figure 11(c) results in an ultimate strength of 465 p.s.i., when the ultimate strength is calculated by means of the logarithmic spiral method.

However, Figure 11(d) demonstrates the effect of investigating the stability of the layered system of Figure 11(c) on an entirely different basis. The possibility of failure of the bituminous surface by squeezing out between the tire and base course is examined by a method described in detail elsewhere (10, 11, 12, 13, 14, and 15). The results of this investigation are illustrated in Figure 11(d). For the shape of the tire pressure distribution curve and other conditions shown in Figure 11(d), these results indicate that under any tire inflation pressure greater than about 100 p.s.i. this particular bituminous surface (c = 10 p.s.i., $\phi = 25^0$) would fail by being squeezed out between the tires and the base course, since some portion of the tire pressure distribution curve would be above the pavement stability curve; that is, the applied pressure on some part of the bituminous surface would exceed its stability. Consequently, in this case the ultimate strength of the layered system is not 465 p.s.i. as given by the

logarithmic spiral method, Figure 11(c), but is about 100 p.s.i., Figure 11(d), as given by the investigation of its resistance to being squeezed out between the tire and base course. If the conditions of design require a higher unit load than 100 p.s.i. to be carried, Figure 11 indicates that a bituminous pavement having a higher stability against failure by squeezing action than that illustrated ($c = 10$ p.s.i. and $\phi = 25^\circ$) must be selected.

The data shown in Figure 11 demonstrate the necessity for applying the three criteria outlined at the beginning of this paper to every flexible pavement design problem.

1. Sufficient thickness to prevent subgrade failure.
2. Adequate shear strength in the layers close to the loaded area to avoid failure along shear surfaces entirely within the base and surface.
3. Examination of the stability of each layer against failure by squeezing action.

It is obvious that a different ultimate strength rating will usually be given by each of these three criteria, and that flexible pavement design in general should be guided and controlled by the ultimate strength value that is most critical.

FLEXIBLE PAVEMENT DESIGN IN GENERAL

From the general shape of a logarithmic spiral curve, it is apparent that the lowest point of the critical spiral may be located at an appreciable depth below the loaded area on the pavement surface. For the corresponding wheel loads, tire pressures, and pavement thicknesses recommended by design methods, or by charts of design curves, developed by the Canadian Department of Transport (2, 3, 4, 5, and 6), the U.S. Corps of Engineers (8), and others (1, 7, and 9), it has been found that the critical logarithmic spiral will usually penetrate well into the subgrade. Consequently, for ordinary flexible pavement design requirements, the critical logarithmic spiral intersects the surface course, base course, and subgrade. This means that the ultimate strength method based on the critical logarithmic spiral failure surface already described can be applied to flexible pavement design in general.

In this case, the problem consists essentially of determining c and ϕ values for an equivalent homogeneous material that will have the same ultimate strength as that of the three layer system of Figure 12, subgrade, base and surface, comprised of three different materials, each with its own c and ϕ values. On the

basis of these overall c and ϕ values for the equivalent homogeneous material, the critical logarithmic spiral failure curve can be established, from which the ultimate strength of the three-layer system is then calculated. The procedure is similar to that already outlined for a two-layer system. It is described in Appendix C.

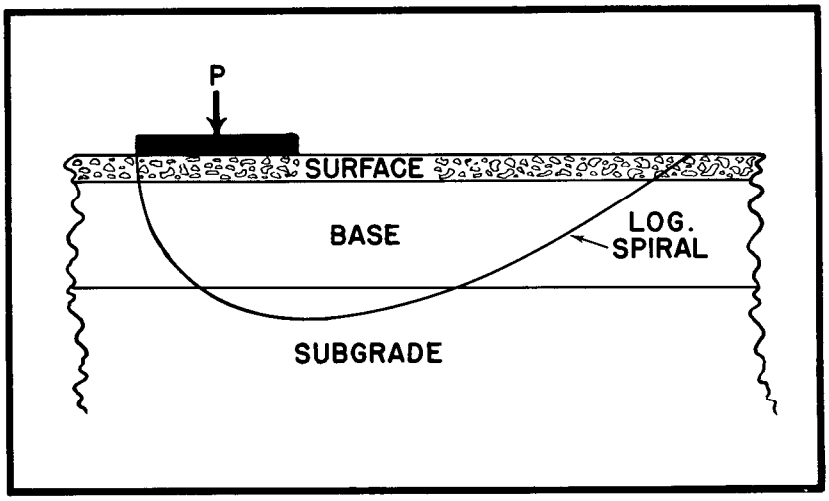

Fig. 12. Flexible Pavement Thickness Design.

In Table V, ultimate strength values are given for a three layer system of bituminous surface, base course, and subgrade, each having the c and ϕ values and the thicknesses listed. Three strip loading widths were employed, 10, 12, and 22 inches. For each strip loading width, the only variable is the value of cohesion c of the base course, every other factor being held constant. The data in column 5 demonstrate that the logarithmic spiral has penetrated well into the subgrade in each case, since its maximum depth of penetration "z" considerably exceeds the combined thicknesses of surface and base. Other investigators have indicated that the ultimate strength for a circular bearing area is from 20 to 30 per cent larger than for a strip load of the same width (29, 30). Since it is usual to base airport and highway pavement design on circular contact areas, ultimate strength values for circular bearing areas are shown in the right-hand column of Table V, and were obtained by increasing the ultimate strengths for strip loading by 25 per cent.

Table V. Ultimate Strength of Flexible Pavement

Surface Course c = 10 p.s.i., $\phi = 40^0$
Base Course c = Variable, $\phi = 45^0$
Subgrade c = 8 p.s.i., $\phi = 10^0$
Strip Loading

Width of Loaded Strip Inches	Thickness of Bituminous Surface Inches	Thickness of Base Course Inches	Total Thickness Base and Surface Inches	Depth of Penetration of Critical Logarithmic Spiral Below Surface "z" Inches	Ultimate Strength	
					Strip Loading p.s.i.	Circular Bearing Area p.s.i.
		When c = 0 for Base Course				
10	2	6	8	13	134	167
12	3	11	14	18.5	173	216
22	3	17	20	29.5	145	182
		When c = 1 p.s.i. for Base Course				
10	2	6	8	13.2	141	176
12	3	11	14	18.4	184	230
22	3	17	20	29.6	152	190
		When c = 5 p.s.i. for Base Course				
10	2	6	8	13.2	167	209
12	3	11	14	18.3	235	294
22	3	17	20	29.6	183	229

The data of Table V demonstrate that for the otherwise constant conditions listed for each of the three loaded widths, the ultimate strength of the flexible pavement structure increases as the cohesion c value of the base course is increased from 0 to 1 to 5 p.s.i. The effect on the ultimate strength is small when the cohesion c of the base course is changed from 0 to 1 p.s.i., but the ultimate strength is increased by from 25 to 35 per cent when the cohesion c of the base is increased from 0 to 5 p.s.i. (for the cases covered by Table V). For example, for the flexible pavement conditions illustrated by Figure 13, if all other factors are kept constant, the incorporation of a binder into the base course to change its cohesion c from zero to 5 p.s.i. would increase the ultimate strength of this particular flexible pavement structure from 216 p.s.i. (when c = 0) to 294 p.s.i. (when c = 5 p.s.i.). This represents an increase of 36 per cent in ultimate strength.

Consequently, on the basis of the logarithmic spiral method described in this paper, Figure 13 and the data of Table V emphasize again that increasing the cohesion c of any one layer of the flexible pavement structure within the logarithmic spiral, without sacrificing angle of internal friction ϕ, results in an important overall increase in the ultimate strength of the structure.

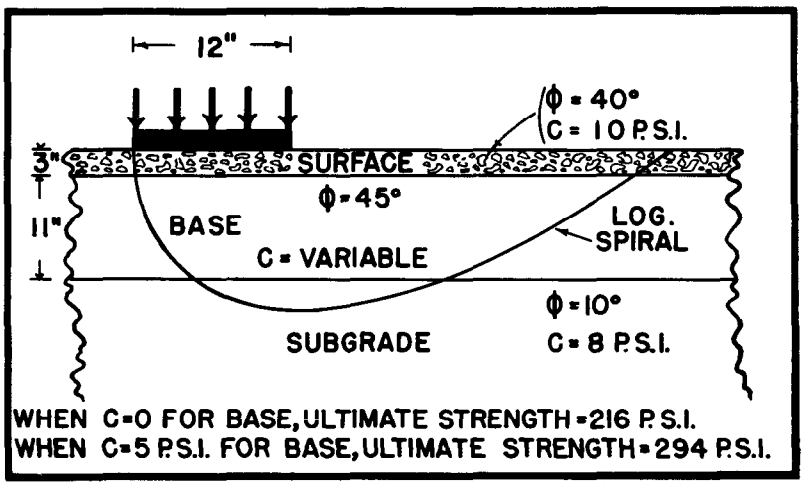

Fig. 13. Influence of Magnitude of Base Course Cohesion On Ultimate Strength of a Flexible Pavement.

Influence of Base Course Quality
On Flexible Pavement Thickness Requirements

Figures 14(a) and 14(b) indicate the considerable reduction in flexible pavement thickness required to develop a specified ultimate strength q = 112 p.s.i., as the angle of internal friction ϕ of cohesionless base course material is increased from 40° to 50°; that is, as the shearing strength of the base course is increased. It should be emphasized in connection with Figure 14 that every factor is maintained constant except the shearing strength and thickness of the base course.

Figure 14(b) demonstrates that as the angle of internal friction ϕ of the base course is increased from 40° to 50°, the required thickness of cohesionless base can be decreased from 12 to 7.2 inches, the developed ultimate strength for the three layer flexible pavement system being 112 p.s.i. in all cases. This represents a reduction in base course thickness of 40 per cent.

The results illustrated in Figure 14(b) seem reasonable, since it would ordinarily be expected that for a given overall ultimate strength requirement the thickness of base course could be decreased as its quality (shearing strength) is increased. On the other hand, actual field tests by the Canadian Department of Transport and the U.S. Corps of Engineers tend to indicate that flexible pavement thickness requirements are independent of the

quality of the base course material. For example, the Corps of Engineers permits no reduction in thickness if high quality base course material is employed for the full depth of base and sub-base, in place of materials ranging from lower quality at the bottom of the sub-base to highest quality in the top layer of the base.

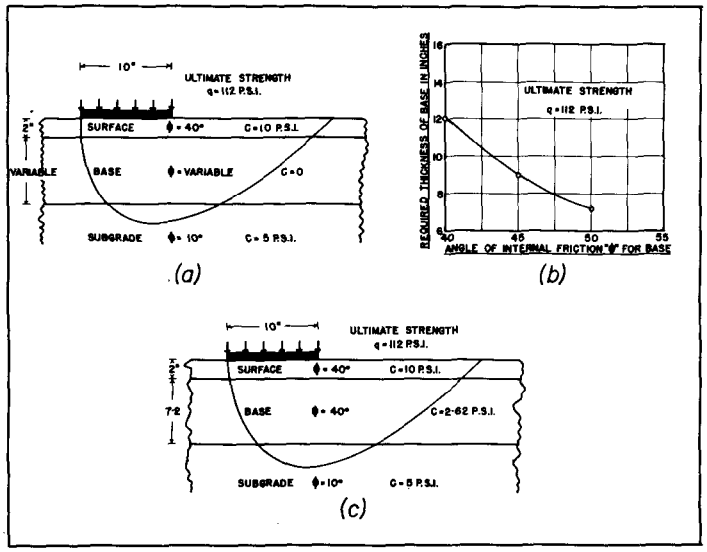

Fig. 14. Influence of Base Course Strength Characteristics On Base Course Thickness Requirements.

How are the results illustrated in Figure 14(b), indicating that higher base course quality permits a considerable reduction in flexible pavement thickness, to be reconciled with the findings of the Corps of Engineers and Canadian Department of Transport based on full scale field tests, that no reduction in thickness can be permitted even when highest quality base course material is employed for the full depth of sub-base and base? This divergence between theory and practice would be explained if, as seems probable, current construction methods are unable to develop *in the field* the large difference in the angles of internal friction of various base course materials that can be easily demonstrated by laboratory tests. Base course materials with high angles of internal friction ϕ usually consist of crushed angular particles with rough faces. These resist compaction to high density under the amount and type of compaction ordinarily

provided in the field. On the other hand, granular materials having a lower angle of internal friction ϕ, e.g. crusher run gravels, are composed of more rounded particles with smoother surfaces. These compact to relatively high density under the usual compactive effort applied during construction. For the usual base course materials ranging from crusher run gravel to crushed stone, it is not unlikely, therefore, that *the effective angle of internal friction* ϕ developed at the end of base course compaction in the field is not greatly different whether the base course materials show quite high or considerably lower angles of internal friction ϕ in laboratory tests. If this explanation is correct, because of inadequate compaction equipment or procedure, a base course aggregate developing an angle of internal friction ϕ of 50^0 in a laboratory test may have an effective angle of internal friction ϕ of only 45^0 or less after compaction into a base course in the field. Consequently, before the much smaller thicknesses of base course materials with high angles of internal friction, indicated by Figure 14(b) to be theoretically possible, can be utilized with confidence in flexible pavement design, compaction equipment and compaction procedures must be developed that will provide in the finished base course in the field the same high angles of internal friction shown by laboratory tests.

Figures 14(a) and 14(b) pertain to cohesionless base course materials. Figure 14(b) demonstrates that if the angle of internal friction ϕ of a cohesionless base course material is 40^0, a base course thickness of 12 inches is required for the conditions illustrated by Figure 14(a). However, this thickness of base is reduced to 7.2 inches if base course material with an angle of internal friction $\phi = 50^0$ is employed. Figure 14(c) indicates the effect of adding a binder to develop cohesion c in the base course material for which $\phi = 40^0$. When c = 2.62 p.s.i. and $\phi = 40^0$, only 7.2 inches of base course are again needed for an ultimate strength of 112 p.s.i. Consequently, for the conditions illustrated by Figure 14, a bituminous bound base course 7.2 inches thick for which $\phi = 40^0$ and c = 2.62 p.s.i. develops the same ultimate strength, 112 p.s.i., in the flexible pavement structure as a whole, as the identical thickness of cohesionless granular material having an angle of internal friction of 50^0. In this case, the introduction of cohesion c = 2.62 p.s.i. into a cohesionless material for which $\phi = 40^0$ confers on it the same strength as that developed by a cohesionless material for which $\phi = 50^0$. This illustrates again the important effect that the introduction or existence of cohesion c in any layer seems to have on the ultimate strength of a flexible pavement.

Base course materials of very high shearing strength (high angles of internal friction ϕ for cohesionless aggregates) are required in flexible pavements for jet aircraft for which tire pressures may be 200 p.s.i., 300 p.s.i., or higher. In many areas such high quality cohesionless base course materials are not locally available. Figure 14 demonstrates that in this case base courses of high shearing strength could be obtained by combining aggregates having relatively low angles of internal friction ϕ with bituminous or similar binders to provide the magnitude of cohesion c required for high stability. Practical verification of the soundness of this solution is provided by the extraordinary strength of sand-asphalt base and surface courses as compared with the instability or lack of strength of the dune, beach, etc. sands from which they are frequently made. As previously mentioned, this principle has been successfully employed for the construction of sand asphalt surfaced roads and airports in Nebraska (33), Florida (34), and elsewhere (35).

Influence of Bituminous Surface Thickness
On the Ultimate Strength of a Flexible Pavement

A problem sometimes debated by highway and airport engineers is whether or not increasing the thickness of the bituminous surface itself substantially increases the overall strength of a flexible pavement. Either curve of Figure 15, based on the ultimate strength approach described in this paper, indicates that the overall strength of a flexible pavement may be greatly increased by increasing the thickness of the bituminous surface. Like Figure 10, the "full cohesion" curve of Figure 15 assumes complete mobilization of the cohesion c of each layer throughout the full length of the spiral, while the "partial cohesion" curve neglects cohesion c of the bituminous surface along the extremity of the spiral remote from the loaded area. The strength increase is from 134 p.s.i. for zero thickness to 203 p.s.i. and 255 p.s.i. for the "partial cohesion" and "full cohesion" curves, respectively, for a surface thickness of 6 inches, representing strength gains of 51 and 90 per cent. Evidence will be presented later indicating that the "full cohesion" curve may more nearly represent the ultimate strength of a flexible pavement developed under field conditions than the "partial cohesion" curve.

The increase in overall flexible pavement strength with increase in surface thickness illustrated in Figure 15 is only possible when the bituminous surface course is sufficiently stable within itself at each thickness to resist squeezing failure between

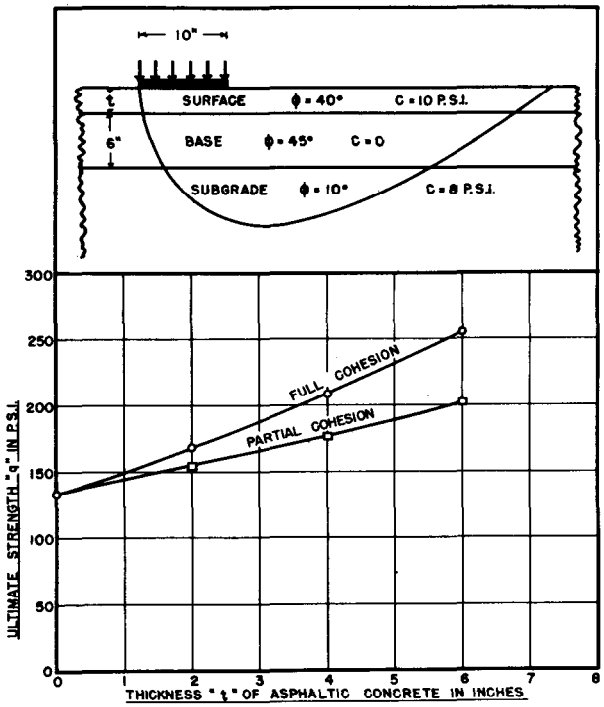

Fig. 15. Influence of Thickness of Asphalt Surface On the Ultimate Strength of a Flexible Pavement.

tire and base course under some lower applied load, as previously pointed out in connection with Figure 11.

Figure 15 demonstrates that overlays of well-designed bituminous concrete can be very effective for increasing the ultimate strength of flexible pavements that are beginning to show signs of distress. Furthermore, the method described in this paper makes it possible to calculate the ultimate strength of a flexible pavement that is starting to show distress and the increase in ultimate strength to be expected by constructing an overlay of specified thickness of any given properly designed bituminous concrete.

Influence of Braking and Acceleration Stresses on Flexible Pavement Thickness Requirements

Braking stresses are created between a tire and pavement when the brakes are applied, while acceleration stresses, acting in the opposite direction to braking forces, are developed whenever a vehicle is being accelerated. Because of the urgency frequently associated with their application, braking stresses are generally more severe than acceleration stresses.

Flexible pavements in service are subjected to direct braking and acceleration stresses. The equivalent of these forces is also exerted indirectly whenever a vehicle changes direction in a horizontal plane, and when it moves on either an uphill or downhill gradient (the tangential component of its own weight), without the application of either brakes or accelerator. Braking and acceleration forces are usually applied in the direction of travel, and they, therefore, tend to shove the pavement either ahead of (for braking), or behind (for acceleration) the wheel.

It has been a relatively common observation for many years that serious waving, rolling, or other distortion can develop at the surfaces of flexible pavements at stop lights, bus stops, stop signs, etc., where there is much stopping and starting of traffic. These deformities result from braking and acceleration stresses if the flexible pavement is otherwise adequately designed. The same types of surface deformation are sometimes observed at the entrance to curves where brakes may be applied to decrease speed, and at the foot of a hill where the accelerator may be depressed to gain or maintain speed as uphill travel is begun. These examples demonstrate that braking and acceleration stresses may frequently provide the most critical conditions of design for flexible pavements that are to carry moving loads. Consequently, the influence of acceleration and braking forces on flexible pavement design should be investigated.

The surface distortion at the locations mentioned in the previous paragraph is sometimes due to movement entirely within the bituminous surface itself, which may not have sufficient stability to resist braking or acceleration forces. When a vehicle changes from downgrade to horizontal movement, or from horizontal to upgrade, the change in direction of motion of the vehicle exerts a larger than normal wheel or axle load on the pavement at these points. It is well known that as the wheel or axle load is increased, a greater thickness of flexible pavement is necessary. At the locations mentioned, therefore, due to the change in direction of vehicle movement, a greater thickness of flexible pavement should be provided.

In addition to the causes for pavement distortion at various locations that have just been described, Figure 16 demonstrates that wherever braking or acceleration stresses are applied, the thickness of a flexible pavement should be increased to resist the effect of these forces themselves. The reason for this becomes clear when Figures 16(b) and 16(c) are compared.

Figure 16(b) represents the condition of vehicle travel in a horizontal plane at uniform speed. In this case, the applied pressure is either the total wheel load or unit pressure exerted on the contact area, and it acts in a vertical direction. Braking or acceleration stresses are assumed to be negligible or entirely absent. As soon as the brakes are applied, Figure 16(c) demonstrates that in addition to the vertical wheel load of Figure 16(b), a braking stress acting tangentially to the surface is added. It

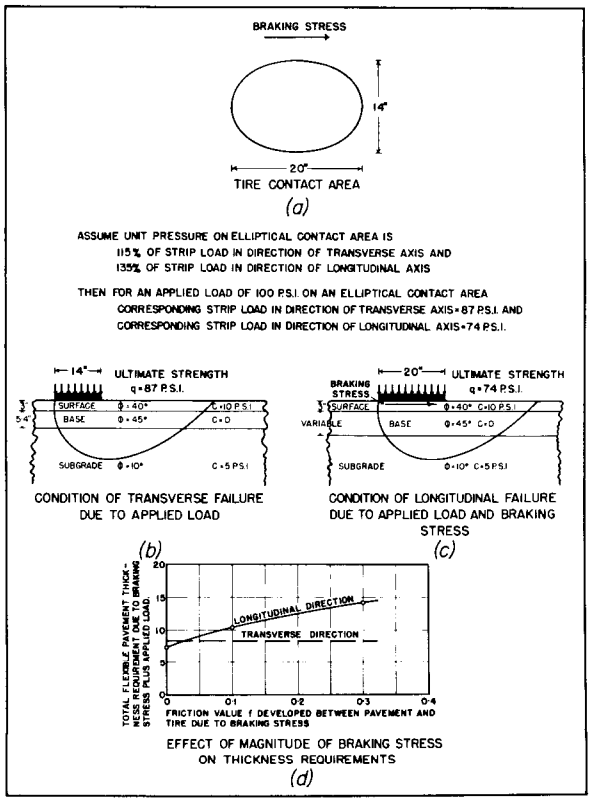

Fig. 16. Influence of Magnitude of Braking Stresses On Flexible Pavement Thickness Requirements.

is apparent that this braking force increases the load moment acting on the pavement structure, since the load moment (about the origin of the logarithmic spiral failure curve) now consists of the sum of the moments of the wheel load and of the braking force. Consequently, if equilibrium is to be maintained, and pavement failure avoided, the flexible pavement must develop a larger reaction moment (also about the origin of the logarithmic spiral failure curve) for the condition of Figure 16(c) (with braking stresses) than that of Figure 16(b) (without braking stresses). This larger reaction moment can be developed by either improving the quality (shearing resistance) of base course or surfacing materials, or increasing their thickness. In Figure 16(c) this greater reaction moment is obtained by increasing the thickness of the cohesionless granular base course.

Figure 16(d) indicates that the increase in flexible pavement thickness required to resist braking action depends upon the intensity of the applied braking stress. The magnitude of the braking force is represented in Figure 16(d) by the friction value f. For example, when f = 0.1, the braking force applied to the pavement is 0.1 of the vertical pressure exerted by the tire; that is, one-tenth of the wheel load. Similarly, when f = 0.3, the braking stress being exerted is three-tenths of the wheel load. The maximum friction value f that can be developed between pavement and tire is, of course, the coefficient of friction. Any attempt to apply a braking stress of larger magnitude than that represented by the coefficient of friction results merely in skidding of the tire on the pavement.

To obtain the comparative data needed for illustrating the influence of braking or acceleration stresses on flexible pavement thickness requirements, the assumptions listed in Figure 16 have been made. Each of these assumptions is believed to be reasonable.

Calculations by the logarithmic spiral method are easier to perform on the basis of strip loading. It has been previously mentioned that for cohesive soils the unit load that can be supported on a circular area is generally accepted to be from 20 to 30 per cent greater than that carried as a strip load (29, 30). For this paper, the increase for circular over strip loading is assumed to be 25 per cent. This is also assumed to apply in general to elliptical loading with the difference that the ratio of elliptical to strip loading depends upon the direction of the strip load relative to the principal axes of the elliptical contact area. The assumption is made that the ultimate load that can be supported on an elliptical contact area is 115 and 135 per cent of

the corresponding ultimate strip loads in the directions of the transverse and longitudinal axes of the contact area. Consequently, if a tire pressure of 100 p.s.i. represents the ultimate load on an elliptical contact area, the corresponding ultimate strip loads in the direction of the transverse and longitudinal axes are 87 and 74 p.s.i., respectively, Figures 16(b) and 16(c).

Figure 16(b) indicates the thickness of cohesionless base course in a flexible pavement structure that must develop an ultimate strength of 87 p.s.i., representing strip loading in the direction of the transverse axis of the contact area. The required thickness of base is 5.4 inches when the bituminous surface is 3 inches thick, giving a total thickness of flexible pavement of 8.4 inches, Figure 16(b). On the other hand, for an ultimate strength of 74 p.s.i., representing strip loading in the direction of the longitudinal axis of the elliptical contact area as illustrated in Figure 16(c), Figure 16(d) shows that a base course thickness of only 4.4 inches is required, which when combined with the 3-inch bituminous surface gives an overall flexible pavement thickness of 7.4 inches. Consequently, Figures 16(b), 16(c), and 16(d) indicate that for the condition of stationary wheel loads, or for vehicle movement at constant velocity, there is greater tendency for flexible pavement failure in the direction of the transverse than of the longitudinal axis of the tire contact area. This is in keeping with the observed performance of flexible pavements in service.

When braking or acceleration stresses are applied, they are normally exerted in the direction of the longitudinal axis of the contact area, and not in the direction of its transverse axis. In Figure 16(d), therefore, the flexible pavement thickness requirement in the direction of the transverse axis of the loaded area is shown as a broken line parallel to the abscissa, indicating that the thickness required to prevent failure in the direction of the transverse axis of the contact area is independent of either braking or acceleration stresses.

It should be pointed out, however, that this is not strictly correct, since in actual practice, as brakes or accelerator are applied, the vehicle tends to rotate in a vertical plane, putting more vertical load on the front wheels in the case of braking stresses, and on the rear wheels for acceleration stresses. This additional vertical load on front or rear wheels increases with increasing intensity of braking or acceleration stresses (increasing values of friction factor f, Figure 16(d)). This increasing vertical pressure with increasing intensity of braking or acceleration stresses requires some increase in thickness as f is

increased. For actual traffic conditions, therefore, the broken line graph in Figure 16(d), representing the thickness of flexible pavement required to prevent failure in the direction of the transverse axis of the contact area as braking stresses are applied, should have some positive slope. The increase in the intensity of vertical pressure and of size of contact area due to braking or acceleration stresses would both have to be measured before the slope of the broken line could be calculated. In the meantime, the horizontal slope given to this broken line in Figure 16(d) is probably not an unreasonable first approximation for the comparative purposes for which it is employed.

As explained previously, the application of a braking or acceleration stress increases the load moment (about the origin of the critical logarithmic spiral) in the direction of the longitudinal axis of the contact area; that is, in the direction of vehicle travel, Figure 16(c). If flexible pavement failure is to be avoided in this direction, this larger load moment must be balanced by the development of a greater reaction moment within the flexible pavement. This greater reaction moment can be provided by increasing the thickness of base course, or bituminous surface, or both. For the conditions represented by Figure 16, this greater reaction moment is obtained by increasing the base course thickness. Figure 16(d) indicates that as the braking or acceleration stresses are increased to develop values of the friction factor f between tire and pavement that are zero, 0.1, 0.2, and 0.3 of the tire inflation pressure (contact area pressure), the thickness of base course must be increased from 4.4 to 7.4 to 9.6 to 11.2 inches, while the total thickness of flexible pavement must be increased from 7.4 to 10.4 to 12.6 to 14.2 inches. Consequently, Figure 16(d) indicates that at relatively low breaking stresses, flexible pavement thickness design *for moving wheel loads* tends to be governed by stability requirements in the direction of the longitudinal (direction of travel) rather than of the transverse axis of the contact area. Furthermore, for the conditions it represents, Figure 16(d) indicates that the flexible pavement thickness required to support *a moving wheel load* for which the tire inflation pressure is 100 p.s.i. is increased from 8.4 inches when braking or acceleration stresses are absent, to 14.2 inches when braking forces developing a friction factor f = 0.3 are applied.

The distortion of flexible pavements that occurs with some frequency at stop signs, stop lights, bus stops, etc., where there is much stopping and starting of traffic, provides ample evidence of the qualitative correctness of the conclusions indicated

by Figure 16(d), and of the need for an appreciably greater thickness of flexible pavement for locations where breaking and acceleration stresses are severe, than for those long sections where vehicles tend to move at a relatively uniform rate of speed.

Investigations by Nijboer (31) and by Goetz and Chen (36) have demonstrated that the value of cohesion c being measured for a bituminous paving mixture in a triaxial test becomes much higher as the rate of strain or rate of loading is increased. This is also true of soil materials to a lesser degree (37). With respect to flexible pavement design, this means that a considerably higher value of cohesion c for a flexible pavement structure will be developed by moving than by stationary wheel loads of the same weight.

The reaction moment of a flexible pavement consists of the sum of the cohesion moment and the weight moment. The cohesion moment is usually considerably greater than the weight moment, Appendix C. The magnitude of the cohesion moment varies directly with the value of cohesion c, Appendices A, B, and C, and Table 6. Consequently, the larger the value of cohesion c, the greater is the reaction moment developed by a given flexible pavement structure. Since a higher value for cohesion c is developed by moving than by stationary wheel loads, a larger reaction moment is also developed within a given flexible pavement by a moving wheel load than when it is stationary. Consequently, all other conditions being equal, a smaller thickness of flexible pavement will support a given wheel load in the form of moving than of stationary traffic.

This is probably true even when braking or acceleration stresses are applied to a vehicle moving at high speed for the purpose of temporarily slowing down or speeding it up, but not bringing it to a stop, since a much higher value for cohesion c is being developed by the flexible pavement under these conditions than occurs under the same wheel load when stationary. Therefore, even though braking or acceleration stresses may be applied temporarily, as long as the vehicle continues to travel at relatively high speed, and is not brought to a stop, a smaller thickness of given flexible pavement is probably adequate for a moving wheel load than when it is stationary.

Consequently, insofar as flexible pavement design is concerned, for given subgrade, base course, and bituminous surfacing materials, and for a specified wheel load, the ultimate strength method based upon a logarithmic spiral failure curve described in this paper indicates that flexible pavement thickness requirements increase in the following order for the traffic conditions listed:

1. Vehicles moving at relatively uniform speed.
2. Stationary vehicles.
3. Bus stops, traffic lights, etc., where braking and acceleration stresses are severe, and there is much stopping and starting of traffic.

It might be asked whether or not Items 1 and 2 listed immediately above should have their order reversed in the case of heaviest highway traffic; that is, whether flexible pavement thickness requirements for the repeated loadings of the highest intensities of highway traffic should be greater for vehicles moving at relatively high speed than when stationary. Sufficient evidence does not seem to have been recorded or published to provide a definite answer to this question as far as highway engineering is concerned. However, in the related field of airport engineering, current flexible pavement design requires a greater thickness of flexible pavement for parking aprons, taxiways, and the ends of runways, where aircraft are stationary or move very slowly, than for the central portions of runways where aeroplanes are usually travelling at high speed for take-off or landing. This greater thickness requirement for aprons and taxiways than for runways is maintained even for airports designed for capacity operations; that is, for the highest possible intensity of aeroplane traffic. Because of their relatively small area, airports probably offer a better opportunity for a direct comparison of flexible pavement thickness requirements for a high intensity of moving versus stationary wheel loads than do highways. Insofar as evidence from current airport engineering provides a guide to highway design, it tends to support the order of flexible pavement thickness requirements listed in the previous paragraph for moving versus stationary wheel loads even for highways.

However, because airport runways are much wider than highways, capacity operations on runways represent fewer repetitions of load at any point on the paved surface than in the case of high intensity traffic on highways. Consequently, for highway traffic of greatest intensity, a highway engineer would probably be exercising reasonable judgment if he selected the thickness requirements for stationary wheel loads to carry moving highway traffic of the same weight. For smaller intensities of highway traffic, the flexible pavement thickness would be correspondingly decreased.

Ultimate Strength of Thick versus Thin Bituminous Surfaces

Each of the four tangents of the W.A.S.H.O. Test Road at Malad City, Idaho, is constructed of five 300-foot sections of flexible pavement. Each 300-foot section has the same overall thickness throughout, but the thickness of the five consecutive sections of each tangent is increased by 4-inch increments to include 6, 10, 14, 18, and 22 inches. On two of the four tangents the thickness of the asphalt surface is 2 inches, while on the other two tangents it is 4 inches thick. However, regardless of the thickness of the asphalt surface itself, the overall thicknesses of sub-base, base course, and asphalt surface are the same on corresponding test sections on the four tangents. For example, the test sections having an overall thickness of 6 inches consist of either 4 inches of asphalt surface and 2 inches of granular base course, or 2 inches of asphalt surface and 4 inches of base course. Similarly, the test sections that are 14 inches in overall thickness consist of either 4 inches of asphalt surface, 2 inches of granular base course, and 8 inches of granular sub-base, or 2 inches of asphalt surface, 4 inches of base course, and 8 inches of sub-base.

When presenting the paper by Miller and Carey (38) for the last annual meeting, Mr. W. N. Carey, Project Engineer for the W.A.S.H.O. Test Road, mentioned that as a result of traffic testing completed up to that time, for the smaller overall thicknesses of flexible pavement (6, 10, and 14 inches), it appeared that the two tangents with 4-inch asphalt surfaces were performing better than the other two tangents where the thickness of asphalt surface was 2 inches; that is, there had been less evidence of distress on corresponding sections where the asphalt surface was 4 inches rather than 2 inches thick.

Figure 17 has been prepared to demonstrate that this difference in the traffic performance of corresponding test sections with 2-inch and 4-inch asphalt surfaces reported by Mr. Carey is precisely the result that would be expected on the basis of the ultimate strength approach to flexible pavement design that has been described in this paper. The two diagrams on the left-hand and right-hand sides of Figure 17 indicate that the overall thickness of flexible pavement is 10 inches in both cases. However, for the left-hand diagram, the flexible pavement consists of 2 inches of asphalt surface and 8 inches of granular base, while for the right-hand diagram it consists of 4 inches of asphalt surface and 6 inches of base. This construction is similar in its thickness dimensions to one of the five test sections of the

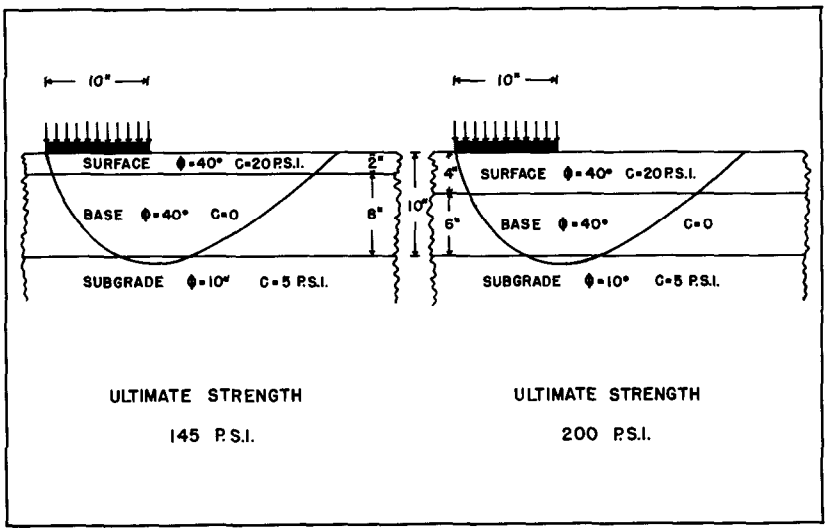

Fig. 17. Influence of Asphalt Surface Thickness on Ultimate Strength For a Given Total Thickness of Surface and Base.

W.A.S.H.O. Test Road. It should be emphasized that the c and ϕ values for each layer, subgrade, sub-base, base course, and asphalt surface, have not been measured for the materials employed for the Test Road itself, and those shown in Figure 17 have been arbitrarily assigned.

The ultimate strengths of the two flexible pavement cross-sections illustrated in Figure 17 were calculated by means of the logarithmic spiral method previously described in this paper (see also Appendix C). As listed in Figure 17 itself, the ultimate strength values were found to be 200 p.s.i. for the flexible pavement section with the 4-inch asphalt surface, but only 145 p.s.i. for that with the 2-inch asphalt surface. Consequently, the cross-section with the 4-inch asphalt surface in Figure 17 has 38 per cent greater ultimate strength than that for which the asphalt surface is 2 inches thick.

It should be emphasized again that the total thickness of flexible pavement is the same for both cross-sections shown in Figure 17, t = 10 inches, and that only the individual thicknesses of the base course and asphalt surface have been varied.

If the ultimate strength values obtained for the two flexible pavement cross-sections illustrated in Figure 17 are even approximately representative of the difference in strengths of corresponding test sections of the W.A.S.H.O. Test Road, they

provide an explanation for the better performance of the tangents with 4-inch asphalt surfaces, as compared with those where the asphalt surface is only 2 inches thick, which has been reported by Mr. Carey. For test sections such as those 6, 10 and 14 inches thick at the W.A.S.H.O. project, that are either underdesigned from the point of view of thickness, or of barely adequate strength, with all other conditions being equal, it would be expected that the test sections of higher ultimate strength would show the superior performance, since the degree of underdesign would be less for these. On the other hand, for those sections that are of adequate strength or are overdesigned, which may be true of the 18- and 22-inch thicknesses of the W.A.S.H.O. Test Road, little difference in the performance of sections with either 2 or 4 inches of asphalt surface would be anticipated, even if the ultimate strength of the sections with 4 inches of asphalt surface were considerably greater. In this latter case, it becomes a matter of comparing two different degrees of flexible pavement overdesign, for which differences in service behaviour would not be expected to develop under normal traffic, unless possibly after a very long time.

It should be pointed out that increasing the thickness of the asphalt surface would not always result in the large increase in strength for the flexible pavement structure as a whole that is illustrated in Figure 17, where the asphalt surface is relatively strong, while the granular base is probably somewhat below average strength. If a granular base of high stability (high angle of internal friction ϕ) were combined with a much weaker asphalt surface (lower c and ϕ values), then, for a given overall depth of base and surface, increasing the thickness of the asphalt surface would result in a much smaller increase of strength for the entire flexible pavement structure than that shown in Figure 17. Variations in thickness of the asphalt pavement itself will also have less influence on the ultimate strength of the overall flexible pavement structure when the depth of granular base and sub-base is unusually great. Consequently, the strength advantage to be gained by increasing the thickness of the bituminous surface layer depends upon the relative stabilities and thicknesses of the base course and bituminous surfacing materials. In all cases, of course, an engineer will wish to determine which practical combination of thicknesses of base course (including sub-base) and bituminous surface will provide an adequate flexible pavement structure for the traffic anticipated, at the smallest overall cost.

Incidentally, Figure 17 provides another illustration of the importance of the presence of cohesion c in any layer on the

ultimate strength of a flexible pavement. It will be noted that the angle of internal friction ϕ is the same for both base and surface courses, $\phi = 40^{0}$. The overall thickness of base and surface is constant, t = 10 inches. In a sense, therefore, the asphalt surface consists of the top layer of base course to which cohesion c = 20 p.s.i. has been added. By adding cohesion c = 20 p.s.i. to the top 4 inches of the base course (diagram on the right-hand side) instead of to only the top 2 inches of base (diagram on the left-hand side of Figure 17), the ultimate strength of the flexible pavement structure has been increased by 38 per cent in this particular case.

Influence of Paved Shoulder on the Ultimate Strength of a Flexible Pavement

The paved surface on each of the four tangents of the W.A.S.H.O. Test Road in Southern Idaho is 24 feet wide, which provides two 12-foot lanes for the trucks applying test traffic of specified axle loadings.

During his presentation of the paper by Miller and Carey (38) on the progress of the W.A.S.H.O. project of the last annual meeting of the Highway Research Board, Mr. W. N. Carey reported that traffic testing during the first full year (1953) had produced failure on portions of the thinner test sections of flexible pavement. Generally speaking, however, these failures had been largely confined to the outer wheel path extending from 4 to 6 feet inward from the edge of the pavement. Relatively little failure had occurred on the corresponding inner wheel path occupying the inner six feet of the 12-foot traffic lanes on these same test sections.

Carefully performed moisture and density tests spaced at short intervals across the 12-foot traffic lane showed no difference in either subgrade or base course moisture and density values between the inner and outer 6-foot sections. Consequently, failure of the outer 6 feet of pavement adjacent to the shoulder with no failure of the corresponding inner 6 feet could not be ascribed to differences in moisture contents and densities of the underlying subgrade and base. Mr. Carey reported that after studying these results, the Advisory Committee for the W.A.S.H.O. Test Road recommended that the shoulders be paved adjacent to portions of several of the test sections where failure had not yet occurred. These sections of paved shoulder were added during the latter part of 1953, and their influence will be observed during the 1954 traffic testing.

Figure 18 demonstrates that the ultimate strength approach to flexible pavement design described in the present paper provides an explanation for

(a) the failure of the flexible pavement in the outer wheel path but not in the corresponding inner wheel path of the 12-foot traffic lanes at the W.A.S.H.O. project, and
(b) the improved flexible pavement performance to be anticipated during 1954 traffic testing for the portions of test sections for which paved shoulders have been provided.

Since there was no difference in subgrade or base course moisture and density values, it might be asked first of all why

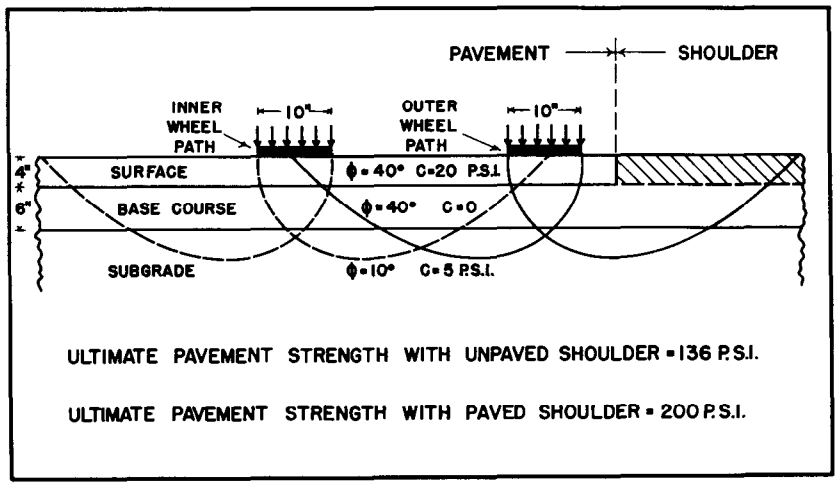

Fig. 18. Influence of Paved Shoulder on Ultimate Strength of Flexible Pavement.

failure developed in the outer wheel path (6 feet nearest to the shoulder) of the thinner test sections, but not in the corresponding inner wheel path (6 feet nearest the centre of the 24-foot pavement). The ultimate strength concept based upon the logarithmic spiral failure curves illustrated in Figure 18 provides an explanation. The logarithmic spiral failure curves under the inner wheel path (broken line failure curves in Figure 18) lie entirely within the paved area. Consequently, they are able to develop the cohesion c of the bituminous pavement at both extremities of the logarithmic spiral. This is also true for the full line logarithmic

spiral curve directed toward the centre of the pavement from the outer wheel path.

On the other hand, the full line logarithmic spiral under the outer wheel path directed toward the right of Figure 18 cuts through the cohesionless gravel shoulder of the road. Only the extremity of this spiral immediately below the outer wheel path intersects the asphalt pavement, the other end of the spiral terminating in the gravel shoulder. Consequently, this spiral differs from those under the inner wheel path in that it can mobilize the cohesion c of the asphalt pavement at only one of its extremities.

For the particular conditions illustrated in Figure 18, the ultimate strength developed by the flexible pavement under the inner wheel path, where both extremities of the logarithmic spiral failure curve intersect the bituminous pavement, is 200 p.s.i. On the other hand, the ultimate strength developed by the flexible pavement under the outer wheel path, where the logarithmic spiral failure curve intersects the gravel shoulder, is only 136 p.s.i. Consequently, the ultimate strength of the flexible pavement under the inner wheel path is 47 per cent greater than that under the outer wheel path for this particular case. This, therefore, provides an explanation for the failure under the outer wheel path of portions of the thinner test sections at the W.A.S.H.O. Test Road, without accompanying failure under the corresponding inner wheel path.

Figure 18 indicates that by paving the shoulder there would be no greater tendency for failure in the outer wheel path than for the inner wheel path at the W.A.S.H.O. project, provided there were no differences in moisture and density values for the underlying subgrade and base course. For Figure 18 it is assumed that the thickness and all other characteristics of the pavement placed on the shoulder are identical with those for the paved road surface. It can be seen from the logarithmic spiral failure curves under the outer wheel path of Figure 18 that by paving the shoulder the ultimate strength of the flexible pavement under the outer wheel path would become equal to that under the inner wheel path (assuming no difference in subgrade or base course moisture and density). Consequently, for the case represented by Figure 18, paving the shoulder would increase the ultimate strength of the flexible pavement under the outer wheel path by 47 per cent. It is to be expected, therefore, that the parts of the thinner sections of flexible pavement at the W.A.S.H.O. project along which a paved shoulder was constructed during the latter part of 1953 will show marked superiority during the

balance of the traffic testing program over those portions for which the shoulder has been left unpaved.

It is obvious that the effective ultimate strength value for the entire width of a paved roadway is the ultimate strength developed by the flexible pavement under the weakest wheel path, which Figure 18 indicates is most likely to be the wheel path nearest the shoulder. This applies even to multi-lane highways, since by convention the driving lane is the one nearest the road shoulder.

From even casual observation of road performance, it has been well known for many years that the portions of bituminous pavements near the shoulders have usually shown greater tendency for distress or failure than the centre of the pavement. During the early stages of the development of low-cost paved road construction about twenty to twenty-five years ago, failure of the outer third (adjacent to the shoulders) of low-cost bituminous pavements was particularly common, since the need for base courses of adequate thickness had not become generally recognized. This distress or failure of the outer portions of bituminous pavements has usually been attributed to the entrance of moisture into the base and subgrade under the pavement edges. The increased moisture content lowers the strength of the foundation under the edges of the pavement, causing the outer portions to deform or fail. On the other hand, Figure 18 indicates that even if there were no loss of subgrade or base course strength under the edges of bituminous pavements, there is greater tendency for failure of the outer than of the inner wheel path solely because of the presence of the usual earth or gravel shoulder, the difference in ultimate strength being 47 per cent for the particular conditions illustrated.

Bituminous pavements have been placed on many roads which are so narrow that the width of shoulder is only a foot or so, and in extreme cases may even be measured in inches. In these cases, the critical logarithmic spiral failure curves under the outer wheel path intersect the ditch slope beyond the shoulder and develop a smaller reaction moment than for the wide shoulder condition of Figure 18. For these very narrow roads, therefore, the per cent difference in ultimate strength values between the inner and outer wheel paths could be considerably greater than that illustrated by Figure 18 for roads with wide unpaved shoulders, which is 47 per cent.

As a first impression, highway engineers may feel that the construction of bituminous surfaces on road shoulders would add considerable to the overall cost of a flexible pavement. However,

as will be pointed out, a substantial decrease in the overall thickness of flexible pavement for the main roadway appears to be possible if the road shoulders were paved. Consequently, an economic study of each individual project might indicate that for many cases paved shoulders would not add materially, if at all, to the overall cost.

It should be particularly noted in this connection that current flexible pavement thickness requirements for highways are controlled by the thicknesses needed to prevent failure of the outer wheel paths. Since a uniform thickness over the cross-section is normally employed, this means that the inner wheel path is usually overdesigned. For example, for the conditions represented by Figure 18, if the thicknesses of base and surface shown were just adequate for the outer wheel path, the inner wheel path is overdesigned by 47 per cent. By paving the shoulder adjacent to the bituminous pavement proper, the outer wheel path would be protected against loss of strength due to entrance of moisture into the foundation under the pavement edge, and would be materially strengthened by the presence of the pavement on the shoulder. Therefore, a paved shoulder would tend to make the flexible pavement under the outer wheel path as strong as that under the inner wheel path. Consequently, a substantial reduction in overall flexible pavement thickness requirements for highways might be possible if the shoulders were paved. This reduction in flexible pavement thickness across at least the entire width of the bituminous surface proper, usually 24 feet for a 2-lane pavement, and frequently from shoulder to shoulder when the full depth of base is carried from ditch slope to ditch slope, which may be 40 or more feet, might be sufficient to pay for a large portion or even the entire cost of the paved shoulders. In addition, the intangible, but very positive, value of firm paved shoulders to motorists in general merits consideration for primary highways particularly.

Insofar as airports are concerned, since most airplane traffic is confined to the central third of runways, paving shoulders or runways would not provide the substantial benefit that appears to be possible for highways. Since traffic tends to concentrate on the central third of the width of paved runways, the outer two thirds of the pavement function as very wide paved shoulders in a sense. This in itself may be a major factor contributing to the well-recognized smaller flexible pavement thickness requirements for runways than for highways for capacity traffic of the same wheel loading.

Incidentally, Figure 18 and reported W.A.S.H.O. Test Road experience to date furnish evidence that the curves of Figures 10 and 15 labelled "partial cohesion" provide ultimate strength values that are much too conservative (too small). It will be recalled that these "partial cohesion" curves represent the entire ultimate strength that a flexible pavement can develop provided that cohesion c of the bituminous pavement is mobilized for only the extremity of the critical spiral failure curve that is immediately below the loaded area. On the other hand, the "full cohesion" curve includes the influence of cohesion c at both extremities of the spiral. If the "partial cohesion" curve of Figure 15 represented the entire ultimate strength developed by a flexible pavement, it would make no difference to the ultimate strength value whether the shoulder was paved or unpaved. Furthermore, if the "partial cohesion" curve of Figure 15 indicated the total ultimate strength that could be mobilized by a flexible pavement, the ultimate strengths developed under either the inner or outer wheel paths of Figure 18 would be exactly the same, and both would be equal to 136 p.s.i., assuming no difference in foundation strength for either wheel path. In this case, failure of the flexible pavement under both the inner and outer wheel paths of the W.A.S.H.O. Test Road would have been expected to tend to occur in exactly the same amount. However, as previously mentioned, Mr. W. N. Carey has reported (38) complete failure of the outer wheel path of some sections of the W.A.S.H.O. project, without any signs of distress appearing in the corresponding inner wheel path. Consequently, the "partial cohesion" curves in Figures 10 and 15 do not represent the entire ultimate strength that can be mobilized by a flexible pavement. The marked difference in flexible pavement behaviour under the outer and inner wheel paths at the W.A.S.H.O. project indicates that the ultimate strength actually developed by a flexible pavement could be illustrated by a curve which at least lies between those labelled "partial cohesion" and "full cohesion" in Figures 10 and 15. If W.A.S.H.O. Test Road performance is typical of that of flexible pavements in general, their ultimate strengths are apparently closer to, and may even be represented by, the curve labelled "full cohesion." In other words, there is considerable evidence that there is a tendency for cohesion c of each layer intersected to be mobilized throughout the full length of the critical logarithmic spiral failure curve, and not just over some portion of its length near the loaded area.

SAFETY FACTOR FOR ULTIMATE STRENGTH VALUES FOR FLEXIBLE PAVEMENT DESIGN

The ultimate strength values derived on the basis of the logarithmic spiral method described in this paper could not ordinarily be employed directly for flexible pavement design, because the deflection developed by the load at ultimate strength would usually damage the bituminous surface. This is similar to the situation in foundation design where, if the ultimate strength of the underlying soil were employed for the design of footings, the large ensuing settlement would normally damage the structure seriously. When designing footings, a safety factor of about 3 is frequently applied to the measured ultimate strength of the soil (29).

Consequently, a factor of safety must usually be applied to the ultimate strength of a flexible pavement as calculated by the logarithmic spiral method, to protect the bituminous surface against damage by the excessive deflection that an applied wheel load equal to the ultimate strength would cause. This immediately leads to the problem of what the magnitude of this safety factor should be.

Factors of safety in actual use for flexible pavement design and construction for highways and airports are unknown. Nevertheless, they could be determined. Actual experience in many areas has indicated what the flexible pavement design should be for any given wheel load, subgrade support, and traffic intensity. For design purposes, the size of the contact area is usually taken to be equal to the wheel load divided by the tire inflation pressure and is assumed to be circular in shape. By using the diameter of this circle as the width of a strip loading, and knowing the c and ϕ values for subgrade, base course, and bituminous surface, and the density of each layer, an ultimate strength value for the flexible pavement can be determined by the logarithmic spiral method. The ultimate strength for the strip loading can be increased by from 20 to 30 per cent to give the corresponding ultimate strength for a circular area of the same diameter as the strip load width. The ratio of this calculated ultimate strength for the circular area in p.s.i., to the tire inflation pressure in p.s.i. employed for the original design, represents the safety factor being used.

Since the flexible pavement thickness required for any given wheel load and inflation pressure varies with traffic intensity, the safety factor to be employed should also vary with the density of traffic. It appears that the safety factor being employed

for flexible pavements for airport runways for capacity operations is somewhat smaller than that for highways for densest traffic, since the concentration of traffic is greater on a heavily travelled highway than on the busiest runway.

GENERAL COMMENTS

1. One of the criticisms of the logarithmic spiral method described in this paper for determining the ultimate strength of flexible pavements, that may occur to the reader, is that no allowance has been made for the discontinuities to be expected where the spiral crosses the boundaries between different layers. This objection may be quite valid. On the other hand, the lack of complete homogeneity of soils in embankments and slopes does not seem to interfere with the reasonable accuracy obtained when circular arcs are assumed for the shape of the failure surfaces when analysing their stability. In stability investigations, these circular arcs are assumed to cut through soil layers of different shearing strengths without discontinuity. In addition, as pointed out early in the paper, the surface profile of the rutting and upheaval of a flexible pavement that has failed under excessive wheel loads is at least qualitatively similar to that of a homogeneous soil which has been overloaded by traffic. Consequently, the shapes of the surfaces of shear failure cannot be greatly different in these two cases, and in this paper they are assumed to be logarithmic spirals. It may be, therefore, that any actual discontinuities tending to occur wherever the logarithmic spiral crosses a boundary between two layers of quite different materials are not too important insofar as stability analysis by the logarithmic spiral method is concerned.
2. When attempts are made to analyse the stability of a layered system by assuming that discontinuities occur whenever the logarithmic spiral crosses a boundary between two layers, serious difficulties immediately arise. For example, different origins might be expected for the portions of the spirals in the several layers. The positions of the origins for the various spirals through the different layers would depend upon the amount of discontinuity assumed. In addition, about which of these origins or other common point is the load moment to be taken?

   If a common origin is assumed, but the shape of the logarithmic spiral within each layer is established on the basis of its c and ϕ values, a discontinuous failure curve of quite

improbable shape is obtained. Furthermore, locating the required common origin for the lowest developed ultimate strength by trial and error is such a time-consuming task that this approach would be of little practical utility for design purposes, particularly since the ultimate strength values it provides do not seem to be greatly different from those obtained by the much simpler method described in the present paper.

Consequently, if discontinuities of the spiral at the boundaries between the layers of a flexible pavement are assumed, other difficulties immediately arise that tend to discourage the use of the method due to the excessive time and trouble they involve, and they might even lead to greater error in the calculation of the ultimate strength of a flexible pavement than occurs if the discontinuities are disregarded, as has been done in this paper.

3. When analysing the stability of slopes by means of the circular arc method, the shearing resistance of the soil is assumed to be mobilized simultaneously along the whole length of the failure arc, which may be several hundred feet. Good agreement between actual field performance and the stability values calculated on this basis are usually reported. Consequently, the assumption made in this paper that the shearing resistances of the materials in the different layers of a flexible pavement are mobilized simultaneously throughout the entire length of a logarithmic spiral failure curve, which is at most only a few feet in length, may not be unreasonable.
4. A major conclusion indicated by the data of this paper is the important contribution that the existence of cohesion c in any one or more layers makes to the ultimate strength of a flexible pavement. Figures 10, 15, 17, and 18 testify to its important influence when cohesion c occurs in the bituminous surface but not in the base. On the other hand, the large increase in ultimate strength that results from the introduction of cohesion c into the base course material is illustrated in figures 13 and 14.

   Figure 7 has demonstrated that vinders that provide cohesion c for base course or surfacing materials may function as lubricants rather than as cements, if an excess is employed. In their capacity as lubricants, they tend to reduce the angle of internal friction ϕ of the aggregate. It is well illustrated in Figure 7 that the introduction of even a slight excess of binder will result in a net loss of ultimate strength, if the influence of the reduction in ϕ is greater than the effect of the increase in c that may still occur.

In cases where the lubricant property of current common binders such as clay or bituminous materials is too pronounced, e.g. the stabilization of heavy clay soils with bituminous binders, methods for reducing their lubricant quality and increasing their effectiveness as plastic cements (higher cohesion c) should be considered. As an alternative, new inexpensive binders, that will perform more nearly as desired, might be investigated.

5. Since Professor Burmister's layered system theory of flexible pavement design is based upon the elastic properties of the material in each layer, it will result in the same strength rating for either cohesionless materials or those containing a binder to give cohesion c, if their moduli of elasticity are the same. The logarithmic spiral method employed in this paper, on the other hand, indicates that while two materials, one cohesionless, and the other cohesive with both c and ϕ values, might have the same moduli of elasticity, the cohesive material may develop either a higher or lower ultimate strength than the other depending upon the relative values for ϕ of the two materials. Therefore, while its modulus of elasticity is the most important characteristic of the material in each layer from the point of view of Burmister's theory, the c and ϕ values are the most important properties of the material in each layer of a flexible pavement when its strength is analysed by the logarithmic spiral method. Consequently, for the same layered system of base course and surfacing materials, a different strength rating will probably be given by Professor Burmister's theory based upon elastic properties and a critical surface deflection, than by the logarithmic spiral method based upon ultimate strength and a factor of safety. No data are presently available for determining the magnitude and range of the differences in safe loading given by the two methods.
6. While the calculations required for the logarithmic spiral method described here are somewhat time-consuming, they are relatively simple and straight-forward and can be quickly mastered by any qualified, interested individual. The basic charts presented in Appendix C materially reduce the amount of calculation otherwise required. It is quite likely that additional basic charts can be devised that will reduce the time spent on calculation still further.

SUMMARY

1. Three criteria for flexible pavement design are listed.
2. Heavier airplanes for air transport, and a greater number of trucks with heavy axle loadings on highways, have increased the thickness of flexible pavement required to prevent subgrade failure.
3. The high tire inflation pressures of jet aircraft have increased the tendency for flexible pavement failure along shear planes entirely within the base and surface course, when the base course is of great depth.
4. A method is described for calculating the ultimate strength of a flexible pavement on the basis of the c and ϕ values for each layer, and assuming a logarithmic spiral failure curve. In essence, this method involves the determination of c and ϕ values for an equivalent homogeneous material having the same ultimate strength as the layered system of the flexible pavement.
5. Examples of the application of this method are given for calculating ultimate strength values for one-, two-, and three-layer flexible pavement systems.
6. This method indicates that the ultimate strength of cohesionless aggregates increases with increasing angle of internal friction ϕ. The ultimate strength of any given cohesionless aggregate can be materially increased by incorporating a binder to provide cohesion c, provided the lubricating quality of the binder does not seriously reduce the angle of internal friction ϕ of the aggregate.
7. Examples are included to show that the overall ultimate strength of a flexible pavement containing a cohesionless base course of low to moderate stability can be greatly increased by incorporating a binder that introduces cohesion c into the base course.
8. The important contribution that the existence of cohesion c in any layer, surface, base, or sub-base, makes to the ultimate strength of a flexible pavement is one of the major conclusions indicated by the data of this paper.
9. The utilization of this ultimate strength method to guide the stabilization of both cohesionless and cohesive soils is described, and the fact that it provides conclusions that are in at least qualitative agreement with field experience is pointed out.
10. This method indicates that either additional thickness of flexible pavement, or higher quality sub-base, base course,

and bituminous surfacing materials are required at bus stops, traffic lights, etc., due to the severe braking and acceleration stresses that occur wherever there is much stopping and starting of traffic.

11. Calculations show that for the same overall thickness of flexible pavement, an appreciably higher ultimate strength will be developed by a 4-inch than by a 2-inch thickness of well-designed bituminous surfacing.
12. For the usual flexible pavement on highways with earth or gravel shoulders, this method shows that the ultimate strength of the flexible pavement under the inner wheel path is likely to be appreciably greater than that under the outer wheel path. This is supported by the pavement failure pattern reported for the W.A.S.H.O. Test Road.
13. Considerable evidence is presented to show that the ultimate strength of a flexible pavement on a highway would be materially increased by providing paved shoulders.
14. An example is included to show that a flexible pavement with a bituminous surface of low stability may fail because the bituminous surface is squeezed out between tire and base course, rather than by shearing failure along a logarithmic spiral through surface, base, and subgrade; that is, squeezing failure of a bituminous surface of low to moderate stability may occur under a smaller applied load than would be required to cause failure along the critical logarithmic spiral through surface, base, and subgrade. This example warns that all three of the criteria listed at the beginning of this paper must be kept in mind when designing a flexible pavement.
15. To summarize its most important findings very briefly, this study indicates that the ultimate strengths of flexible pavements could be greatly increased, or conversely, their overall thickness requirements could be materially reduced by,
    (a) the proper use of binders either to introduce cohesion c into base course materials, or to increase any existing c value they may possess,
    (b) increasing the thickness of well-designed bituminous surfaces, and
    (c) paving the shoulders of highways.

    Economic studies would indicate the projects for which the application of any one or more of these three major findings would lead to satisfactory flexible pavement performance at lower overall cost.

16. Appendices A, B, and C contain sample calculations illustrating the application of the ultimate strength method based on logarithmic spiral failure curves to actual flexible pavement design problems.

ACKNOWLEDGMENTS

The material presented in this paper forms part of an extensive investigation of airports in Canada that was begun by the Canadian Department of Transport in 1945. Air Vice-Marshall A. T. Cowley, Director of Air Services, has the general administration of this investigation. It comes under the direct administration of Mr. Harold J. Connolly, Chief Construction Engineer, Mr. George W. Smith, Assistant Construction Engineer, and Mr. E. B. Wilkins. In their respective districts, the investigation is carried on with the generous cooperation of District Airway Engineers G. T. Chillcott, R. A. Bradley, F. L. Davis, O. G. Kelly, L. Millidge, and W. D. G. Stratton.

It is a pleasure to make grateful acknowledgment to Mr. C. L. Perkins for the very able manner in which he carried through the large number of calculations involving the logarithmic spiral required for this paper. Familiarity with these calculations has enabled him to work out procedures that shorten the number of trials for the required solutions. Mr. Perkins developed the use of polar co-ordinate graph paper described in Appendix C to simplify the determination of the lengths of the arcs of a logarithmic spiral that are intercepted by each layer of a flexible pavement. He also recognized the relationships outlined in Appendix D that give the exact position (relative to one extremity of the loaded area) of the ordinate on which the centres of the critical logarithmic spirals for cohesionless and for cohesive, frictionless, homogeneous soils are located. The author also wishes to express his warm appreciation to Mr. Perkins for his skilful drafting of the various diagrams for this paper.

LITERATURE CITED

1. "Thickness of Flexible Pavements," Current Road Problems No. 8-R, Highway Research Board (1949).
2. Norman W. McLeod, "Airport Runway Evaluation in Canada," Highway Research Board Research Report No. 4 B, October (1947).
3. Norman W. McLeod, "Airport Runway Evaluation in Canada—Part 2," Highway Research Board Research Report No. 4 B—Supplement, December (1948).
4. Norman W. McLeod, "A Canadian Investigation of Load Testing Applied to Pavement Design," Special Technical Publication No. 79, American Society for Testing Materials, April, 1948.
5. Norman W. McLeod, "A Canadian Investigation of Flexible Pavement Design," The Association of Asphalt Paving Technologists, Proceedings, Volume 16 (1947).
6. Norman W. McLeod, "Economical Flexible Pavement Design Developed from Canadian Runway Study," Engineering News-Record, April 28, May 12, May 26, and June 9, 1949.
7. E. H. Davis, "Pavement Design for Roads and Airfields," Road Research Technical Paper No. 20, Road Research Laboratory, London (1951) H. M. Stationery Office.
8. Engineering Manual, Corps of Engineers, U. S. Army, Part XII, Chapter 2, July (1951).
9. L. A. Palmer and James B. Thompson, "Pavement Evaluation by Loading Tests at Naval and Marine Corps Air Stations," Highway Research Board Proceedings, Vol. 27 (1947).
10. Norman W. McLeod, "The Rational Design of Bituminous Paving Mixtures," Highway Research Board Proceedings, Vol. 29 (1949).
11. Norman W. McLeod, "A Rational Approach to the Design of Bituminous Paving Mixtures," The Association of Asphalt Paving Technologists, Proceedings, Vol. 19 (1950).
12. Norman W. McLeod, "Application of Triaxial Testing to the Design of Bituminous Pavements," American Society for Testing Materials, Special Technical Publication No. 106 (1951).
13. Norman W. McLeod, "Influence of Tire Design on Pavement Design and Vehicle Mobility," Highway Research Board, Proceedings, Vol. 31 (1952).
14. Norman W. McLeod, "Rational Design of Bituminous Paving Mixtures with Curved Mohr Envelopes," The Association of Asphalt Paving Technologists, Proceedings, Vol. 21 (1952).
15. Norman W. McLeod, "The Design of Bituminous Mixtures with Curved Mohr Envelopes," The Association of Asphalt Paving Technologists, Proceedings, Volume 22 (1953).
16. D. M. Burmister, "The Theory of Stresses and Displacements in Layered Systems and Applications to the Design of Airport Runways," Highway Research Board, Proceedings, Vol. 23 (1943).
17. "Soil Mechanics for Road Engineers," Road Research Laboratory, London (1952), H. M. Stationery Office.
18. Karl Terzaghi, "Theoretical Soil Mechanics," John Wiley and Sons Inc., New York (1943).
19. D. P. Krynine, "Soil Mechanics," McGraw-Hill Book Co. Inc., New York (1941).

20. Donald W. Taylor, "Fundamentals of Soil Mechanics," John Wiley and Sons Inc. (1948).
21. G. G. Meyerhof, "The Ultimate Bearing Capacity of Foundations," Geotechnique, Vol. 2, No. 4, December (1951).
22. C. A. Hogentogler, "Engineering Properties of Soil," McGraw-Hill Book Co. Inc., New York (1937).
23. George B. Sowers and George F. Sowers, "Introductory Soil Mechanics and Foundations," The MacMillan Co., New York (1951).
24. W. S. Housel, "Internal Stability of Granular Materials," American Society for Testing Materials, Proceedings, Vol. 26, Part 2 (1936).
25. Harmer E. Davis and Richard J. Woodward, "Some Laboratory Studies of Factors Pertaining to the Bearing Capacity of Soils," Highway Research Board, Proceedings, Vol. 29 (1949).
26. D. P. Krynine, Discussion, Highway Research Board, Proceedings, Vol. 29 (1949).
27. L. Fox, "Computations of Traffic Stresses in a Simple Road Structure," Road Research Technical Paper No. 9, Road Research Laboratory, London (1948), H. M. Stationery Office.
28. E. S. Barber, Discussion, Highway Research Board, Proceedings, Vol. 29 (1949).
29. G. G. Meyerhof, "The Tilting of a Large Tank of Soft Clay," The South Wales Institute of Engineers, Proceedings (1951).
30. Karl Terzaghi and Ralph B. Peck, "Soil Mechanics in Engineering Practice," John Wiley and Sons Inc., New York (1948).
31. L. W. Nijboer, "Plasticity as a Factor in the Design of Dense Bituminous Road Carpets," Elsevier Publishing Co. Inc., New York (1948).
32. W. R. Greathead, "Soil as an Engineering Material at Two Major Airports in South Africa," The South African Institution of Civil Engineers Transactions, April (1951).
33. Paul F. Critz and C. M. Duff, "Bituminous Treatment of Sandy Soils in Nebraska," Public Roads, Volume 22, No. 10, December (1941).
34. H. C. Weathers, "Sand Bituminous Stabilization," Highway Research Board, Proceedings, Volume 17 (1937).
35. U.S. Corps of Engineers, "Symposium on Asphalt Paving Mixtures," Highway Research Board, Research Report No. 7-B, June (1949).
36. W. H. Goetz and C. C. Chen, "Vacuum Triaxial Technique Applied to Bituminous Aggregate Mixtures," The Association of Asphalt Paving Technologists, Proceedings, Volume 19 (1950).
37. P. C. Rutledge, Review of "Cooperative Triaxial Shear Research Program of the Corps of Engineers," Soil Mechanics Fact Finding Survey Progress Report, Waterways Experiment Station, Vicksburg, Mississippi, U.S.A., April (1947).
38. Earl V. Miller and William N. Carey, Jr., "Report of W.A.S.H.O. Road Test," Highway Research Board, Proceedings, Volume 33 (1954).

APPENDIX A

Sample Calculation for Ultimate Strength of a Homogeneous Soil by the Logarithmic Spiral Method

The objective of this sample calculation is the determination of the maximum applied strip load that the homogeneous soil can support without failure for the conditions illustrated in Figure 19, assuming the failure curve to be a logarithmic spiral.

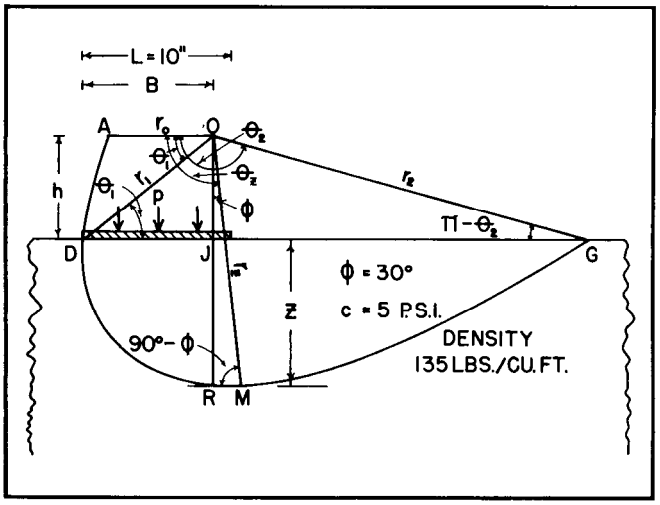

Fig. 19. Illustrating the Logarithmic Spiral Method for Calculating the Ultimate Strength of a Homogeneous Soil.

The method requires balancing load moment against reaction moment for the incipient failure (equilibrium) condition. A critical logarithmic spiral is associated with the maximum load that can be applied. The origin of this critical spiral is determined by the trial and error method. Barber (28) has published three tables of basic data concerning the logarithmic spiral that greatly facilitate a number of the calculations that must be made.

For this sample calculation, the following conditions are given (Figure 19):

Strip Loading
Width of Loaded Strip = L = 10 inches
$\phi = 30^{\circ}$
c = 5 p.s.i.
Soil Density = w = 135 pounds per cubic foot

The following information is required:

(1) Ultimate strength q of the soil in p.s.i.
(2) Depth z of the deepest penetration of the critical logarithmic spiral.

As previously shown, the equation for a logarithmic spiral is

$$r = r_0 e^{\theta \tan \phi} \tag{1}$$

where

r_0 = the initial radius vector
r = any other radius vector
θ = angle between the two radius vectors r_0 and r, measured in radians
e = the base for natural logarithms, 2.71828
ϕ = the angle of internal friction of the material subjected to load

The reaction moment consists of a weight moment plus a cohesion moment. The weight moment is due to the greater weight of material above the spiral to the right than to the left of the ordinate through its origin. The cohesion moment results from the shearing resistance due to cohesion c acting along the length of the spiral. The calculation of the weight moment will be illustrated first.

Step 1

Assume for the first trial that the centre of the critical spiral lies on a radius vector through the left extremity of the loaded area making an angle $\theta_1 = 30^0$, and at a horizontal distance B to the right of the left extremity of the loaded area, Figure 19.

Step 2

Calculate values for $\frac{r_1}{r_0}$, $\sin \theta$, $\frac{r_2}{r_0}$, $\pi - \theta_2$, θ_2, r_0, and r_0^3, all of which are required for determining the weight moment.

By substitution in equation (1), it is found that $\frac{r_1}{r_0} = 1.35$ (see also Barber's Table A, which is based on equation (1), and gives values of $\frac{r}{r_0}$ for different values of θ and ϕ).

$$\sin \theta_1 = \sin 30^0 = 0.5$$

To evaluate $\frac{r_2}{r_0}$, solve the following identity by trial and error.

$$\frac{r_1}{r_0} \sin \theta_1 = \frac{r_2}{r_0} \sin (\pi - \theta_2)$$

from which

$$\frac{r_2}{r_0} = 5.73$$

and

$$\pi - \theta_2 = 6.8^0$$

$$\theta_2 = 180^0 - 6.8^0 = 173.2^0$$

From Figure 19 by inspection

$$r_0 = \left(\frac{B}{\cos \theta_1}\right)\left(\frac{1}{\frac{r_1}{r_0}}\right) = \left(\frac{B}{\cos 30^0}\right)\left(\frac{1}{1.35}\right) = 0.853B$$

$$r_0^3 = 0.621B^3$$

Step 3

Barber (28) lists the following equation for the moment of a sector of a logarithmic spiral,

$$M = \frac{r_0^3}{3 + 27 \tan^2 \theta} \left[e^{3 \theta \tan \phi} \left(\sin \theta + 3 \cos \theta \tan \theta\right) - 3 \tan \phi\right] \quad (2)$$

and in his Table C has tabulated values for $\frac{M}{r_0^3}$ for a wide range of values of θ and ϕ.

The weight moment for the first trial spiral, $\theta_1 = 30^0$, is calculated as follows:

Weight moment of spiral sector OADMGO = 15.69 B^3 w (Barber's Table C (28))

Weight moment of spiral sector OADO = 0.16 B^3 w (Barber's Table C (28))

Weight moment of triangle ODJO $= \left(\frac{B}{2}\right)(B \tan \theta_1)\left(\frac{B}{3}\right)(w) = 0.10\ B^3\ w$

Weight moment of triangle OJGO $= \frac{B \tan \theta_1}{(2)(3)} (B \tan \theta_1 \cot (\pi - \theta_2))^2 w$

$= 2.27\ B^3\ w$

Weight moment of section DMGD $= M_{OADMGO} + M_{OADO} + M_{ODJO} - M_{OJGO}$

$= 15.69\ B^3\ w + 0.16\ B^3\ w = 0.10\ B^3\ w - 2.27\ B^3\ w$

$= 13.68\ B^3\ w$

Therefore, the required value for the weight moment for the first trial spiral = 13.68 B^3 w.

Step 4

The cohesion moment for the length of the first trial spiral actually in the soil must now be calculated.

The moment of the length of a section of a logarithmic spiral is equal to twice the area subtended by the section from its origin. Barber (28) lists the following equation for the area of a sector of a logarithmic spiral,

$$A = \frac{r_0^2}{4 \tan \theta} \left(e^{2 \theta \tan \phi} - 1\right) \quad (3)$$

and in his Table B has tabulated values for $\frac{A}{r_0^2}$ for a wide range of values of θ and ϕ.

Consequently,

$$\text{cohesion moment} = 2c \text{ (area of sector of spiral)}$$
$$= 2c \text{ (area OADMGO - area OADO)}$$
$$\text{Area of sector of spiral OADMGO} = 13.78\ r_0^2 \text{ (Barber's Table B (28))}$$
$$\text{Area of sector of spiral OADO} = 0.36\ r_0^2 \text{ (Barber's Table B (28))}$$

from which

$$\text{cohesion moment} = 2c\ (13.78\ r_0^2 - 0.36\ r_0^2)$$
$$= 26.84\ r_0^2\ c$$

but

$$r_0 = 0.853\ B \qquad \text{(See Step 2 above)}$$

Therefore, the required value for the cohesion moment for the first trial spiral = $19.54\ B^2\ c$.

Step 5

Consequently, for the first trial spiral

$$\text{Total reaction moment} = \text{weight moment plus cohesion moment}$$
$$= 13.67\ B^3\ w + 19.54\ B^2\ c$$

Step 6

Repeat the calculations for Steps 1 to 5 to obtain similar expressions for the total reaction moment when θ_1 is assumed to be 35°, 40°, 45°, and 50°. These are summarized in Table VI.

It should be pointed out in connection with Table VI that the expressions obtained for the reaction moments when assumed values for θ_1 = 30°, 35°, 40°, 45°, and 50°, will always hold for a homogeneous soil for which ϕ = 30°, regardless of the value of cohesion c. Consequently, the reaction moment expressions listed in Table VI do not again have to be calculated as long as the angle of internal friction ϕ = 30° for a homogeneous soil. Similarly, other expressions for reaction moments for assumed values of θ_1 need to be calculated only once when ϕ = 40°, and so on.

It will be observed that reaction moment expressions are given for assumed values of θ_1 in 5° intervals in Table VI. A limited number of calculations indicate that this results in values for ultimate strength that may be sufficiently accurate for practical design.

Step 7

For this sample calculation it has been assumed that c = 5 p.s.i., ϕ = 30°, and w = 135 pounds per cubic foot. By substitution of these values for w and c in the reaction moment expressions in Table VI, the minimum reaction

Table VI. Calculation of Reaction Moments for Different Assumed Values of θ_1 for a Homogeneous Soil for Which $\phi = 30^0$

θ_1	$\frac{r_1}{r_0}$	sin θ_1	$\frac{r_2}{r_0}$	$\pi - \theta_2$	θ_2	r_0	r_0^3	Weight Moments					Cohesion Moment	Total Reaction Moment
								OADMGO	OADO	ODJO	OJGO	Total		
30°	1.35	0.5000	5.73	6.8°	173.2°	0.853B	$0.621B^3$	$15.69B^3w$	$0.16B^3w$	$0.10B^3w$	$-2.27B^3w$	$13.68B^3w$	$19.54B^2c$	$B^2(13.68wB+1^{\wedge}54c)$
35°	1.42	0.5736	5.64	8.3°	171.7°	0.858B	$0.632B^3$	$14.91B^3w$	$0.23B^3w$	$0.12B^3w$	$-2.68B^3w$	$12.58B^3w$	$19.00B^2c$	$B^2(12.58wB+19.00c)$
40°	1.50	0.6428	5.55	10.0°	170.0°	0.872B	$0.664B^3$	$14.57B^3w$	$0.27B^3w$	$0.14B^3w$	$-3.18B^3w$	$11.80B^3w$	$18.81B^2c$	$B^2(11.80wB+18.81c)$
45°	1.57	0.7071	5.45	11.8°	168.2°	0.898B	$0.725B^3$	$14.68B^3w$	$0.35B^3w$	$0.17B^3w$	$-3.83B^3w$	$11.37B^3w$	$19.02B^2c$	$B^2(11.37wB+19.02c)$
50°	1.66	0.7660	5.34	13.7°	166.3°	0.940B	$0.830B^3$	$15.36B^3w$	$0.47B^3w$	$0.20B^3w$	$-4.72B^3w$	$11.31B^3w$	$19.74B^2c$	$B^2(11.31wB+19.74c)$

moment appears to occur for $\theta_1 = 40^0$, and is given by the expression $11.80\ w\ B^3 + 18.81\ B^2\ c$.

It should be noted, however, that each reaction moment expression in Table VI contains the term B^3 in the weight moment portion, and B^2 in the cohesion moment item. (In Figure 19, B is the horizontal distance from the left hand extremity of the loaded area to the ordinate through the origin of the spiral, and is given by DJ.) The value of B (see Step 10 below) varies somewhat with the values of c, ϕ, and θ_1. Consequently, the minimum reaction moment obtained by substituting values for c and w in tables of reaction moments such as Table VI should be checked by substituting the value for B calculated for reaction moment expressions at and on each side of this apparent minimum, to ensure that the minimum reaction moment has been determined.

In this particular case, substitution of the values for w and c gives a minimum reaction moment that is unchanged by the values found for B.

Therefore,

$$\text{the minimum reaction moment} = 11.80wB^3 + 18.81B^2c$$

Step 8

From inspection of Figure 19, and since L = 10, it is apparent that

$$\text{Load moment} = (Lp)\left(B - \frac{L}{2}\right) = 10p\ (B - 5)$$

Step 9

Equating the load moment to the minimum reaction moment gives

$$10p\ (B - 5) = 11.80wB^3 + 18.81B^2c$$

which, upon rearranging, becomes

$$p = \frac{11.80wB^3 + 18.81B^2c}{10\ (B - 5)} \tag{4}$$

but

$$w = 135 \text{ pounds per cu. ft.} = 0.0783 \text{ pounds per cu. in.}$$

and

$$c = 5 \text{ p.s.i.}$$

Substitution of these values for w and c in equation (4) gives

$$p = \frac{0.92\ B^3 + 94.05\ B^2}{10\ (B - 5)} \tag{5}$$

Step 10

In equation (5), p = unit applied load, while B = the horizontal distance from the left extremity of the loaded area to the ordinate through the origin of the critical logarithmic spiral. It is necessary to find the value for B that will result in the minimum value for p; that is, to find the origin of the spiral

that will provide the smallest ultimate strength q. This is obtained by differentiating equation (5) with respect to B, equating the derivative to zero, and solving the resulting quadratic equation for B.

Differentiating equation (5), simplifying, and equating the resulting equation to zero, gives

$$\frac{dp}{dB} = B^2 + 43.6\,B - 511.1 = 0 \qquad (6)$$

Solving equation (6) for B gives

$$B = 9.6 \text{ inches.}$$

Consequently, the origin of the required critical logarithmic spiral is located on the radius vector making an angle $\theta_1 = 40^\circ$, at the point of intersection of this radius vector with the ordinate spaced 9.6 inches to the right of the left hand extremity of the loaded strip, Figure 19.

Step 11

The ultimate strength q is obtained by substituting the value 9.6 for B in equation (5), and solving for p, which gives

$$p = 206 \text{ p.s.i.}$$

Therefore, the ultimate strength q for a homogeneous soil for which c = 5 p.s.i. and $\phi = 30^\circ$, and for the other conditions illustrated in Figure 19, is 206 p.s.i.

Step 12

To find the depth z of the deepest penetration of the critical logarithmic spiral below the ground surface.

From Figure 19,

Angle OMR = $90 - \phi$, since the tangent to a logarithmic spiral always makes an angle of $90 - \phi$ with the radius vector at the point of tangency.

Also,

$$\text{Angle OMR} = 180 - \theta_z$$

Consequently,

$$90 - \phi = 180 - \theta_z$$

or

$$\theta_z = 90 + \phi$$

In addition,

$$z + h = r_z \cos(\theta_z - 90^\circ) = r_z \cos\phi$$

but,

$$h = B \tan\theta_1$$

Therefore,

$$z = r_z \cos \phi - B \tan \theta_1 \tag{7}$$

The value of each term in equation (7), except r_z, has already been evaluated.

$$\cos \phi = \cos 30^0 = 0.866$$

$$B = 9.6$$

$$\tan \theta_1 = \tan 40^0 = 0.8391$$

r_z can be evaluated from the general equation for the logarithmic spiral,

$$r_z = r_0 e^{\theta_z \tan \phi} \tag{8}$$

for which

$$r_0 = 0.870\ B = (0.870)\ (9.6) = 8.35$$

$$\theta_z = 90 + \phi = 90 + 30 = 120^0 = 2.0944 \text{ radians}$$

$$\tan \phi = \tan 30^0 = 0.5774$$

Substituting these values in equation (8) and solving, gives

$$r_z = 28.0 \text{ inches.}$$

All terms on the right hand side of equation (7) have now been evaluated. Substituting these values in equation (7) gives

$$z = (28.0)\ (0.866) - (9.6)\ (0.8391) = 16.2 \text{ inches.}$$

Consequently, the maximum penetration of the critical logarithmic spiral below the ground surface, z, is 16.2 inches.

APPENDIX B

Sample Calculation for the Ultimate Strength of a Two-Layer System by the Logarithmic Spiral Method

The objective of this sample calculation is the determination of the maximum applied strip load that a two-layer system consisting of a bituminous surface on a great depth of base course can support without failure for the conditions illustrated in Figure 20, assuming the failure curve to be a logarithmic spiral.

In essence, the method employed requires the determination of c and ϕ values for an equivalent homogeneous material having the same ultimate strength as the layered system. After these c and ϕ values have been determined, the ultimate strength of the equivalent homogeneous material can be obtained by the method outlined in Appendix A. It is assumed, of course, that this method is capable of providing c and ϕ values for an equivalent homogeneous material having the same ultimate strength as the layered system.

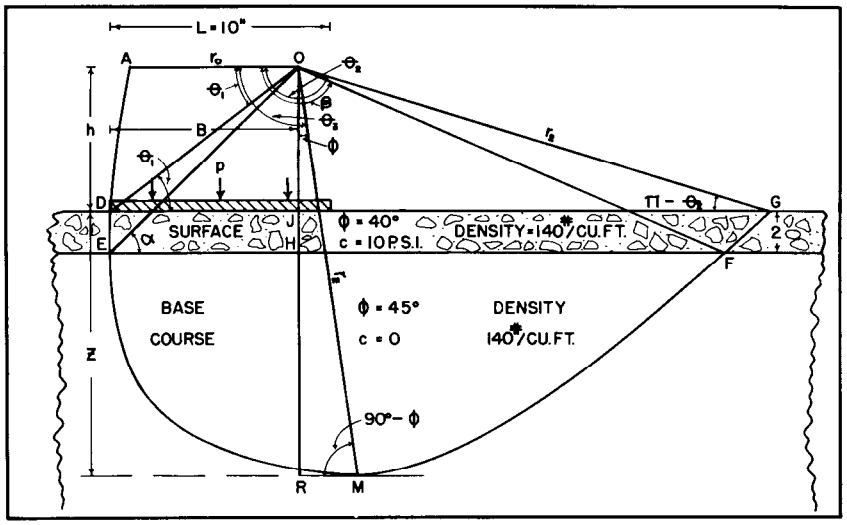

Fig. 20. Illustrating the Logarithmic Spiral Method for Calculating the Ultimate Strength of a Two-Layer System of Flexible Pavement.

There is a different material in each layer of the two-layer system of Figure 20, and each has its own c and ϕ values. To find the values of c and ϕ for an equivalent homogeneous material having the same ultimate strength as the two-layer system, the method of successive approximations is employed, assuming in all cases that the failure curve is a logarithmic spiral.

As the first step in this method, single values for c and ϕ for the equivalent homogeneous material are assumed, and the critical logarithmic spiral is determined as described in Appendix A. Based on the actual values of c and ϕ for each layer traversed by the spiral, overall average values for c and ϕ assumed to be acting along the full length of the spiral can be calculated. These calculated average values for c and ϕ will usually be different than those arbitrarily assumed for this spiral. A second critical spiral is, therefore, determined, based on a homogeneous material having the average values for c and ϕ calculated for the first spiral. Using the procedure just outlined for the first spiral, overall average values for c and ϕ acting along the full length of the second spiral can be calculated. Using this second set of average values for c and ϕ, a third critical spiral is determined, from which a third set of overall average values for c and ϕ can be calculated, and used for establishing the fourth spiral. This process can be repeated as often as required.

As illustrated in Figure 21, each successive spiral approaches more nearly to the ultimate spiral that would result from many successive approximations. Table IV demonstrates that the differences in overall average values for c and ϕ, and in the values of ultimate strength, become progressively smaller between successive approximations. Consequently, the number of successive approximations to be used in any given case depends upon the degree of accuracy needed for practical design. For the conditions covered by

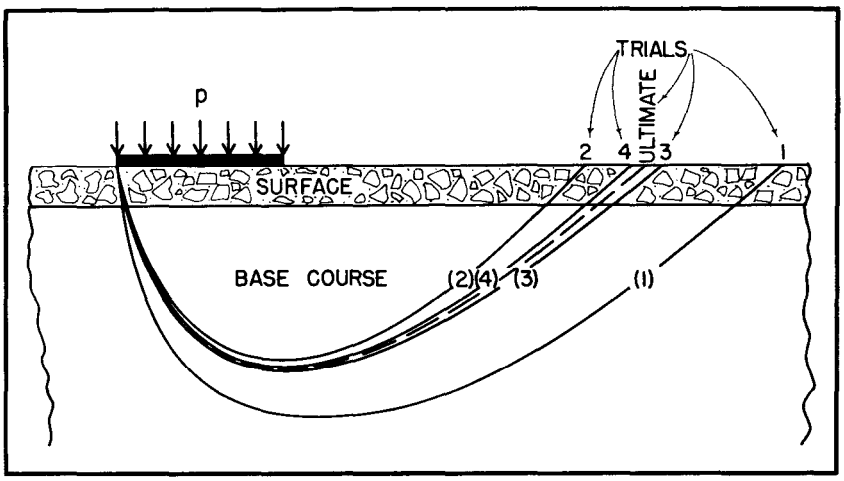

Fig. 21. Illustrating Relative Positions of Logarithmic Spirals Resulting from Successive Trials When Applying the Method of Successive Approximations.

Table IV, even the second successive approximation would provide the accuracy required.

The successive steps required for the application of this method will be outlined in a sample calculation based on the following conditions illustrated in Figure 20.

Strip Loading

Width of Loaded Strip = L = 10 inches

For Surface Course, c = 10 p.s.i., $\phi = 40^0$

For Base Course, $\phi = 45^0$, c = 0

Thickness of Surface Course = 2 inches

Density of both layers = w = 140 lbs./cu.ft. = 0.081 lbs./cu.in.

The following information is required:

(1) Ultimate strength q of the two-layer system in p.s.i.
(2) Depth z of the deepest penetration of the critical logarithmic spiral.

The successive steps required for the determination of the ultimate strength of the two-layer system will be described first.

Step 1

Arbitrarily assume c and ϕ values for the homogeneous material that is to have the same ultimate strength as that of the given two-layer system. With more experience, it may be possible to assume a set of c and ϕ values in this first step that are not greatly different from the ultimate values for c

and ϕ determined at the end of the successive approximation procedure. These will be intermediate between those for the surface course and the base course; that is, c will be somewhere between 0 and 4 p.s.i., and ϕ somewhere between 40° and 45°. Since the angles of internal friction ϕ of the base and surface course are not greatly different, the c and ϕ values for the base course will be selected for the first approximation in this case.

The arbitrarily assumed values for c and ϕ for the equivalent homogeneous material for the first step, therefore, are c = 0 p.s.i. and ϕ = 45°.

Step 2

Determine the critical spiral for a homogeneous material for which c = 0 p.s.i. and ϕ = 45°, by the trial and error method outlined in Appendix A. The ultimate strength q for this homogeneous material as calculated from the critical spiral = 318.5 p.s.i. (Table IV).

Step 3

On the basis of the actual values of c and ϕ in each of the two layers traversed by this spiral, determine overall average values for c and ϕ assumed to be acting along the full length of the spiral. The overall average value for ϕ will be calculated first.

Step 4

Calculate the total length of this first spiral (below ground level), and also the length of each of the left-hand and right-hand portions of the spiral lying entirely within the surface course.

The length of the arc DMG of the spiral is found by integrating the following equation:

$$\text{Length of arc DMG} = \frac{r_0 \sqrt{\tan^2 \phi + 1}}{\tan \phi} \left[e^{\theta \tan \phi} \right]_{\theta_1}^{\theta_2} \qquad (9)$$

By the procedure of Step 2, Appendix A,

$$r_0 = 4.965 \text{ inches}$$

$$\theta_1 = 53°12' = 0.9285 \text{ radians}$$

$$\theta_2 = 174°30' = 3.0457 \text{ radians}$$

$$\tan \phi = \tan 45° = 1.000$$

Substituting these values in equation (9) and simplifying,

$$\text{Length of arc DMG} = 129.856 \text{ inches}$$

To find length of arc of spiral DE, angle α must be first evaluated:

$$B = 7.500 \text{ inches (Procedure of Appendix D)}$$

$$OJ = B \tan \theta_1$$

$$\tan \theta_1 = \tan 53°12' = 1.33673$$

$$OJ = (7.500)\,(1.33673) = 10.025 \text{ inches}$$

$$OH = OJ + 2 \text{ inches} = 12.025 \text{ inches}$$

$$\frac{OH}{OE} = \sin \alpha$$

Also

$$OE = r_0\, e^{\alpha \tan \phi} = 4.965\, e^{\alpha}$$

Then

$$\frac{OH}{\sin \alpha} = 4.965\, e^{\alpha}$$

or

$$\sin \alpha\, e^{\alpha} = \frac{12.025}{4.965} = 2.42195 \tag{10}$$

Solving equation (10) by trial and error gives

$$\alpha = 59^{\circ}19' = 1.0353 \text{ radians}$$

$$\text{Length of arc DE} = \frac{r_0 \sqrt{\tan^2 \phi + 1}}{\tan \phi} \left[e^{\theta \tan \phi} \right]_{\theta_1}^{\alpha} \tag{11}$$

Substituting known values for each term on the right-hand side of equation (11) and simplifying gives

$$\text{Length of arc DE} = 2.003 \text{ inches}$$

By a similar series of calculations, it is found that

$$\text{Length of arc FG} = 3.237 \text{ inches}$$

Therefore,

$$\text{Total length of spiral in bituminous surface} = 2.003 + 3.237 = 5.240 \text{ inches}$$

$$\text{Total length of spiral in base course} = 129.856 - 5.240 = 124.616 \text{ inches}$$

Step 5

To obtain the overall average value for ϕ along the whole spiral DMG,

$$(129.856)\,\phi_{av} = (5.240)\,(\phi = 40^{\circ}) + (124.616)\,(\phi = 45^{\circ})$$

$$\phi_{av} = \frac{(5.240)(40) + (124.616)\,(45)}{129.856}$$

$$= 44^{\circ}48'$$

Therefore, the overall average value for ϕ along the length of the first spiral is 44°48'.

Step 6

To obtain the overall average value for cohesion c along the whole spiral DMG,

$$(129.856)\, c_{av} = (5.240)\,(c = 10) + (124.616)\,(c = 0)$$

$$c_{av} = \frac{(5.240)\,(10) + (124.616)\,(0)}{116.16}$$

$$= 0.4035 \text{ p.s.i.}$$

Therefore, the overall average value for cohesion c along the length of the first spiral is 0.4035 p.s.i.

Step 6 (Alternative)

As an alternative to the method just given in Step 6, an average value for cohesion c can be obtained by equating the sum of the cohesion moments for the two portions of the spiral, DE and FG, entirely within the surface course, to the cohesion moment for the entire spiral, DMG, resulting from the use of this overall average value for cohesion c.

The general equation for the cohesion moment of an arc of a logarithmic spiral is

$$\text{cohesion moment of arc of spiral} = \frac{c r_0^2}{2 \tan \phi} \left[e^{2 \theta \tan \phi} \right]_{\theta_1}^{\theta_2} \qquad (12)$$

From the conditions for this sample calculation, Figure 20, cohesion c = 10 p.s.i. for the portion of the spiral within the bituminous surface, and c = 0 for the base. Consequently, cohesion moments for the different parts of the spiral can be calculated.

$$\text{Cohesion moment for arc DE} = \frac{c r_0^2}{2 \tan \phi} \left[e^{2 \theta \tan \phi} \right]_{\theta_1}^{\alpha} \qquad (13)$$

Substituting known values for each term on the right hand side of equation (13), and simplifying, gives

$$\text{Cohesion moment for arc DE} = 187.9 \text{ inch lbs.}$$

$$\text{Cohesion moment for arc FG} = \frac{c r_0^2}{2 \tan \phi} \left[e^{2 \theta \tan \phi} \right]_{\beta}^{\theta_2} \qquad (14)$$

Substituting known values for each term on the right-hand side of equation (14), and simplifying, gives

$$\text{Cohesion moment for arc FG} = 2366.5 \text{ inch lbs.}$$

$$\text{Cohesion moment for arc DMG} = \frac{c_{av} r_0^2}{2 \tan \phi} \left[e^{2 \theta \tan \phi} \right]_{\theta_1}^{\theta_2} \qquad (15)$$

Substituting known values for each term on the right hand side of equation (15), and simplifying, gives,

Cohesion moment for arc DMG = 5369.0 c_{av} inch lbs.

Equating these cohesion moments,

$$5369.0\ c_{av} = 187.9 + 2366.5 = 2554.4$$

for which,

$$c_{av} = \frac{2554.4}{5369.0} = 0.476 \text{ p.s.i.}$$

Consequently, the overall average value for cohesion c along the length of this first spiral, as obtained by the moment method, is 0.476 p.s.i.

Step 7

Since the overall average value for cohesion c obtained as an arithmetic average is somewhat smaller than that given by the moment method, it is used here because it is more conservative.

Average values for c and ϕ given by the first spiral (first approximation), which are to be used for the spiral representing the second approximation, therefore, are

$$c = 0.404 \text{ p.s.i.}$$

$$\phi = 44°48'$$

It will be observed that these average values for c and ϕ calculated for the first spiral are somewhat different from the values of c = 0 p.s.i. and $\phi = 45°$ that were arbitrarily assumed for its construction.

The method of successive approximations must, therefore, be continued until the overall average values for c and ϕ calculated for any spiral are very nearly the same as the values of c and ϕ used for its determination. Expressed in another way, this method must be continued until the overall average values for c and ϕ calculated for spirals representing two successive approximations are quite close to each other (Table IV and Figure 21).

Step 8

Determine the critical logarithmic spiral (second successive approximation) for a homogeneous material for which c = 0.404 p.s.i. and $\phi = 44°48'$, by the trial and error method outlined in Appendix A. The ultimate strength q for this homogeneous material as calculated from this second critical spiral = 383.2 p.s.i. (Table IV).

Step 9

Calculate overall average values for c and ϕ as given by this second critical spiral, using the procedure described in Steps 4, 5, and 6. These overall average values are found to be c = 0.401 p.s.i. and $\phi = 44°48'$. These values are used for the third successive critical spiral.

Step 10

Determine the critical logarithmic spiral (third successive approximation) for a homogeneous material for which c = 0.401 p.s.i. and $\phi = 44°48'$, by the trial and error method outlined in Appendix A. The ultimate strength q for this homogeneous material as calculated from this third critical spiral = 382.8 p.s.i. (Table IV).

Step 11

While three successive approximations are sufficient in this case, in general this procedure must be repeated for as many further successive approximations as may be required for the accuracy needed; that is, until the per cent difference in ultimate strength values between two successive approximations is as small as desired.

From Table IV, it will be observed that the ultimate strength given by the third critical spiral (third successive approximation) is only 0.1 per cent higher than that found for the second critical spiral. In this case, therefore, either the second or third critical spiral provides an ultimate strength value of sufficient accuracy for practical design.

Figure 21 demonstrates that the critical spirals given by each successive approximation in the above steps lie alternately on either side and successively closer to the ultimate critical spiral that would result from many successive approximations.

Step 12

Determine the value for z, representing the deepest penetration of any logarithmic spiral below the ground surface, by the procedure illustrated in Step 12, Appendix A. The value of z for the third critical spiral of Table IV is found to be 27.7 inches.

APPENDIX C

Sample Calculation for the Ultimate Strength of a Three-Layer System by the Logarithmic Spiral Method

The objective of this sample calculation is the determination of the maximum applied strip load that a three-layer system, consisting of a bituminous surface, base course, and subgrade, can support without failure for the conditions illustrated in Figure 22, assuming the failure curve to be a logarithmic spiral.

Generally speaking, the method employed requires the determination of c and ϕ values for an equivalent homogeneous material having the same ultimate strength as the layered system. After these c and ϕ values have been determined, the ultimate strength of the equivalent homogeneous material can be obtained by the method described in Appendix A. It is assumed, of course, that this method is capable of providing c and ϕ values for an equivalent homogeneous material having the same ultimate strength as the layered system.

There is a different material in each layer of the three-layer system of Figure 22, and each has its own c and ϕ values. To find the values of c and ϕ for an equivalent homogeneous material having the same ultimate strength as

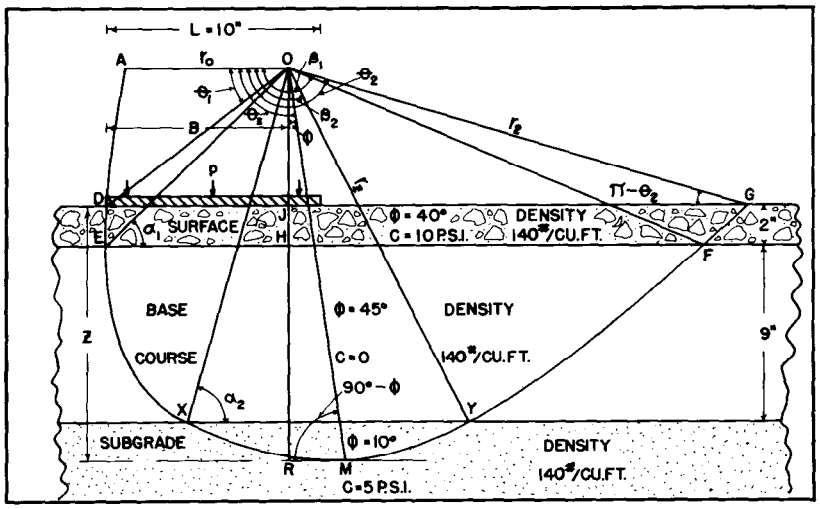

Fig. 22. Illustrating the Logarithmic Spiral Method for Calculating the Ultimate Strength of a Three-Layer Flexible Pavement System.

the three-layer system, the method of successive approximations is employed, assuming in all cases that the failure curve is a logarithmic spiral.

As the first step in this method, a value for c and a value for ϕ for the equivalent homogeneous material are assumed, and the critical logarithmic spiral is determined as described in Appendix A. Based on the actual values of c and ϕ for each layer traversed by the spiral, overall average values for c and ϕ assumed to be acting along the full length of the spiral can be calculated. These calculated values for c and ϕ will usually be different from those arbitrarily assumed at the beginning for this spiral. A second critical spiral is, therefore, determined, based on a homogeneous material having the average values for c and ϕ calculated for the first spiral. Using the procedure just outlined for the first spiral, overall average values for c and ϕ acting along the full length of the second spiral can be calculated. Using this second set of average values for c and ϕ, a third critical spiral is determined, from which a third set of overall average values for c and ϕ can be calculated and used for establishing the fourth spiral. This process can be repeated until the ultimate strength values given by two successive trial spirals are close enough for practical design.

The number of trials required can be reduced by a modification of the above procedure. For example, instead of using c and ϕ values calculated for the second trial spiral to establish the third trial spiral, the original and calculated values for c and ϕ for the second trial spiral are averaged, and these average values for c and ϕ are used to establish the third trial spiral.

The successive steps required for the application of the logarithmic spiral method to the determination of the ultimate strength of a three-layer flexible pavement system will be outlined in a sample calculation based upon the following conditions illustrated in Figure 22.

Strip loading

Width of loaded strip = L = 10 inches

For surface course, c = 10 p.s.i., $\phi = 40^0$

For base course, c = 0 p.s.i., $\phi = 45^0$

For subgrade, c = 5 p.s.i., $\phi = 10^0$

Density of all three layers = w = 140 lbs. per cu. ft.
= 0.081 lb. per cu. ft.

The following information is required:

(1) Ultimate strength q of the three-layer system in pounds per square inch.
(2) Depth z of the deepest penetration of the critical logarithmic spiral.

The successive steps required for the determination of the ultimate strength of the three-layer system will be described first.

Some Useful Graphs

Before proceeding with the sample calculation itself, several useful graphs, that have been developed to reduce the number of calculations required to determine the ultimate strength of a multi-layered flexible pavement system by means of the logarithmic spiral method, will be described.

The calculation of values for each of the variables listed in Table VI of Appendix A is a time-consuming task, even when such tables are prepared for values of the angle of internal friction ϕ at relatively wide intervals of 10^0. Furthermore, values of θ_1 at 5^0 intervals as given in Table VI for an angle of internal friction $\phi = 30^0$, are not closely spaced enough to pinpoint the values of θ_1 at which the minimum cohesion moment and minimum weight moment occur. For a situation like this, graphs are desirable because of the continuous spectrum of values for each variable that their use makes possible.

Figures 23, 24, 25, 26, and 27 provide values for each of the important variables listed in Table VI pertaining to materials with a continuous range of angles of internal friction ϕ from 0^0 to 60^0.

Figure 23 illustrates the values for the numerical coefficients K_w and K_c associated with the weight moment and cohesion moment, respectively, for a relatively wide range of values for θ_1 for a material with an angle of internal friction $\phi = 30^0$. Figure 23 consists of a graphical plot of data taken from Table VI, which applies only when the angle of internal friction ϕ of the material is 30^0. For example, from the second row of data in Table VI, $\theta_1 = 35^0$, the weight moment is $12.58\ B^3\ w$, from which $K_w = 12.58$, while the cohesion moment is $19.0\ B^2\ c$, so that $K_c = 19.0$. The same values can be read from Figure 23.

It is obvious from Figure 23 that values for the numerical coefficients K_w and K_c both go through minimums as the value of θ_1 is varied through the appropriate range. It is also apparent that θ_1 for the minimum value of K_w does not coincide with the value of θ_1 at which the minimum value of K_c occurs. Minimum K_c is observed at $\theta_1 = 40^0$, while minimum K_w occurs at $\theta_1 = 48.5^0$. As the angle of internal friction ϕ increases, the θ_1 values at which minimum K_w and minimum K_c occur become much closer together, but diverge as ϕ becomes smaller. This is well illustrated in Figure 25.

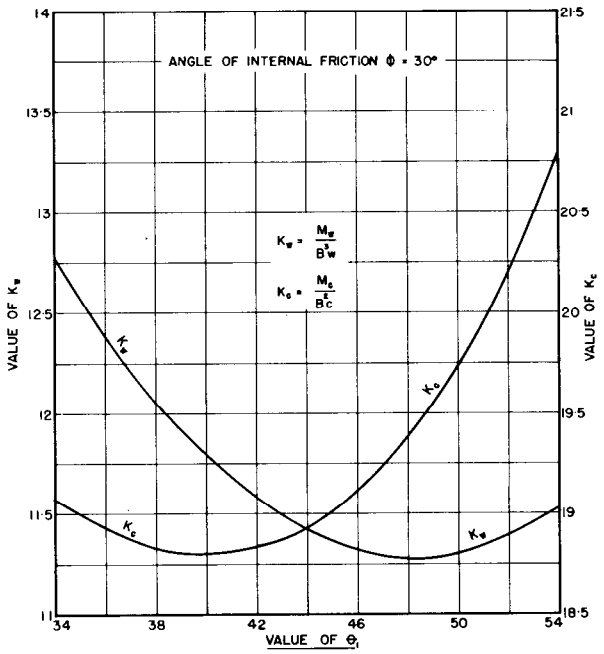

Fig. 23. For a Given Value of Angle of Internal Friction ϕ, Illustrating Graphical Determination of the Values of θ_1 at which Minimum Values of K_w and K_c Occur.

Graphs similar to that of Figure 23 have been prepared for angle of internal friction ϕ of 2, 4, 10, 20, 30, 40, 50, and 60°.

It is one of the principal purposes of graphs like Figure 23 to provide the minimum values of K_c and K_w, since these particular values of K_w and K_c are required for the determination of the reaction moment associated with the maximum load that can be applied. Figure 24 is a graph of the minimum values of K_c and K_w for materials with angles of internal friction ϕ varying from 0° to 60°. Figure 24 indicates that the minimum values of K_w become quite small for materials with angles of internal friction ϕ less than about 15°. This means that for materials with angles of internal friction from 0° to about 15°, the weight moment is quite small relative to the cohesion moment; that is, the total reaction moment consists largely of the cohesion moment. When ϕ = 0°, the reaction moment, of course, is equal to the cohesion moment, and the weight moment is zero.

Figure 25 illustrates the relationship between angle of internal friction ϕ, and the values of θ_1 at which minimum values of K_w and K_c occur. However, the overall reaction moment required is associated with a single value of θ_1. This particular value of θ_1 must lie between the values of θ_1 for minimum K_w and minimum K_c. For example, if ϕ = 30°, the value of θ_1 pertaining to the minimum overall reaction moment will be between θ_1 = 40° (minimum K_c) and θ_1 = 48.5° (minimum K_w). The required single value of θ_1 between these

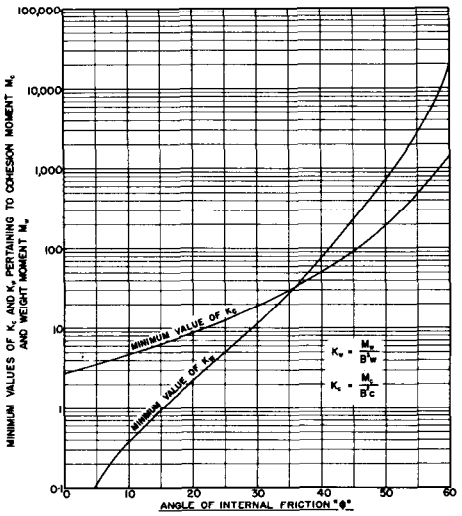

Fig. 24. Graph Showing Relationship between Angle of Internal Friction ϕ and Minimum Values of K_C and K_W Pertaining to Cohesion Moment M_C and Weight Moment M_W Respectively.

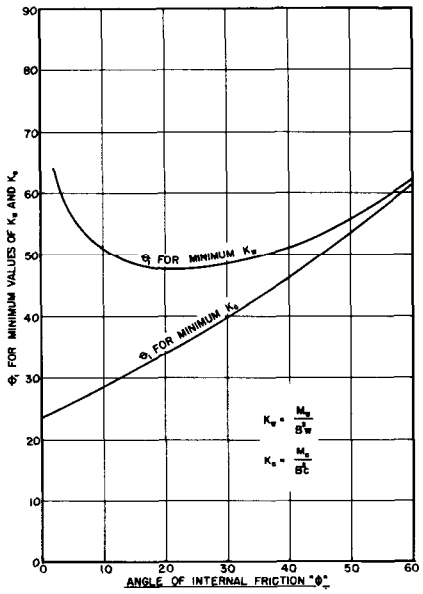

Fig. 25. Graph Showing Relationship between Angle of Internal Friction ϕ and Magnitude of θ_1 for Corresponding Minimum Values of K_W and K_C.

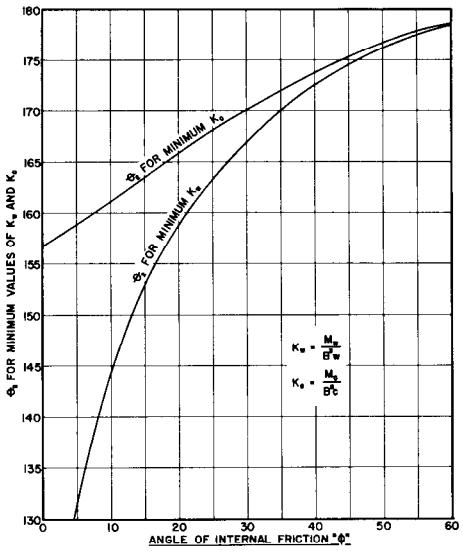

Fig. 26. Graph Showing Relationship between Angle of Internal Friction ϕ and Magnitude of θ_2 for Corresponding Minimum Values of K_w and K_c.

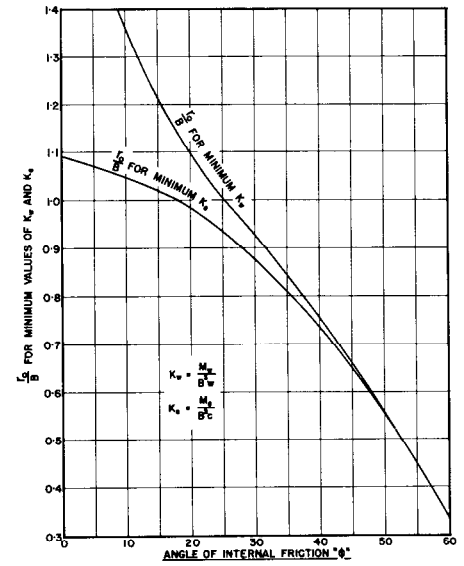

Fig. 27. Graph Showing Relationship between Angle of Internal Friction ϕ and Magnitude of r_0/B for Corresponding Minimum Values of K_w and K_c.

limits can be established on the basis of the relative magnitudes of the cohesion moment and the weight moment. For example, if the minimum cohesion moment is one-half the minimum weight moment for a material having an angle of internal friction $\phi = 30^0$, the value of θ_1 needed for determining the required overall reaction moment is $40^0 + (2/3)(48.5 - 40) = 45.7^0$. It should be added that θ_1 can vary appreciably from the single value established by this method without having any marked effect on the value of the overall reaction moment.

Figure 26 provides values of θ_2 for corresponding minimum values of K_c and K_w for materials with angles of internal friction ϕ up to 60^0. For any given problem, the required single value of θ_2 can again be determined on the basis of the relative magnitudes of the cohesion and weight moments.

In Figure 27, the values of $\frac{r_0}{B}$ associated with the minimum values of K_c and K_w for materials with angles of internal friction ϕ from 0^0 to 60^0 are given. In this case also, the single value of $\frac{r_0}{B}$ required for the solution of the problem is intermediate between those given by the two curves, and depends upon the ratio of the cohesion and weight moments.

When the procedure of Appendix B is followed, one of the most time-consuming phases of the solution is the calculation of the lengths of the portions of the logarithmic spiral lying within each layer of the flexible pavement. Before the lengths of the arcs of the spiral within each layer can be calculated, the size of the angles θ_1, α, θ_2, and β in Figure 20, or θ_1, α_1, α_2, θ_2, β_2, and β_1, in Figure 22 must be accurately determined to within a small fraction of a degree, since they serve as the limits of integration in the equation for the length of an arc of a spiral (Equation (9), Step 4, Appendix B). Determining the sizes of these angles accurately is a lengthy procedure because of the trial and error method involved at one stage, Step 4, Appendix B.

By using polar coordinate graph paper of rather large size (e.g. 17 x 11 inches), Figure 28, the size of the different angles θ_1, α_1, α_2, θ_2, β_2, and β_1 can be read directly from the graph to the nearest one-tenth of a degree, which provides sufficient accuracy for the solution of practical problems. In this case, the origin of the polar coordinate paper must also be the origin of the logarithmic spiral. The spiral itself can be easily drawn, Figure 28.

The information provided by the graphs of Figures 24, 25, 26, 27, and 28 will now be utilized to facilitate the solution of the three-layer flexible pavement problem described earlier in Appendix C, and illustrated by Figure 22.

Step 1

Arbitrarily assume c and ϕ values for the homogeneous material that is to have the same ultimate strength as that of the given three-layer system.

The arbitrarily assumed values for c and ϕ for the first step are

$$c = 5 \text{ p.s.i. and } \phi = 30^0$$

Step 2

From Figure 24 read off minimum values of K_w and K_c for $\phi = 30^0$.

$$K_w = 11.35$$

$$K_c = 18.85$$

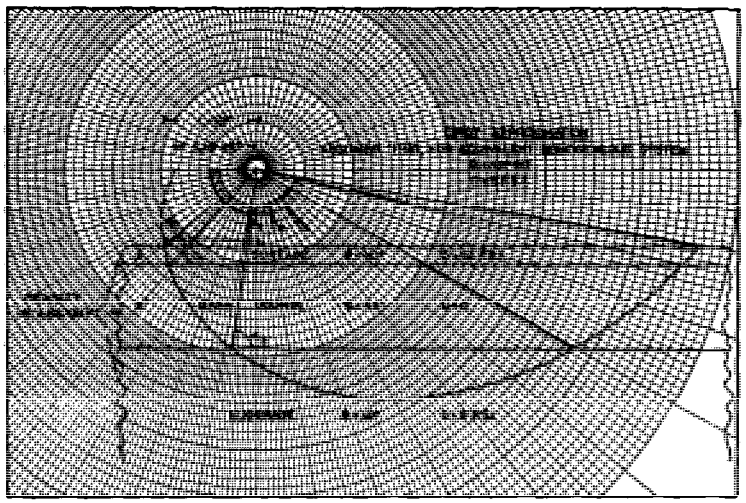

Fig. 28. Illustrating Graphical Procedure Based on Polar Coordinates for Simplifying Calculation of Ultimate Strength of a Three Layer Flexible Pavement System by the Logarithmic Spiral Method.

Substitute these values in the reaction moment equation

$$M_R = B^3 K_w w + B^2 K_c c \tag{16}$$

giving

$$M_R = 11.35 B^3 w + 18.85 B^2 c$$

but

$$w = 0.081 \text{ lbs./cu. in.}$$

and

$$c = 5 \text{ p.s.i.}$$

Therefore,

$$M_R = 0.919 B^3 + 94.25 B^2 \tag{17}$$

Step 3

From inspection of Figure 22, and since L = 10, it is apparent that the load moment is given by

$$M_L = 10p (B - 5) \tag{18}$$

Step 4

Equating the load moment to the reaction moment gives

$$10p (B - 5) = 0.919 B^3 + 94.25 B^2$$

which, upon rearranging, becomes

$$p = \frac{0.919\ B^3 + 94.25\ B^2}{10\ (B - 5)} \tag{19}$$

Step 5

It is necessary to find the value of B, for which p will be a minimum, since this minimum value of p will be the ultimate strength q. The value of B that will give a minimum value of p is found by differentiating equation (19) with respect to B, equating the derivative to zero, and solving the resulting quadratic equation for B.

Differentiating equation (19), simplifying, and equating the resulting equation to zero gives

$$\frac{dp}{dB} = B^2 + 43.78\ B - 512.79 = 0 \tag{20}$$

Solving equation (20) for B gives

$$B = 9.61$$

Step 6

The ultimate strength q is the value of p obtained by substituting the value 9.61 for B in equation (19), and solving for p, giving

$$p = 206.5 \text{ p.s.i.}$$

Step 7

To establish the origin of the critical logarithmic spiral for which the ultimate load q is a minimum, it is necessary to determine the value of θ_1 in addition to B. From Figure 25, it is apparent that minimum values of K_w and K_c do not occur at the same value of θ_1. Since only one value of θ_1 can be used to determine the origin of the critical spiral, a weighted average of the two values of θ_1 must be taken. This weighted average value for θ_1 is established on the basis of the relative magnitudes of the cohesion moment M_c and the weight moment M_w.

$$\begin{aligned} M_w &= 0.919\ B^3 && \text{(from equation (17))} \\ &= (0.919)\ (886.3) \\ &= 814.5 \\ M_c &= 94.25\ B^2 && \text{(from equation (17))} \\ &= (94.25)\ (92.3) \\ &= 8696.1 \end{aligned}$$

Consequently, the cohesion moment M_c is more than ten times as large as the weight moment M_w. It will be remembered that the total reaction moment $M_R = M_w + M_c$.

Step 8

From Figure 25,

$$\text{for } K_w \text{ (minimum)}, \ \theta_1 = 48.42^\circ$$
$$\text{for } K_c \text{ (minimum)}, \ \theta_1 = 39.8^\circ$$

Consequently,

$$\text{for } M_w \text{ (minimum)}, \ \theta_1 = 48.42^\circ, \text{ and}$$
$$\text{for } M_c \text{ (minimum)}, \ \theta_1 = 39.8^\circ.$$

The weighted average value of θ_1 to be employed for locating the origin of the critical spiral will be closer to 39.8° than to 48.42°, because the cohesion moment M_c is more than ten times as large as the weight moment M_w. The required value of θ_1 is

$$48.42 - \frac{M_c}{M_c + M_w}(49.42 - 39.8)$$
$$= 48.42 - \frac{8696.1}{8696.1 + 814.5}(8.62)$$
$$= 48.42 - 7.88$$
$$= 40.54^\circ = 40^\circ 32'$$

Therefore, the value of θ_1 required to establish the origin of the critical spiral is $\theta_1 = 40^\circ 32'$.

Step 9

It is not necessary to calculate the value of θ_2, but preknowledge of its value provides a useful check on the accuracy employed when drawing in the spiral on polar coordinate graph paper, Figure 28.

From Figure 26,

$$\text{for } M_w \text{ (minimum)}, \theta_2 = 166.8^\circ$$
$$\text{for } M_c \text{ (minimum)}, \theta_2 = 170.0^\circ$$

Only one value of θ_2 can be used to determine the origin of the critical spiral, and it must lie between the two values 166.8° and 170.0°. Its value is established on the basis of the relative magnitudes of the cohesion moment M_c and the weight moment M_w, following the procedure of Step 7. This gives

$$\theta_2 = 169^\circ 43'$$

Step 10

From Figure 27

$$\text{for } M_w \text{ (minimum)}, \frac{r_0}{B} = 0.926$$

for M_c (minimum), $\frac{r_0}{B} = 0.873$

Again, only one value of $\frac{r_0}{B}$ can be employed for establishing the origin of the critical spiral. Following the procedure of Step 7, a weighted average value is found for $\frac{r_0}{B}$, which is

$$\frac{r_0}{B} = 0.878$$

However,

$$B = 9.61 \qquad \text{(Step 5)}$$

Therefore,

$$r_0 = (0.878)\,(9.61)$$
$$= 8.42 \text{ inches.}$$

Step 11

On the basis of the values for B, θ_1, and r_0 obtained in Steps 5, 8, and 10, the critical logarithmic spiral can be drawn, Figure 28. Read values of the angles α_1, α_2, β_1, β_2, *from the graph (Figure 28) to the nearest one-tenth* degree. As a check, the value of θ_2 provided by the spiral should be read as close as possible from the graph, and compared with the calculated value of θ_2 from Step 9.

From Figure 28

$$\alpha_1 = 48°48'$$
$$\alpha_2 = 83°00'$$
$$\beta_1 = 166°45'$$
$$\beta_2 = 149°30'$$
$$\theta_2 = 169°42'$$

Step 12

The total length of the spiral (below the pavement surface), and the lengths of the portions of the spiral lying within each layer of the three-layer system, Figures 22 and 28, can now be calculated.

The length of the arc DMG of the spiral is found by integrating the following equation,

$$\text{Length of arc DMG} = \frac{r_0\sqrt{\tan^2\phi + 1}}{\tan\phi}\left[e^{\theta \tan\phi}\right]_{\theta_1}^{\alpha_2} \qquad (9)$$

It has already been determined that

$$r_0 = 8.43$$
$$\theta_1 = 40°32'$$

$$\theta_2 = 169^\circ 43'$$

$$\tan \phi = \tan 30^\circ = 0.57735$$

Substituting these values in equation (9), and simplifying,

$$\text{Length of arc DMG} = 67.953 \text{ inches}$$

Similarly,

$$\text{Length of arc DE} = \frac{r_0\sqrt{\tan^2 \phi + 1}}{\tan \phi} \left[e^{\theta \tan \phi}\right]_{\theta_1}^{\alpha_1} \tag{21}$$

By inspection, from Figure 28

$$\alpha_1 = 48^\circ 48',$$

and the other variables were previously evaluated.

Substituting these values in equation (21), and simplifying,

$$\text{Length of arc DE} = 2.204 \text{ inches.}$$

In a similar manner, since values for α_2, β_2, β_1, and θ_2 can be read from the drawing (Figure 28), by suitable substitution in equations similar to equation (21), it is found that

$$\text{Length of arc EX} = 11.343 \text{ inches}$$

$$\text{Length of arc XY} = 37.143 \text{ inches}$$

$$\text{Length of arc YF} = 14.439 \text{ inches}$$

$$\text{Length of arc FG} = 2.824 \text{ inches}$$

Therefore,

$$\text{Total length of spiral in bituminous surface} = 2.204 + 2.824 = 5.028 \text{ inches}$$

$$\text{Total length of spiral in base course} = 11.343 + 14.439 = 25.782 \text{ inches}$$

$$\text{Total length of spiral in subgrade} = 37.143 \text{ inches}$$

Step 13

A method for obtaining an overall average value for the angle of internal friction ϕ along the whole spiral DMG has been illustrated in Step 5, Appendix B. Consequently,

$$(67.953)\ \phi_{av} = (5.028)(\phi = 40^\circ) + (25.782)(\phi = 45^\circ) + (37.143)(\phi = 10^\circ)$$

from which

$$\phi_{av} = \frac{(5.028)(40) + (25.782)(45) + (37.143)(10)}{67.953}$$

$$= 25°30'$$

Therefore, the overall average value for ϕ along the length of the first spiral is 25 deg. 30 min.

Step 14

A method for obtaining an overall average value for cohesion c along the whole spiral DMG has been illustrated in Step 6, Appendix B. Consequently,

$$(67.953)\, c_{av} = (5.028)(c = 10) + (25.782)(c = 0) + (37.143)(c = 5)$$

from which

$$c_{av} = \frac{(5.028)(10) + (25.782)(0) + (37.143)(5)}{67.953}$$

$$= 3.47 \text{ p.s.i.}$$

Therefore, the overall average value for cohesion c along the length of the first spiral is 3.47 p.s.i.

Step 15

The values of c and ϕ arbitrarily assumed for the construction of the first spiral were

$$c = 5 \text{ p.s.i.}$$
$$\phi = 30°$$

The overall average values of c and ϕ calculated for this first spiral were

$$c = 3.47 \text{ p.s.i.}$$
$$\phi = 25°30'$$

The c and ϕ values calculated for the spiral are, therefore, appreciably different than those arbitrarily assumed for its construction. Consequently, the method of successive approximations must be continued until the overall average values for c and ϕ calculated for the spiral are very nearly the same as those used for its construction.

Step 16

Using the procedure of Steps 1 to 15, determine the critical logarithmic spiral (second successive approximation) for a homogeneous material for which c = 3.47 p.s.i. and $\phi = 25°30'$, the values of c and ϕ calculated for the first trial spiral.

This second critical spiral gives an ultimate strength value of 99.3 p.s.i., an overall average value of c = 2.96 p.s.i., and an overall average value of $\phi = 29°45'$.

These calculated overall average values for c and ϕ for the second spiral, c = 2.96 and ϕ = 29°45', are still appreciably different than those employed for its construction, c = 3.47 p.s.i. and ϕ = 25°30'. Consequently, a third trial is necessary.

Step 17

To lessen the gap between original and resultant values of c and for the spiral, take as the original values for c and ϕ for the third successive approximation the average of the original and resultant values for c and ϕ for the second trial spiral. Consequently, the values of c and ϕ to be used for the third trial spiral are

$$c = \frac{3.47 + 2.96}{2} = 3.22 \text{ p.s.i.}$$

$$\phi = \frac{25°30' + 29°45'}{2} = 27°38'$$

By using this method of averaging original and resultant values for c and ϕ for the previous spiral (except the first), the number of trials (successive approximations) can be materially reduced.

The third trial spiral drawn on the basis of these averaged values for c and ϕ gives an ultimate strength of 110.91 p.s.i., an overall average value of c = 3.18 p.s.i., and an overall average value of ϕ = 27°50'.

Step 18

For the fourth successive approximation, take as the original values for c and ϕ the average of the original and resultant values for the third trial spiral. The c and ϕ values to be used, therefore, are

$$c = \frac{3.22 + 3.18}{2} = 3.20 \text{ p.s.i.}$$

$$\phi = \frac{27°38' + 27°50'}{2} = 27°44'$$

The fourth trial spiral based on these averaged values for c and ϕ gives an ultimate strength of 110.8 p.s.i., an overall average value of c = 3.22 p.s.i., and an overall average value of ϕ = 27°37'.

It is clear that the values for c, ϕ, and ultimate strength q, resulting from the fourth trial spiral, are almost identical with those provided by the third trial. It would, therefore, be of no practical value to make a fifth successive approximation.

Consequently, the required value for the ultimate strength q of this three-layer flexible pavement system is

$$q = 110.8 \text{ p.s.i.}$$

Figure 29 demonstrates that the critical spirals given by each successive approximation in the above steps lie alternately on either side, and successively closer to the ultimate critical spiral that would result from many successive approximations.

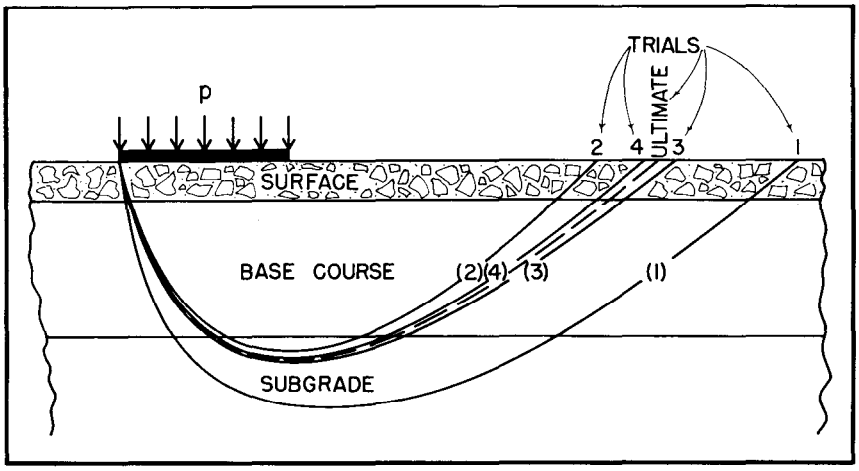

Fig. 29. Illustrating Relative Positions of Logarithmic Spirals Resulting from Successive Trials When Applying the Method of Successive Approximations.

Table VII. Ultimate Strength of Three-Layer System

For Surface Course c = 10 p.s.i., $\phi = 40^0$
For Base Course c = 0 p.s.i., $\phi = 45^0$
For Subgrade c = 5 p.s.i., $\phi = 10^0$
Thickness of Surface Course = 2 inches
Thickness of Base Course = 9 inches
Density of Surface, Base, and Subgrade = 140 lbs./cu.ft.
= 0.081 lbs./cu. in.

Strip Loading
Width of Loaded Strip = 10 inches
Values of c, ϕ, and q for Successive Trials

Successive Approximation No.	Cohesion c p.s.i.	Angle of Internal Friction ϕ	Ultimate Strength q p.s.i.
1	5.0	30^0	206.5
2	3.47	$25^0 30'$	99.3
3	3.22	$27^0 38'$	110.9
4	3.2	$27^0 44'$	110.8

Step 19

Determine the value for z, representing the deepest penetration of any given logarithmic spiral below the ground surface, by the procedure illustrated in Step 12, Appendix A. For the fourth trial spiral, from Step 18 above, it is found that

$$z = 14.7 \text{ inches}$$

Step 20

Prepare a table of the values for c, ϕ, and ultimate strength q associated with each trial, or successive approximation, Table VII.

It is quite apparent from Table VII that there is little difference between the ultimate strength values for the third (110.9 p.s.i.) and fourth (110.8 p.s.i.) trials. The c and ϕ values for the third and fourth trials are also nearly the same. Consequently, only three trial logarithmic spirals were required to determine the ultimate strength of this three-layer flexible pavement with sufficient accuracy for ordinary practical design.

APPENDIX D

Location of the Origin of the Critical Logarithmic Spiral

The principles involved in the determination of the ultimate strength of a homogeneous soil by means of a logarithmic spiral failure curve have been illustrated by the sample calculation of Appendix A. The critical logarithmic spiral is the curve along which failure is assumed to occur if the ultimate strength of the material is exceeded. The origin of this critical spiral must be found by trial and error, and it lies on a radius vector through an extremity of the loaded area and making an angle θ_1 with the horizontal, Figure 19.

Appendix D presents a simple mathematical proof that the exact position of the origin of the critical logarithmic spiral along this radius vector is located by,

1. the intersection of the radius vector with the ordinate marking 75 per cent of the distance toward the opposite extremity of the loaded area *for cohesionless soils*, (c = 0), and
2. the intersection of the radius vector with the ordinate through the opposite extremity of the loaded area (100 per cent of the distance toward the opposite extremity) *for cohesive frictionless soils*, (ϕ = 0).

Figure 19 will be employed to illustrate these two mathematical proofs. The conditions illustrated by Figure 19 are:

1. Strip loading.
2. Width of loaded strip = L.
3. Horizontal distance from one extremity of the loaded area to the ordinate through the origin of the critical logarithmic spiral = B.

The problem consists of finding the distance B as a fraction or percentage of the total width L of the contact area for:

(a) cohesionless soils (c = 0),
(b) cohesive, frictionless soils (ϕ = 0), and
(c) soils with both cohesion and friction (c and ϕ).

Case 1. Cohesionless Soils (c = 0)

When using the logarithmic spiral method for determining the ultimate strength of a soil, the load moment M_L must be equated to the reaction moment M_R, which in turn consists of the sum of the weight moment M_w and the cohesion moment M_c. Consequently, for the critical logarithmic spiral, at equilibrium,

$$M_L = M_R = M_w + M_c$$

From Figure 19, by inspection,

$$M_L = pL\left(B - \frac{L}{2}\right)$$

and from Appendix A,

$$M_R = M_w + M_c = B^3 K_w w + B^2 K_c c$$

It was explained in Appendix C that K_w and K_c are numerical coefficients in the general expressions for the weight moment M_w and the cohesion moment M_c, respectively. See also Table 6 of Appendix A.

Consequently,

$$pL\left(B - \frac{L}{2}\right) = B^3 K_w w + B^2 K_c c$$

from which

$$p = \frac{B^3 K_w w + B^2 K_c c}{BL - \frac{L^2}{2}} \tag{22}$$

For cohesionless soils c = 0. Therefore, for cohesionless soils equation (22) becomes

$$p = \frac{B^3 K_w w}{BL - \frac{L^3}{2}} \tag{23}$$

It is required to find the value of B that will result in the minimum value for p, since the minimum value for p is the required ultimate strength q. At the same time, this value for B also locates the ordinate on which the origin of the critical logarithmic spiral failure curve must lie.

The value of B that will give a minimum value for p for cohesionless soils is obtained by differentiating equation (23) with respect to B, equating the derivative to zero, and solving the resulting equation for B. This operation gives the following:

$$\frac{dp}{dB} = \frac{\left(BL - \frac{L^2}{2}\right)(3B^2 K_w w) - B^3 K_w w L}{\left(BL - \frac{L^2}{2}\right)^2}$$

from which, upon simplification,

$$3\left(B - \frac{L}{2}\right) - B = 0$$

or

$$B = \frac{3L}{4} = 0.75\ L$$

Therefore, the origin of the critical logarithmic spiral for cohesionless soils lies on the ordinate that marks off 75 per cent of the width of the contact area when measured from the extremity of the loaded area intersected by the spiral itself.

Case 2. Cohesive, Frictionless Soils ($\phi = 0$)

The development of the mathematical proof for the location of B for Case 2, cohesive frictionless soils, is identical with that for Case 1 down to equation (22),

$$p = \frac{B^3 K_w w + B^2 K_c c}{BL - \frac{L^2}{2}} \tag{22}$$

For cohesive, frictionless soils, $\phi = 0$, and the value of the weight moment expression, $B^3 K_w w$ of equation (22) is zero, since $K_w = 0$ when $\phi = 0$, Figure 24. Therefore, for cohesive, frictionless soils equation (22) becomes

$$p = \frac{B^2 K_c c}{BL - \frac{L^2}{2}} \tag{24}$$

As for Case 1, the value of B that results in a minimum value for p is obtained by differentiating equation (24) with respect to B, equating the derivative to zero, and solving the resulting equation for B. This operation gives the following,

$$\frac{dp}{dB} = \frac{\left(BL - \frac{L^2}{2}\right) 2B K_c c - B^2 K_c c L}{\left(BL - \frac{L^2}{2}\right)^2} = 0$$

from which, upon simplification,

$$2\left(B - \frac{L}{2}\right) - B = 0$$

or

$$B = L$$

For cohesive, frictionless soils, therefore, the origin of the critical spiral lies on the ordinate through the opposite extremity of the contact area to that intersected by the spiral itself.

Case 3. Soils with Both Cohesion and Friction (c *and* ϕ)

While there is no simple mathematical proof covering the location of B in this case, it can be inferred from Cases 1 and 2 that for soils with both cohesion and friction, the origin of the critical spiral lies on the radius vector at its intersection with an ordinate somewhere between 75 and 100 per cent of the distance toward the opposite extremity of the contact area from that intersected by the spiral itself. For this case, therefore, B is greater than 0.75 L, but less than L, or as expressed in mathematical symbols,

$$0.75\,L < B < L \tag{25}$$

The exact location of B between these two limits depends upon the relative magnitudes of cohesion c and angle of internal friction ϕ of the soil material. When ϕ is large and c is small, B approaches 0.75 L, while for the reverse, B approaches L.

That the position of B for the critical logarithmic spiral for soils with both c and ϕ values lies between 0.75 L and L is illustrated by the sample calculations of Appendices A, B, and C. For each of these sample calculations, L = 10 inches, and B should, therefore, have values between the limits of 7.5 and 10 inches.

From Step 10 in Appendix A for which c = 5 and $\phi = 30^0$, B = 9.6 inches.
From Step 4 in Appendix B for which c = 0 and $\phi = 45^0$, B = 7.5 inches.
From Step 5 in Appendix C for which c = 5 and $\phi = 30^0$, B = 9.6 inches

It happens that the distribution of c and ϕ values for these three sample calculations from Appendices A, B, and C cover a relatively narrow range. Nevertheless, the corresponding values of B for the critical spirals indicate the correctness of equation (25).

Discussion

MR. EDMUND THELEN: I'd like to ask how cohesion c was measured.

DR. N. W. McLEOD (Demonstrating on blackboard): The term cohesion c, as employed in this paper, has the same significance as in the field of soil mechanics. It can be most easily understood by reference to a Mohr or Coulomb diagram, Figure A(2), in which the shear strength s developed along the plane of failure through the material, Figure A(1), is the ordinate axis, while the stress acting normal or perpendicular to the plane of failure is plotted as the abscissa. On a Mohr or Coulomb diagram, cohesion c is represented by the intercept on the ordinate axis (shear stress axis) that is made by the Coulomb or Mohr envelope, Figure A(2). Expressed in another way, and illustrated

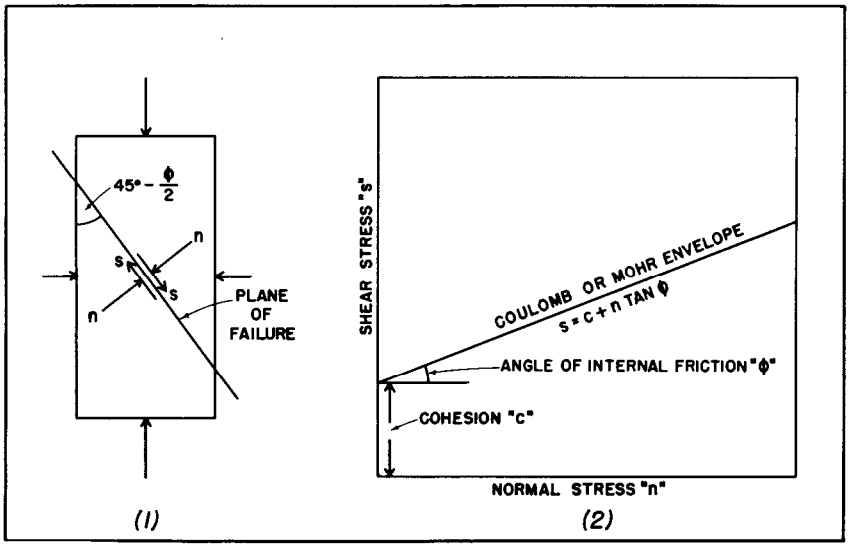

Fig. A. Mohr or Coulomb Diagram.

by Figure A(2), cohesion c represents the maximum shear strength that can be developed along the failure plane through a material, Figure A(1), when the normal stress n acting on the plane of failure is zero. For the soil and aggregate materials considered in soil mechanics, and for most bituminous paving mixtures, the Coulomb or Mohr envelope is usually a straight line which is a graphical representation of the well-known Coulomb equation $s = c + n \tan \phi$, Figure A(2), where s is the maximum shear strength that can be developed along the failure plane, Figure A(1), c is the cohesion c already defined, n is the normal stress on the plane of failure, Figure A(1), also referred to previously, and ϕ is the angle of internal friction indicated by the angle between the Coulomb or Mohr envelope and the horizontal. From even casual inspection of the Coulomb equation, it is seen that the shearing strength s of a soil, aggregate, or bituminous surfacing material can be increased by increasing the values of either c, ϕ, or n. The triaxial test can be used to measure the values of c and ϕ for each of these materials. As indicated in the paper, when all other factors remain constant, the ultimate

strength of a flexible pavement can be greatly increased by increasing the value of c or ϕ, or both, for the material in any one or more layers of the flexible pavement system.

MR. JOHN GRIFFITH (Supplemented by written discussion): Dr. McLeod has stated that only one assumption was made in his proposed solution—namely, that the failure curve is of the shape of a logarithmic spiral. I would like to submit, however, that a number of other assumptions are necessary in problems of this nature. One is that strength characteristics reflected by a single load application, as in the triaxial and other empirical tests, are assumed to be the same as strength characteristics measured by repetitive load applications. We know that in flexible pavements any failures which occur do so under a large number of repetitive loads. The assumption, then, is that the single load application in the triaxial test provides a direct measure of strength which is applicable to repetitive loading conditions. This is definitely an assumption and I, for one, do not believe that it can be substantiated.

Further assumptions must be made with regard to density and moisture content conditions under which the tests are run. We know that moisture contents vary in the pavement structure and also that there are some changes in density under traffic. These variables result in still other assumptions in the triaxial test procedure as discussed by Dr. McLeod.

Still another assumption is to the effect that laboratory compaction procedures give the same density and structure, or particle orientation, as achieved in the field. From the number of laboratory compaction procedures now being used and the several papers which have been presented on this subject, one would gather that it is at least debatable that any compaction procedure can be definitely relied upon to give unquestionable results insofar as density and particle structure are concerned. In fine-grained soils particularly, it is extremely doubtful that we can ever reproduce the structure provided by mother nature. We will probably find it difficult to reproduce density and particle structure conditions which are achieved by construction equipment.

There are other variables in this problem such as those resulting from frost and climatic factors, possible physical changes in the various construction materials over a period of time, the effects of unpredictable traffic patterns and loading conditions, etc., that we have no way of evaluating in precise terms. These factors certainly are not evaluated in a precise

manner in Dr. McLeod's triaxial solution, nor are they in other approaches to this problem. Either they are not considered at all or certain simplifying assumptions are made in an effort to take them into account in the solution of the problem.

I submit, therefore, that there are a number of assumptions and omissions in Dr. McLeod's proposed "rational" solution, rather than the single admitted assumption that the failure curve is in the shape of a logarithmic spiral.

In conclusion, I wish to again register a protest on the implication that this is a rational, theoretical and precise solution. In my opinion, it is fully as empirical as other more commonly used procedures and methods of analysis which are usually admitted to be "empirical." If and when a truly "rational" procedure for pavement design is ever reached, it will likely be of such a complex nature that only our most outstanding mathematicians will be able to handle it. I have no doubt, however, but that Dr. McLeod will be in the forefront of this development. Notwithstanding any comments and objections, I feel that Dr. McLeod is to be highly complimented on the originality of his thinking and for making the results of his studies available to all of us.

DR. McLEOD (Supplemented by written discussion): Mr. Griffith's frank disagreement with the attempt made in this paper to outline a rational approach to flexible pavement design is warmly welcomed and greatly appreciated. Lack of agreement has the stimulating effect of forcing one to re-examine and further justify or clarify his own point of view.

The comments that have just been expressed by Mr. Griffith probably reflect the thinking of a large school of highway and airport engineers who not only favour the empirical approach to flexible pavement design, but have actually convinced themselves that the difficulties in the way of the development of a rational method of flexible pavement design are insuperable, or nearly so. These beliefs of those who belong to this school of thought are sincerely held, and merit careful consideration by all engineers who are interested in this field.

It is clearly recognized that almost our entire storehouse of published information concerning the strength or stability of flexible pavements consists of the results of purely empirical tests such as C.B.R., North Dakota Cone, Hveem Stabilometer, Florida Bearing Value, Texas Punching Shear, Unconfined Compression, Marshall, Hubbard-Field, etc. Practicing engineers are, therefore, tied to these empirical tests as a basis for the

design of flexible pavements, if they intend to utilize our accumulated experience in this field. Any engineer who attempts to use a rational approach to flexible pavement design is to a very considerable extent travelling over unexplored territory, and is more or less on his own. However, *an experienced engineer,* when using a rational method of flexible pavement design, is on firmer ground than a first impression may convey, since there are many points at which the conclusions indicated by the rational approach can be checked at least qualitatively with the known performance of flexible pavements in service. Some of these have been referred to in the present and previous papers by the author.

It is precisely because the current methods ordinarily employed for the design of flexible pavements are entirely empirical throughout, that it is worth while for highway and airport engineers to pause occasionally and reflect on the fact that in this respect the status of flexible pavement design today is where general structural design was over a century ago before theoretical stress analysis came into general use. No doubt there were many engineers at that time who adopted and maintained the attitude that the empirical approach to the design of bridges, buildings, and other structures, an approach that had been gradually developed and tested over a period of seventy centuries or more, was entirely adequate and that the untried theories of stress analysis being proposed could be dismissed as a product of the over-active imaginations of a few mathematicians, and were much too complicated in any case to ever come into general use.

While some of the structures, aqueducts, bridges, buildings, etc. built by the Romans from fifteen hundred to two thousand years ago, are still in service, our present knowledge of stress analysis indicates that they were usually greatly overdesigned and, therefore, very wasteful of construction materials. Of course, those that were underdesigned because of the empirical methods of design employed, collapsed during construction or shortly afterward. Serious overdesign and underdesign is the penalty that the empirical approach can always be expected to inflict in the fields where it is utilized, since the safety factor being used cannot be determined.

The invention and rapid development of railroad transportation throughout the world in the latter half of the nineteenth century is considered to have greatly accelerated the acceptance of rational methods of structural design based upon the theoretical stress analysis. The tremendous number of bridges alone that were required for railroad extension across vast undeveloped

areas made it imperative that their cost be kept to a minimum compatible with safety. Rational design made this possible. It is doubtful that the growth of the continent-wide network of railroads, and the accompanying large scale development of industry and agriculture in North America during the past century, could have proceeded at anything approaching the spectacular rate actually achieved, if the wasteful empirical methods of structural design employed previous to that time had been followed. To a not inconsiderable degree, therefore, the phenomenal development of the North American continent during the past hundred years has been due to the enormous reduction in construction and manufacturing costs that rational methods of design based upon theoretical stress analysis have made possible. As pointed out in the paper, there is a possibility that the introduction of high tire inflation pressures on jet aircraft, and the gradually increasing axle loads on highways, may stimulate and accelerate the development of a rational approach to flexible pavement design.

It is a rather curious anomaly of mental attitudes that engineers, who would insist on applying the *rational methods* of soil mechanics to the design of bridge or building footings, embankments, earth dams, etc. in any given area, are satisfied to accept without question one or more of the current *empirical methods* if asked to design a flexible pavement in the same locality, even though the latter appears to be a specialized problem in soil mechanics. The necessity for utilizing these empirical methods of flexible pavement design for current projects is not disputed, since it is realized that an engineer on the job has little alternative at the present time. Faced with the need for immediate decisions, he must make use of whatever tools and information past research has made available, and these have been essentially empirical.

It is the casual, continued, unquestioning acceptance of these empirical methods of flexible pavement design that is surprising, particularly in an age when the advantages of the rational approach to the solution of scientific problems have been so strikingly demonstrated by the brilliant achievement of unlocking the energy of the atom. This comment applies particularly to those who are responsible for research in the flexible pavement field. It is disconcerting to find that so little research effort is being expended on attempts to develop rational methods for designing flexible pavements, especially when, as should be well known, one empirical method may reject as poor design what another empirical method would approve as good design;

for example, Marshall versus Hveem Stabilometer. There is even a tendency for some of the research going on in this field to be directed to the development of additional empirical tests, which only add to the existing confusion, instead of endeavouring to come to grips with the problem on a fundamental basis.

In the related field of rigid pavements, since portland cement concrete is considered to have the properties of an elastic material, principles of theoretical stress analysis can be utilized similar to those that have been so successfully applied to the design of steel structures for many decades. Nevertheless, it was not until papers by Westergaard were published in 1926 and 1933, that the design of rigid pavements was placed on a rational basis which has been almost universally accepted.

Now, nearly thirty years later, it would seem to be about time that some serious effort was being devoted to the development of a rational method of flexible pavement design that would receive general approval on a national and international scale. Nevertheless, the existing stock of fundamental information on this subject is still so meagre, and so little is yet known about the actual mechanism of failure of flexible pavements when overloaded, that it has not been possible so far to take even the first important step toward a rational method of design, which requires deciding whether the design of flexible pavements should be based upon elastic behaviour, plastic properties, or a combination of both. Consequently, much basic work remains to be done in this field.

While it is recognized that the task of developing one or more generally acceptable rational methods for the design of flexible pavements is far from easy, a number of investigators have made a start in this direction, and the contributions of Gray, Housel, Goldbeck, Palmer, Barber, Vokac, and Glossop and Golder, among others, are well known. Publication in 1943 of the results of Professor Burmister's outstanding study of the flexible pavement design problem based upon the elastic properties of a layered system requires special mention, while a further attempt has been made from the entirely different point of view of plastic behaviour in the author's paper that has just been presented.

In his discussion, Mr. Griffith has made a number of specific criticisms, to which the author would like to reply.

He suggests that the triaxial test is not suitable for determining the strength characteristics of the materials employed for the various layers of a flexible pavement, since he believes that only one application of load can be made, whereas a flexible pavement

may be subjected to many hundreds of thousands of load repetitions during its service life. This criticism is not valid, however, since triaxial procedure has been devised for applying any number of load applications from one to a great many. Consequently, if it is actually required, repetitive loading can be employed for the triaxial test. On the other hand, so little is still known about the way or ways in which overloaded flexible pavements fail, that the author is not at this time prepared to admit that it is necessary to introduce repetitive loading into the triaxial test for routine design.

In the somewhat related field of plate bearing tests, analysis of data from many hundreds of large scale load tests on steel plates having diameters from 12 to 42 inches, carried out by the Canadian Department of Transport on existing runways at Canadian airports, has indicated simple relationships between loads supported at one, ten, one hundred, one thousand, etc. repetitions, for a given total deflection and rate of loading. Consequently, if for any given load Mr. Griffith cares to name the number of repetitions that he considers critical, it is just possible that this load will be found to be a rather definite fraction of the load that can be applied for one application in the triaxial test.

Carefully performed triaxial tests have demonstrated that clays develop much greater strength under transient than under sustained loads. This tends to be true of materials in general. As explained in the paper itself, rapidly moving loads (transient) develop considerably higher values of cohesion c within a flexible pavement than stationary loads. Therefore, the ultimate strength mobilized by a given flexible pavement tends to be considerably higher under moving than under stationary wheel loads. For most flexible pavements, this additional ultimate strength may be more than adequate to compensate for the destructive influence, e.g. possibly fatigue, of a large number of repetitions of load represented by moving traffic. Consequently, it is by no means certain that a repetitive procedure for the triaxial test, as suggested by Mr. Griffith, is always necessary or desirable when this test is used for flexible pavement design.

It might be noted in this regard that for reasons contained in the paper itself, the severity of traffic loading to which flexible pavements are subjected in service would appear to rank in decreasing order as follows:

(1) vehicles applying braking and acceleration stresses at locations where there is much stopping and starting of traffic, e.g. bus stops and traffic lights,

(2) stationary vehicles, and
(3) vehicles moving at a high but relatively uniform rate of speed.

Mr. Griffith refers to the difficulty of preparing laboratory test specimens that will reproduce the density, moisture, and structure that various flexible pavement materials will eventually acquire in the field, and for this reason he questions the value of triaxial tests applied to flexible pavement design. However, this problem is no more serious with respect to the triaxial test than to any of the empirical tests that are currently employed, usually without question, for the design of flexible pavements. It should be noted that these same factors must be considered in connection with the preparation and testing of test specimens required for the design of many other earth structures such as embankments, earth dams, retaining walls, building foundations on either natural or filled ground, etc. Nevertheless, these difficulties have not been considered serious enough to prevent the use of rational methods of design in these related fields. Consequently, uncertainties concerning the moisture content, density, and method of compaction to be selected for the preparation of test specimens do not provide any more valid reason for objecting to the application of the results of the triaxial test to the design of flexible pavements than to the use of this test as the basis for the design of the various types of earthwork construction for which it has been long employed.

The other objections listed by Mr. Griffith are in the same category. For example, earth dams are exposed to the various factors of frost, climate, changing moisture content, drawdown, etc., which are either identical with or more serious than those to which flexible pavements are subjected. However, they do not prevent earth dam engineers from using rational methods of design, even though the failure of an earth dam would ordinarily be a much more serious matter from the point of view of loss of life and property damage, than the failure of a flexible pavement on an airport runway or highway. Probably it is just because the failure of an earth dam would often be catastrophic that earth dam engineers feel that they must make use of a rational method of design in spite of some uncertainty concerning the magnitudes of a number of the variables that must be included. Furthermore, to avoid excessive costs, they are ordinarily restricted to a safety factor that is higher than unity but less than two.

The effects of "unpredictable traffic patterns and loading conditions, etc. that we have no way of evaluating in precise

terms," to quote another of Mr. Griffith's criticisms, apply as forcibly to the bridges, multi-level traffic interchanges, etc., that must be built on any highway system, as to the long miles of flexible pavement between them. Uncertainties concerning the magnitudes of these variables do not prevent the design of bridges and similar structures by rational methods. Bridge engineers make the best possible estimate of the "traffic patterns and loading conditions" to be expected, and design these structures accordingly. The same approach would be employed when applying a rational method to the design of flexible pavements.

In the final paragraph of his discussion, Mr. Griffith states, "I wish to again register a protest on the implication that this is a rational, theoretical, and precise solution. In my opinion, it is fully as empirical as other more commonly used procedures and methods of analysis which are usually admitted to be 'empirical'."

As previously pointed out, all of the factors that Mr. Griffith has listed as being insurmountable to the development of a rational method of flexible pavement design have not stopped the evolution and wide-spread use of rational methods of design in related fields where each of these factors, and some that are even more formidable, must be considered. For example, the identical factors enumerated by Mr. Griffith did not prevent the derivation of a rational method of design for rigid pavements that within a very few years became universal in its application. Earth dam design is another excellent example.

The general nature of his remarks tends to give the impression that Mr. Griffith would be unwilling to acknowledge that any proposed method of flexible pavement design could be labelled "rational," unless it took into account each of the factors he has listed, and could still be applied on the basis of a safety factor approaching unity. It should be observed in this connection that the strength of steel has probably been more thoroughly investigated than that of any other material. Nevertheless, even in the field of steel structures, which have been designed according to the rational methods of theoretical stress analysis for the past hundred years or so, a safety factor ranging from 3 to 10 or more is employed, depending upon the nature of the applied load and other conditions.

It is well known that what are ordinarily referred to as safety factors are actually factors of ignorance. They are introduced into rational methods of design for the specific purpose of making due allowance for variables similar to those listed by

Mr. Griffith, for which uncertainty exists concerning their magnitude and effect. Consequently, for any rational method of flexible pavement design that may be developed and applied, it is to be expected that a safety factor will have to be employed to provide for the uncertain influence of variables that cannot be accurately or completely evaluated. In this respect, a rational method of design for flexible pavements will be no different from those in other fields where the use of rational methods has been commonplace for many years.

In spite of our present inability to evaluate precisely the different factors listed by Mr. Griffith, flexible pavements continue to be built. In some manner or other, each of the difficulties he has mentioned is being either consciously or unconsciously considered when choosing the design to be employed, whether this selection is based upon empirical tests, past experience, or inspired guess. It is precisely because flexible pavements are built on this basis at the present time that some are underdesigned and fail prematurely, while others are greatly overdesigned. Either condition represents a serious wastage of materials and construction effort, that could be avoided by a rational method of design.

Before any favoured rational method of flexible pavement design can be applied, however, the safety factor to be employed must be determined. As pointed out in the paper itself, this safety factor could be evaluated for existing flexible pavement construction in any given area where conditions are relatively uniform. From this information, the magnitude of the safety factor that seemed to avoid both overdesign and underdesign could be established. The size of the safety factor to be employed would probably vary somewhat from locality to locality, depending upon each particular set of local conditions. It would also vary within each locality depending upon the critical wheel or axle loading and volume of traffic to be carried.

Among the many other advantages of rational over empirical methods of design, brief mention should be made of one in particular. The application of rational methods will very often reveal solutions to problems that would not even be dreamed about by minds that are married to the empirical approach. Rational methods indicate the most effective use of materials, and how they should be combined or assembled to provide maximum performance for the least expenditure. For example, if the rational method of flexible pavement design described in this paper has any merit, it indicates that the overall thicknesses of flexible pavements could be reduced substantially by:

(1) the proper use of plastic binders either to introduce cohesion c into the base course materials, or to increase any existing c value they possess, always provided, of course, that the angle of internal friction ϕ is not materially reduced,
(2) increasing the thickness of well-designed bituminous surfaces, and
(3) paving the shoulders of highways.

In addition, among other findings it has indicated that greater flexible pavement thickness is needed at bus stops and traffic lights, etc., where there is much stopping and starting of traffic, and that, with all other factors being equal, the ultimate strength of a flexible pavement is greater under the inner (nearer the centre) than under the outer wheel path (nearer the shoulder) of an ordinary highway with earth or gravel shoulders.

The various empirical tests employed for flexible pavement design, C.B.R., Hveem Stabilometer, North Dakota Cone, Marshall, etc., either singly or in combination could not be made to provide similar conclusions. Even if the results given by the particular rational method described in this paper should be over-optimistic in any respect, it nevertheless illustrates the supreme advantage that even a relatively elementary rational approach has over the best empirical methods, namely, it is capable of indicating solutions to problems that would not even be suspected on the basis of the empirical approach.

To summarize this reply to Mr. Griffith's criticisms very briefly:

(1) The factors that Mr. Griffith has listed as being insurmountable to the development of a rational method of flexible pavement design have not prevented the evolution and widespread acceptance of rational methods of design in closely related fields such as rigid pavements, earth dams, embankments, retaining walls, etc.
(2) The continued, unquestioning acceptance of empirical methods of flexible pavement design prevents engineers from acquiring an understanding of the fundamental factors that actually control the performance of flexible pavements in service, and blinds them to possible solutions to problems in this field that even a relatively elementary rational method of flexible pavement design would reveal.

This reply to Mr. Griffith's brief comments is much longer than could ordinarily be justified. However, empirical methods of design for flexible pavements are so firmly entrenched, and have such a large following, that the author has been glad to have

the opportunity, provided by Mr. Griffith's criticisms, of presenting some of the merits of the case for a rational approach to flexible pavement design.

MR. DON E. STEVENS: Dr. McLeod, would you repeat the description of your method for combining cohesion with angle of internal friction. I believe that in some instances you related ultimate strength with angle of internal friction. Then you also covered the situation where the influence on ultimate strength obtained by combining cohesion with the angle of internal friction was shown. What is the derivation of your method?

DR. McLEOD: In the equation for a logarithmic spiral, the angle of internal friction appears as a power term. Consequently, as soon as the angle of internal friction for a material has been measured by a triaxial or direct shear test, its value can be introduced directly into the equation. The size of the angle of internal friction controls the curvature of the logarithmic spiral failure curve. After the logarithmic spiral failure curve has been established, the problem becomes one of pure mechanics. Load moment is balanced against reaction moment. Both moments are taken about the origin of the spiral. If cohesion is absent, the reaction moment becomes the net weight moment of the material contained within the spiral. If cohesion is present, the reaction moment consists of the net weight moment plus the cohesion moment. The cohesion moment is due to cohesion c acting along the whole length of the spiral through the material. The principal problem involved is finding the critical logarithmic spiral; that is, the spiral that will just support the smallest applied load. Obviously, if a certain spiral failure curve will just carry a certain load, while another spiral will fail under a much smaller load, the second spiral is more critical than the first. Locating the critical logarithmic spiral requires the use of the trial and error method. Examples of the procedure employed are contained in Appendices to the paper.

MR. STEVENS: I would like to ask a second question, Dr. McLeod. I was impressed by the increase in ultimate strength values that occur when even a small amount of cohesive material is introduced into any part of the flexible pavement structure. Does this imply that the introduction of cohesion into a base course is chiefly of value only if the base course is otherwise going to be overloaded, or can we assume from your paper that the introduction of cohesion into a base course might so increase its ultimate strength that it would be possible to reduce the thickness of base?

DR. McLEOD: Concerning Mr. Stevens' first point, there is nothing to be gained from increasing the ultimate strength of a flexible pavement beyond that needed to support the traffic loads to be carried, since the unnecessary extra strength represents wasted materials and construction effort. However, for the case mentioned by Mr. Stevens, where the base course material is too weak to support the applied load, if it consists of cohesionless sand or gravel of low stability, the method described in the paper indicates that its bearing capacity might be increased greatly by incorporating a binder that would provide measurable values of cohesion c. An excellent practical example of the successful application of this method occurred in the sand hill region of Nebraska, where unstable cohesionless dune sands were converted into stable road surfaces by mixing in liquid asphalts, which furnished cohesion c. Consequently, in areas where highly stable granular materials are not available, but large quantities of unstable sands or gravels exist, it should be worth while to investigate the cost of improving the stability of these local materials by the introduction of cohesive binders versus the expense of importing stable granular materials such as crushed stone. The most readily available inexpensive cohesive materials are usually tars and asphalts, with clays being in the same category. It is believed that the success or failure of the stabilization of different soils with either clay or bituminous materials can be explained in terms of the ultimate strength approach described in the paper.

As a matter of fact, the adoption of a rational method of flexible pavement design would probably do more to extend the development and use of soil stabilization than any other single factor that could be introduced. This is particularly true of the more clayey types of soils which tend to be borderline or deficient in stability even when bituminous or similar binders are added. By means of a rational method of flexible pavement design, it could be determined by calculation whether or not the use of a proposed stabilized soil material was capable of providing a flexible pavement of the required strength. If the particular stabilized soil was incapable of developing the strength needed, a rational method would indicate the property or porperties that must be improved to provide the necessary stability. Furthermore, the required minimum thickness of the stabilized soil layer could be quickly calculated.

MR. STEVENS: Do you feel that increasing the ultimate strength of the base course would make it possible to reduce the thickness of base required?

DR. McLEOD: That conclusion is definitely indicated by the rational approach to flexible pavement design described in this paper. However, as with most engineering materials, the matter of economics is involved. Is it cheaper to use a certain required thickness of a given granular material, or a smaller thickness of the same granular material to which a binder has been added to increase its ultimate strength? Or would a reduced thickness of a cohesionless aggregate of greater stability be cheaper than either? The method outlined in the paper provides quantitative answers to problems such as these. It indicates the thickness of each of the different materials that would be required, and this in turn makes it possible to compare their costs in place in an overall highway or airport pavement structure that must support a given wheel load and traffic intensity.

MR. WM. FORD: I am interested in the advantages of introducing a bituminous binder into the base course material in order to reduce base course thickness. One of your diagrams indicated an increase in strength of nearly 40 per cent for the flexible pavement as a whole, by adding a binder to a granular base. Does this mean that by incorporating an asphalt or similar binder into the base, the required thickness of base could be reduced from say eight inches of crushed stone or gravel to five inches of the same aggregate that had been treated with asphalt?

DR. McLEOD: It should be explained that for the example shown in one of the slides (Figure 13 of the paper), the increase of approximately forty per cent in the strength of the overall flexible pavement structure obtained by adding a binder to the base course, would in general, only hold for the particular combination of flexible pavement layers illustrated by this diagram. If the values for cohesion c and angle of internal friction ϕ shown for each layer were changed appreciably, the increase in ultimate strength obtained by adding a binder to the base might be even more than 40 per cent, but could also conceivably be very much less. Furthermore, if the binder added to the base seriously decreased its angle of internal friction ϕ, there could actually be a decrease in the strength of the overall flexible pavement.

MR. FORD: I would like to make the point, however, that I am interested strictly in the base; that is, in a comparison of the strength of water-bound or traffic-bound macadam versus that of a bituminous-bound macadam base. If you were to eliminate the other factors, such as the wearing surface and subgrade and considered only the base course, would it not be possible for your

method to demonstrate that by incorporating bituminous binder the strength of the base would be so greatly increased that the base course thickness requirement could be reduced in the ratio of eight to five or some similar value?

DR. McLEOD: The question you have raised is a very important one. Nevertheless, there would seem to be considerable danger in concentrating too much attention on a particular layer such as the base course, and neglecting its effect on the flexible pavement as a whole. The ultimate strength of the overall flexible pavement is of greater importance than the strength of any specific layer. The stability of the material in any one layer might be increased by 100 per cent or more by means of some particular treatment, without providing more than a relatively modest increase in strength for the flexible pavement as a whole. The thickness of the layer might be too small to exert much effect.

A flexible pavement usually consists of at least three layers, subgrade, base course, and bituminous surface. The ultimate strength of a flexible pavement depends upon the values of the angle of internal friction ϕ and cohesion c of each layer, and upon the individual thicknesses of base course and surface. Consequently, the angle of internal friction ϕ and cohesion c for the material in each layer must be measured by either triaxial compression or direct shear tests, and the thicknesses of base and surface must be known, before the ultimate strength of the flexible pavement as a whole can be calculated.

For your particular problem, therefore, it would be necessary to obtain values of the angle of internal friction ϕ and cohesion c for the traffic-bound or water-bound macadam base, for the same base after treatment with a bituminous binder, for the subgrade and for the bituminous surface, together with the thickness of the surface and of the base, before calculations could be undertaken to determine whether or not the addition of a bituminous binder to the base would result in an increase in strength of the flexible pavement as a whole, and by how much. If for any reason so much bituminous binder were added to the base that it functioned at least in part as a lubricant and decreased the base course stability, a loss in ultimate strength of the flexible pavement structure could occur. On the other hand, Figures 7, 13, 14, and 17 of the paper tend to indicate that by adding a carefully controlled amount of bituminous binder to the usual granular base, an increase in the ultimate strength of the overall flexible pavement could be expected. Nevertheless, the per cent increase in

ultimate strength of a flexible pavement resulting from treatment of the base course would have to be calculated for the particular conditions associated with each project.

Figure 14 of the paper has considerable bearing on your question, for it indicates the effect on base course thickness that could be expected *under a given set of conditions* by adding a binder to the base. With all other factors held constant, including the load supporting value of the overall flexible pavement (112 p.s.i.), introducing a binder into the granular base permitted an appreciable reduction in base course thickness. Without binder, the required thickness of base course ($\phi = 40^0$) was 12 inches. When sufficient binder was incorporated into the same base course to provide cohesion c = 2.62 p.s.i., a relatively low value of cohesion, Figure 14 (c) shows that the base course thickness requirement was reduced to 7.2 inches. This represents a decrease of 40 per cent in base course thickness *for the particular conditions illustrated.*

MR. J. E. DRISCOLL (by letter): Our question concerns a recent full page advertisement by the Portland Cement Association. The advertisement, among other things, indicated that the distribution of wheel load through a portland cement concrete pavement was at an angle approaching the infinite, whereas the load through a flexible pavement was confined to the contact area of the applied load, without benefit of a reduction in unit pressure resulting from lateral distribution (Figure B).

Under ordinary circumstances, it is our belief based on considerable research, that flexible pavements distribute wheel load through the surface, base, and subgrade at an angle of approximately 45°.

Can you prove or disprove the suggested conclusion contained in the advertisement? In any event, we would appreciate your comments.

DR. McLEOD:(by letter): Figure B reproduces the diagram illustrating the distribution of wheel load pressure through a rigid pavement, and through a flexible pavement, that appears in the article to which Mr. Driscoll refers, Figure B(a) pertaining to the rigid pavement, and Figure B(b) to the flexible pavement. When analysed from the point of view of pressure transmission, this diagram is essentially correct. It is intended to indicate that the stress on the subgrade immediately beneath a wheel load on a flexible pavement is much greater than that for the same wheel load on a rigid pavement. It is generally recognized that because of its rigidity, a portland cement concrete slab distributes a given applied wheel load over a much greater area of subgrade

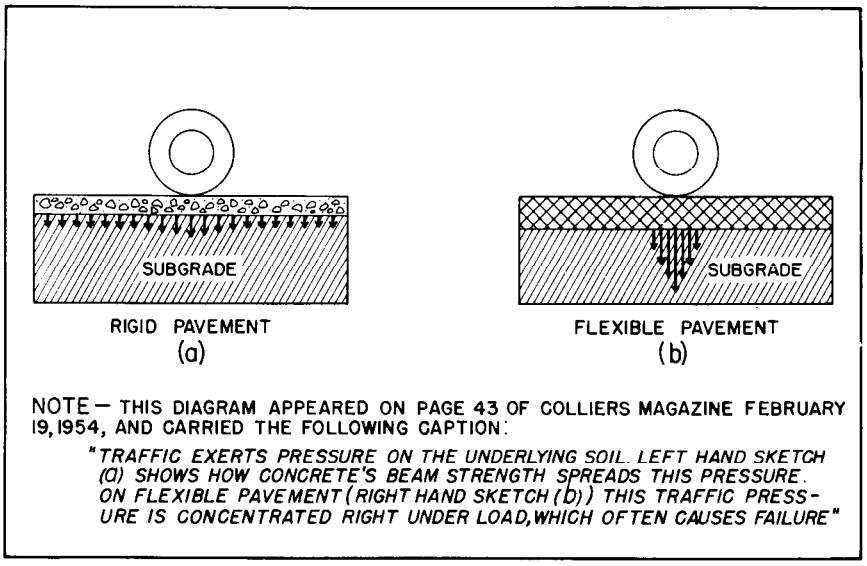

Fig. B. Illustrating Pattern of Pressure Transmission through Rigid and Flexible Pavements.

than a flexible pavement is capable of doing. It is to be emphasized again that Figure B illustrates a fundamental difference between rigid and flexible pavements concerning the manner in which they *transmit* an applied load to the underlying subgrade, rigid pavements applying a small intensity of pressure over a large area of subgrade, while flexible pavements apply higher intensities of pressure over a much smaller area of the subgrade.

However, there is an entirely different way of looking at this problem than that represented by Figure B. How do rigid and flexible pavements compare in their relative abilities *to mobilize the potential supporting value of the underlying subgrade*? This is illustrated diagramatically in Figure C, in which Figure C(a) refers to a rigid pavement and Figure C(b) to a flexible pavement. Figure C demonstrates a generally recognized fundamental difference between rigid and flexible pavements, in that a flexible pavement is considered to be capable of developing several times greater subgrade support than is possible for a rigid pavement.

It is widely accepted that the critical deflection for a rigid pavement under load is approximately 0.05 inch. Applied loads developing a greater deflection of the rigid pavement than this are likely to crack the slab. Consequently, the maximum degree of subgrade bearing capacity that can be mobilized by a rigid pavement is the supporting value of the subgrade in pounds per square inch at 0.05 inch deflection. This is only a small fraction of the potential load carrying capacity of most subgrades.

When a rigid pavement loses contact with the subgrade at any point because of pumping joints, warping stresses due to temperature or moisture gradients through the slabs, etc., it is unable to develop even this relatively small amount of subgrade bearing capacity. Under these conditions, the subgrade support under portions of the rigid pavement may become zero, and the entire applied load must be supported by the beam action of the slabs. It is usually because the subgrade support is seriously decreased or becomes zero, and the bridging strength of the rigid pavement is inadequate, that cracking of slabs occurs at joints, corners, etc.

The precise mechanism of failure of flexible pavements when overloaded is still unknown. However, investigations by The Asphalt Institute and others seem to show that a flexible pavement can withstand a deflection of at least 0.5 inch without failure. The supporting value of a subgrade at 0.5 inch deflection can be

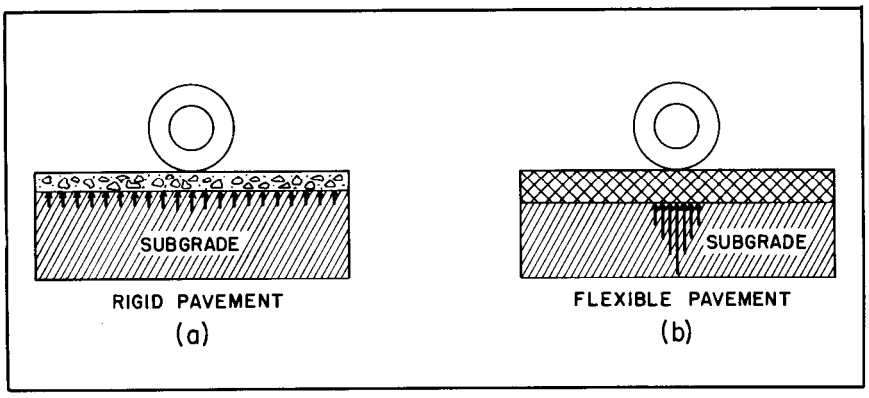

Fig. C. Illustrating Pattern of Subgrade Reaction Mobilized by Rigid and by Flexible Pavements.

from four to five times greater than its supporting value at 0.05 inch deflection for most soils. Therefore, as illustrated by Figure C, a flexible pavement can mobilize from four to five times more subgrade support measured in pounds per square inch than can a rigid pavement. This greater subgrade supporting value is utilized in flexible pavement design and reduces the thickness that would otherwise be required. Furthermore, it is a fundamental characteristic of flexible pavements that they maintain contact at all points with the subgrade. Their flexibility enables them to deform as required to maintain this contact. Consequently, a flexible pavement can be depended upon to adjust itself so as to mobilize a high degree of subgrade support at all times, while under certain conditions previously referred to the subgrade support at some points under a rigid pavement may become zero.

Insofar as articles for popular consumption by a non-technical audience are concerned, proponents of rigid pavements may prefer Figure B, while advocates of flexible pavements might emphasize Figure C. It should be clearly understood, however, that these two figures merely emphasize opposite aspects of the same problem, namely, the action of the loaded pavement on one hand and the reaction of the subgrade on the other. It is widely recognized that both rigid and flexible pavements can be designed and constructed to give many years of satisfactory service performance under any wheel or axle loading and under any traffic intensity. Consequently, any diagram that is intended to create any other impression is both incorrect and misleading.

Mr. Driscoll refers to the average angle of pressure transmission through a flexible pavement from the loaded area and points out that this is often assumed to be 45^0. It is usually further assumed that the transmitted pressure is uniform on any horizontal plane within the zone enclosed by this 45^0 angle of pressure transmission.

Actual measurements have shown that when a soil or aggregate is uniformly loaded on any specified contact area at the surface, the pattern of the distribution of vertical stress on a horizontal plane at any depth below the surface tends to have the shape of a helmet or bell, Figure D. The base of the bell becomes wider and its height becomes shallower at increasing depths below the surface. Consequently, the pressure actually exerted on this horizontal plane is not uniform. The greatest pressure occurs along the vertical axis of the loaded area, and it decreases with increasing radial distance from this axis.

For problems in flexible pavement design, this bell-shaped

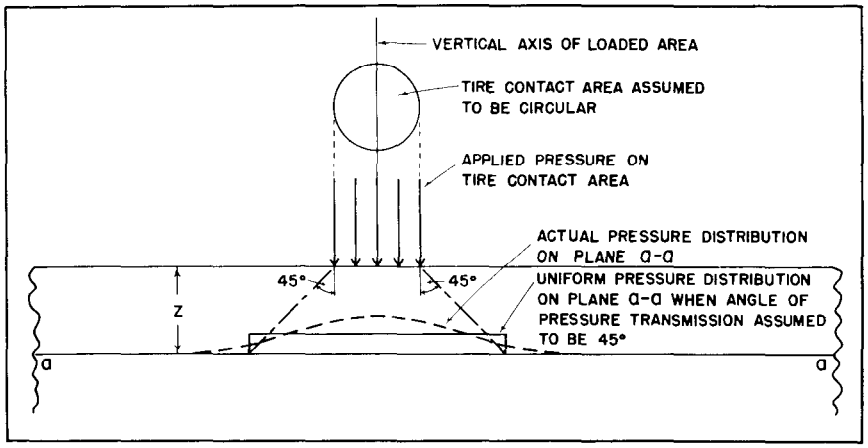

Fig. D. Diagram Illustrating Actual Pressure Distribution on Horizontal Plane At Depth versus Uniform Pressure Distribution Resulting From Assumption of A 45° Angle of Pressure Distribution.

pattern of vertical pressure distribution is not easily handled on a mathematical basis. Consequently, for calculating the required thickness of flexible pavement, several methods employ the assumption that a *uniform* pressure is exerted on any horizontal plane at depth, and that this uniform pressure is applied over the circular area bounded by the frustrum of a cone making an angle of 45° with the vertical through the perimeter of the loaded area (assuming the loaded area to be circular in shape, Figure D). The Gray formula is an example of a flexible pavement thickness equation, which assumes a uniform distribution of pressure within a 45° angle of pressure transmission from the boundary of the loaded area.

It should be noted that certain building codes are much more conservative concerning the assumption of a uniform pressure within a specified angle of pressure transmission from the loaded area, than are these flexible pavement design equations similar to the Gray formula. Some building codes specify that this angle of pressure transmission must not be assumed to be larger than 30°.

Figure D demonstrates that the assumption of uniform pressure within an angle of pressure transmission of 45° gives an average

vertical pressure on the horizontal plane a - a at any depth z that is considerably less than the maximum vertical pressure that is actually exerted along the vertical axis of the loaded area. This has been demonstrated by actual measurement and by calculations based upon the theory of elasticity.

In his paper on flexible pavement design published in 1940 in Volume 20, Proceedings of the Highway Research Board, Mr. A. T. Goldbeck reports that for any specified surface load the vertical pressure actually measured at any given depth along the vertical axis through the loaded area was much greater than the value of the uniform pressure calculated for that depth on the basis of a 45° angle of pressure transmission. Results of laboratory tests in which known loads were applied at the surface of base course materials having thicknesses frequently employed for highways led Mr. Goldbeck to conclude that the average pressures on the subgrade calculated by assuming a 45° angle of pressure transmission through the base course were approximately one half the vertical pressures actually exerted on the subgrade along the vertical axis through the loaded area. Based on Mr. Goldbeck's findings, therefore, the assumption of an average uniform pressure on the subgrade within a 45° angle of pressure transmission could lead to serious underdesign. To avoid this underdesign, Mr. Goldbeck recommended that the average uniform pressure on the subgrade, obtained by assuming a 45° angle of pressure transmission through the base course, be multiplied by 2 for single tires and by 2.5 for dual tires.

If the subgrade must not be overstressed at any point below the loaded area at the surface, Mr. Goldbeck's data and Figure D indicate that design equations based upon uniform pressure within a 45° angle of pressure transmission would result in underdesign. On the other hand, if the subgrade is overstressed at any given point, it will deform and transfer some of the load to adjacent points that are not overstressed. To the extent that this can occur without causing serious distortion of the surface of a flexible pavement, the assumption of uniform pressure within a 45° angle of pressure distribution avoids underdesign.

The most serious criticism that can be made of flexible pavement design equations based upon the assumption of uniform pressure within a 45° angle of pressure transmission is that they give no direction concerning the way in which the supporting value of the subgrade is to be measured or determined. In general, this very important problem is completely ignored, even though the equations themselves contain a factor that is usually considered to represent subgrade support. In reality, this factor does not

actually represent subgrade support, it merely provides values of the average pressures that are transmitted to the subgrade through various depths of base course. These equations do not indicate how an engineer is to know whether or not any given subgrade will be able to support these transmitted pressures. Expressed in another way, these design equations concentrate on the "action" phase of the problem, that is, on the magnitude of the average uniform pressure transmitted to the subgrade, and they give no attention to the "reaction" phase of the problem, that is, to the way in which the subgrade reacts to applied pressure. It is a well-known principle of mechanics that there can be no equilibrium unless action and reaction are equal, or as expressed mathematically for this case where vertical action and reaction are involved, ΔV must be equal to zero.

The magnitude of the support that any given clay or clay loam subgrade can provide depends upon the amount of deflection that occurs under the applied load and upon the size of the loaded area. For a given deflection, the subgrade supports a smaller unit load as the size of the loaded area is increased. For a given size of contact area, the supporting value of the subgrade increases as the deflection is increased, at least until the ultimate load is reached. Although these simple facts are widely known, it is not uncommon to find tables of supporting values for various types of subgrades listed for use in these flexible pavement design equations, without the slightest reference to either deflection or size of contact area. Such tables of subgrade support are practically valueless for flexible pavement design.

These facts should be kept clearly in mind when using design equations based upon a uniform subgrade pressure and a 45^0 angle of pressure distribution. For example, if the strength of a given clay or clay loam subgrade is measured with a bearing plate 12 inches in diameter resting on its surface, a certain value of subgrade support will be obtained at some specified deflection. At a depth of base course of 9 inches, the loaded area of the subgrade is 30 inches in diameter, if the diameter of the loaded contact area at the surface of the base is 12 inches. However, subgrade support in p.s.i. for a loaded area 30 inches in diameter is just one half of supporting value in p.s.i. for a loaded area 12 inches in diameter for the same deflection for many soils. Furthermore, associated with the increasingly larger loaded area of the subgrade at greater depths of base is a smaller deflection, assuming that the deflection at the surface under the applied load remains constant, since deflection decreases with depth under this condition. Due to this smaller deflection at depth, the

developed value of subgrade support is further decreased. Consequently, a different value of subgrade support should be associated with every thickness of base course being investigated by design equations which assume uniform average pressure distribution within a 45^0 angle of pressure transmission. How often is this done? Usually one value of subgrade support is assumed, regardless of the thickness of base course under consideration.

How often is any information available concerning the way in which the supporting value of any subgrade in question varies with the size of the loaded area, and with the deflection that occurs under load? Finally, is there some critical transmitted load or some critical deflection for each subgrade that should not be exceeded insofar as flexible pavement design for heavily travelled highways or busy airports is concerned?

It appears, therefore, that sufficient published data are not yet available to establish whether the angle of pressure transmission through a flexible pavement, that should be associated with the assumption of uniform average pressure distribution on the subgrade, is approximately 45^0 or some other value, and whether this angle is a constant or varies with depth and with characteristics of base course material, etc.